Evaluation of the non-linear properties of two computational models of the peripheral auditory system

Isaac Smart

Thesis submitted in partial fulfilment of the requirements for a Degree of

Master of Audiology

At the University of Canterbury

Department of Communication Disorders

2015

Acknowledgements

Firstly, I would like to thank my supervisor Dr Donal Sinex. Your support and guidance throughout this process has been invaluable, as well as your generous provision of data that made so much of this study possible.

Secondly, I would like to thank my associate supervisor Associate Professor Greg O'Beirne for helping me with the formatting and revisions in the final stages of my thesis.

I would also like to thank the audiology staff and my classmates for their support over the last two years; I am privileged to have you as colleagues.

Lastly, I would like to thank my family and friends, for all their time and effort in helping me stay sane through this project. Thank you especially to my Dad, whose knowledge in programing saved me many hours in debugging software issues and to my Mum, for all the hours spent supporting and proofreading this project so it could be understood by others.

Abstract

The output responses of two computational models of the peripheral auditory system were investigated. The models used were the Carney model, described in Zilany *et al.* (2009) and the Seneff model, as described in Seneff 1988. Of particular interest is the exhibition of the 'synchrony capture' phenomenon. This occurs when the auditory nerve fibre preferentially fires in time sync with a single spectral component within a complex sound. The studies of Sinex *et al.* (2003) and Deng *et al.* (1987) were used for visual comparison to the modelled responses with regards to synchrony capture. Sinex *et al.* (2003) showed synchrony capture in the responses of auditory nerve fibres to components within a harmonic tone against increasing intensity. Deng *et al.* (1987) showed synchrony capture to a component over increasing relative intensity of that component within a harmonic tone. The results revealed that the Seneff model showed strong agreement to the recorded response sets presented in Sinex *et al.* (2003 and Deng *et al.* (1987). The Carney model showed strong agreement to the synchrony capture presented in Deng *et al.* (1987) but responses did not have strong agreement to synchrony capture presented in Sinex *et al.* (2003).

Table of Contents

List of Figures

List of Tables

List of Abbreviations

CF	Characteristic Frequency
F_0	Fundamental Frequency
F_p	Probe Frequency
SPL	Sound Pressure Level
PSTH	Peri-Stimulus Time Histogram
FFT	Fast Fourier Transformation

Introduction

The process of human hearing, like all mammalian hearing utilises vibrations caused by sound waves to mechanically induce electrical signals by the firing of nerve synapses. This process occurs in the cochlea of the inner ear in the form of a travelling wave on the basilar membrane which activates inner hair cells, sending electrical signals up the auditory pathway via the auditory nerve fibres to the brain where the information is perceived as 'sound'.

The perception of sound relies on encoded information derived from the temporal and spectral properties of the stimulus. This encoding determines the various properties that are admitted to the higher components of the auditory pathway. Furthermore, this encoding allows for separation of the auditory signal out from various streams of related sounds. The encoding causes harmonics of a fundamental frequency to be perceived as a single sound; the pitch and timbre being determined by the fundamental frequency and subsequent component patterns respectively (Moore, Peters, & Glasberg, 1985; Moore, Glasberg, & Peters, 1986; Micheyl & Oxenham, 2010).

The encoded information is represented by the firing patterns of the auditory nerve fibres; the neural responses that are activated through the movement of the basilar membrane in reaction to sound vibration.

1.1.1 Neurone Responses

The pattern of neurone firing (the 'spike train') can relay information through either the number of spikes or through the temporal pattern of the spikes. Rate coding of neural firing uses information based on the firing rate exhibited by the neurone over time, for example, increasing in rate as the stimulus intensity increases. The neuronal rate can be reported in a peri-stimulus time histogram (PSTH), in which the neurone firing rates to a stimulus cycle are plotted. The histogram bars are plotted in temporal 'bins', or the average firing rate of a neurone to the stimulus over that time period (Palm, Aertsen, & Gerstein, 1988).

Experiments in 1926 showed that the spike train rate of afferent neurones of muscle fibres increased as the weight loading applied to the fibre was increased (Adrian & Zotterman, 1926). Later experiments showed that rate coding ignores any temporal firing information from either a single neurone or even relative timing in populations of neurones (Stein, Gossen, & Jones, 2005).

Conversely, temporal encoding uses the spike timing of the neurone firing to encode information about the stimulus. Research indicates that the temporal resolution of neural coding to be in the order of 1 millisecond. The precise timing of rate coding may allow for coding of the firing activity that cannot be described by the firing rate alone (Butts *et al.*, 2007). As some stimuli durations will only allow a neurone to fire once, the timing of the spike rather than the average rate of spikes over time may be of more importance, that is, whether or not a neurone fires in the presence of a stimulus and the precise timing of the spike generation (Theunissen & Miller, 1995). This ability to resolve fine temporal information within short time frames may be an important factor for detecting phase differences in sound localisation (Marsalek & Kofranek, 2005), while spike rate may play a role in encoding the intensity level differences also used in sound localisation (Samson & Pollack, 2002).

1.1.2 The Role of the Basilar Membrane

Vibrations of the basilar membrane cause inner hair cells to activate action potentials in the synapsing auditory nerve fibres. Initial observations by von Békésy of the basilar membrane suggested that the vibrations were broadly tuned and passively driven in a linear fashion by the stimulus vibrations alone. These observations showed different stimulus frequencies activating different regions of the membrane with higher frequencies causing the greatest deflection in the basal region and low frequencies causing the greatest deflections in the apical region. Research by Rhode (1971) addressed concerns about extrapolating data from the high intensity stimuli and dead cochlea used by von Békésy to lower intensity levels in living cochlea. Using the Mössbauer technique on living primate cochlea, in which a radioactive source is placed on the basilar membrane and specific photon energies measured to derive source velocity estimates, the measurements in this study indicated nonlinear vibrations for frequencies

which produced the largest deflections in the region under observation and sharp frequency tuning. Further studies have since replicated these findings with refined techniques such as removing the added mass on the basilar membrane introduced by the Mössbauer technique which affected the membrane vibrations. These improvements removed technique interference, allowing subsequent measurements to have greater accuracy (Sellick, Patuzzi, & Johnstone, 1982; Robles, Ruggero, & Rich, 1986; Nuttal & Dolan, 1993; Ruggero, Rich, Recio, Narayan, & Robles, 1997).

The nonlinearity of the basilar membrane is thought to arise from the 'active process', the force generators of which is suggested to be the outer hair cells (Liberman & Dodds, 1984).

1.1.3 Hair Cell Function

As stated above, hearing relies on the function of hair cells sitting on top of the basilar membrane, of which there are two types; the inner hair cells and the outer hair cells. These two cell types have different functions within the hearing system; the inner hair cells synapse with auditory nerve fibres and are responsible for the 'firing' of the nerves, while the outer hair cells are responsible for the nonlinear properties of the basilar membrane vibration, due to their mechanical function in the presence of a sound stimuli (Lim, 1986).

Inner hair cells form a single row closest to the 'inside' edge of the spiral shaped cochlea, while the outer hair cells are arranged in three to five rows, depending on the region of the cochlear, near the 'outer' edge of the spiral. Above both types of hair cells lies the tectorial membrane, hinged at one end, which the stereocilia of the outer hair cells touches. As sound causes the basilar to vibrate, the tectorial membrane moves side to side relative to the top of the hair cells. This shearing action causes a deflection of the stereocilia. In the inner hair cells, this deflection leads to an influx of potassium into the hair cell, resulting in a flow of electrical charge which in turn leads to the generation of an action potential in the synapsed auditory nerve fibres (Ceriani & Mammano, 2012). This process is called mechano-electrical transduction, converting mechanical movement into electrical neural signals (Lim, 1986; Müller, 2008).

Because of the ascending staircase arrangement of stereocilia of the inner hair cell, the gated tip-links that result in the mechano-electrical transduction of the cell, are directional. One consequence of this is half-wave rectification. The hair cell responds to both positive and negative deflections of the basilar membrane, half the stimulus cycle increases the probability of the neurone firing while the other half effects a reduction in firing likelihood (Howard, Roberts, & Hudspeth, 1988; Müller, 2008).

In the outer hair cells, the deflection of stereocilia also results in a change in electrical potential within the cell, although this results in a motor function of the hair cell itself, changing the length, shape and stiffness of the hair cell. This function in turn influences the vibration of the basilar membrane and its response to sound, resulting in the outer hair cells being a key element in the 'active process' and a significant cause of the observed nonlinear response to sound (Lim, 1986; J. F. Ashmore, 1987; Ceriani & Mammano, 2012).

Two main mechanisms have been postulated to explain this 'active process' in the outer hair cells. The first is a voltage-dependent somatic mobility which results from the activity of prestin in the membranes of outer hair cells while the other is dependent on hair bundle mobility driven by calcium currents (J. F. Ashmore, 1987; J. Ashmore *et al.*, 2010).

1.2 Discharge Properties of Auditory Fibres

The auditory nerve is the pipeline from the inner ear to the higher auditory system. The patterns in which the nerve fibres are induced to fire by the stimulus determines the information that is received by the structures higher up in the auditory pathway, with the final representation determining how we perceive the sound. Different variations in this firing pattern are responsible for the perception of the different elements of the stimulus, such as how loud the sound appears to a listener, or the specific pitch (Moore, 2003).

There are physical constraints to how the synapse can encode auditory information. Auditory fibres have a finite rate in which they can fire in response to a stimulus, the maximum rate being saturation of

the fibre. Sachs and Abbas (1974) measured the relationship between the firing rate and the intensity of the stimulus in single auditory nerve fibres in cats. With stimulus tones at the fibre's characteristic frequency, the rate increased rapidly over a range approximately 20 to 30 dB above threshold. It was observed that some fibres saturated at this point, with no further increase in firing rate with increased intensity. However, other fibres continued to increase firing rate for another 30 to 40 dB, albeit at a reduced rate, generating a notable bend in the rate-level function. When the stimulus tone was above the characteristic frequency of the tested fibre, the slope of the rate-level function was observed to decrease with increasing frequency, while measurements with tones lower than the characteristic frequency generated similar rate-level functions to those of tone at characteristic frequency, or increased to a saturation point as the frequency decreased.

Further studies into fibre rate-level functions have observed a close relationship between the spontaneous firing rates of auditory fibres and its dynamic range; the difference between its minimum response threshold and its rate saturation level. Auditory nerve fibres with high spontaneous firing rates typically demonstrate the smallest dynamic range, whereas the opposite is true for fibres with lower spontaneous firing rates (Liberman, 1978; Evans & Palmer, 1980; Winter, Robertson, & Yates, 1990).

Due to the limited dynamic ranges exhibited by auditory nerve fibres, there has been the question of how the human auditory system has the ability to operate with a range of over 100 dB. This is known as the 'dynamic range problem' and has strong implications for understanding how the intensity of a sound is encoded in the peripheral auditory system (Evans, 1981). Measurements with pure-tone stimuli show that the excitation rate at the characteristic frequency placing saturates rapidly, preventing the immediate area from adequately coding for intensity. In order to account for the wide dynamic range measured, intensity coding may be based off the responses produced by the surrounding cochlea area (Viemeister, 1988; Chatterjee & Zwislocki, 1998).

Further research into the dynamic range problem by Wen, Wang, Dean, and Delgutte (2009) suggests that dynamic range adaption occurs in the primary auditory neurones. Measurements from anesthetised neurones in cats appeared to adapt to the distribution of sound levels in a continuous dynamic stimulus

by adjusting towards the most frequently occurring level. While this effect was not as great as that seen in higher level auditory neurones (Dean, Harper, & McAlpine, 2005), this finding suggests that some level of adaptive processing of sound level occurs in the peripheral auditory system, which is subsequently enhanced along the auditory pathway. This finding is supported by measurements that indicate this process of dynamic adaption occurs rapidly enough in the peripheral system to have an impact on the level coding of sounds (Wen, Wang, Dean, & Delgutte, 2012).

The effect of auditory nonlinearity in the responses of auditory nerve fibres to bandlimited noise was examined by Schalk and Sachs (1980). Using maximum driven rate for single tones at the fibre's characteristic frequency as a benchmark, rate-level curves were measured for both narrowband and wideband noise. While narrowband noise produced similar rate-level curves to that of the single tone stimuli, wideband noise responses produced lower discharge rates at the same spectral levels. This observed reduction in rate was noted to have similar properties to that of two-tone suppression, indicating that these nonlinearities may originate from a common mechanism. Furthermore, the rate reduction, or suppressive effects, were most substantial in fibres with low spontaneous rates and less vigorous in fibres with high spontaneous rates. This relationship between spontaneous rate and suppression is supported by findings in phase-locked complex tone discharge patterns (Horst, Javel, & Farley, 1990).

1.2.1 Adaptation

The response of an auditory nerve fibre to a stimulus changes over the stimulus duration. At the onset of a stimulus, the neurone fires maximally, with the rate of action potentials decreasing towards a steady state over the stimulus period. This 'adaptation' to the sound is caused by physiological properties of the synapse, such as a limited replenishment rate of the needed neurotransmitter. After the offset of the tone, before the neurotransmitter levels are replenished, the natural spontaneous activity of the nerve is reduced, slowly recovering over tens of milliseconds to pre stimulus levels (Smith, 1977; Harris & Dallos, 1979).

An investigation into the response properties in feline refractory fibres by Miller, Abbas, and Robinson (2001) indicated a mean absolute refractory period of approximately 330μs after being driven to refractoriness via an intra-cochlear stimulating electrode.

Accurate measurement of the fibre properties is vital in order to accurately model auditory nerve fibre physiology, as this refractory property of nerve fibres can be seen as a form of distortion in the transfer of information, by introducing a regularity into the firing patterns of fibres that may not be present in the stimulus itself. Furthermore, the refractory period may limit the spike timing encoding that can be achieved by an auditory nerve fibre (Gray, 1967).

1.2.2 Frequency Tuning

Research on second order cat auditory neurones performed by Galambos and Davis (1943) indicated that when the stimulus intensity is only just above minimum excitatory levels, an auditory fibre will only respond to a very narrow range of sounds frequencies, that is, the characteristic frequency of the nerve fibre. Iso-intensity curves subsequently demonstrated that as the intensity level of the stimulus was increased, the range of frequencies that were responded to by individual fibres expanded, with the characteristic frequency of each fibre always exhibiting the most excitation. Further research (Evans, 1972) with cochlear neurones from anaesthetised guinea pigs indicated that the shape of frequency tuning curves changed according to the characteristic frequency of the fibre; the region of the cochlea at which it innervates. Tuning curves for high characteristic frequency fibres are steeply sided, with the low frequency tail showing two segments; a steeply sloped segment from approximately 40-70 dB above threshold, with the second segment being defined by a significantly reduced slope. The tuning curves for low characteristic frequency fibres, however, are broader and typically symmetrical in shape (Evans, 1972; Kiang & Moxon, 1974).

There are differing opinions with respect to the tuning sharpness, or bandwidth, of the human cochlea. Some studies claim that the tuning in humans is narrower than that of other mammals (Shera, Guinan, & Oxenham, 2002), while other studies disagree (Ruggero & Temchin, 2005). Complicating the debate

on frequency tuning further is that a number of studies using different estimation methodology show considerable quantitative variation in the frequency tuning between various animal species; some reporting comparable tuning between mammals (Taberner & Liberman, 2005), and others reporting differences in tuning sharpness (Shera *et al.*, 2002).

The ability for the auditory system to select and encode for frequency has a significant impact on the comprehension of speech and music. Frequency selectivity is remarkably stable over a wide range of intensities, only diminishing in ability to analyse concurrently presented frequencies at levels above 70dB SPL (Pick, 1980). Research by Greenberg, Geisler, and Deng (1986) involving two-tone signals in low characteristic frequency cat auditory nerve fibres suggests that while the ability of auditory fibres to represent the spectrum of complex sounds in terms of spatial rate distribution at moderate to high intensities may be compromised (Sachs & Young, 1979), measurements suggest that the temporal discharge properties may compensate, allowing for stable frequency selectivity over a wide range of intensities.

1.2.3 Phase-Locking

Phase-locking is a discharge property that can be observed when the rate of neural firing coincides in phase with the stimulus waveform (Rose, Brugge, Anderson, & Hind, 1967), or in other words, when the stimulus periodicity and the timing of the neural spikes synchronise together. Hence, the temporal structure of the response mimics the periodicity of the waveform. Phase locking occurs in the discharge pattern of sounds up to frequencies of approximately 4-5 kHz, after which the synchrony of the neural spikes and the waveform drops off, often in dramatic fashion. This frequency limit to phase locking is thought to be determined by the low pass filtering present in the membrane of the inner hair cell. This limit is also seen in the decline of the ac/dc ratio that occurs in the inner hair cell potentials with increasing stimulus frequency (Palmer & Russel, 1986). Furthermore, the frequency limit of phase-locking is species dependent, with some mammals such as the guinea-pig having slightly lower limits compared to that of cats or pigeons (Rose *et al.*, 1967; Sachs, Young, & Lewis, 1974).

1.3 Nonlinearity in the Peripheral Auditory System

The vibratory response of the basilar membrane becomes nonlinear due to the interaction with the outer hair cells. Evidence for this was first described in terms of a compressive nonlinearity, or a reduction in gain as stimulus levels are increased, with later studies showing nonlinearity in responses as low as 20 dB SPL up to tested levels of 110dB SPL. This results in the response magnitude on the membrane not growing in proportion to that of the input stimulus (Rhode, 1971; Ruggero *et al.*, 1992). In simple terms, this means that for low and medium intensity sounds, the active mechanism amplifies the sound, with the maximum amount of gain applied at lower intensities and progressively diminishes as the input level increases. This nonlinear process results in responses that do not increase in proportion to increases in amplitude of the stimulus. The response to a stimulus may be at a lower rate than would be expected from a linear system.

Some studies have shown an upper limit to this compressive nonlinearity, in which at high enough intensity levels the response becomes progressively more linear, in particular, observations on the effects of acoustic trauma (Patuzzi, Johnstone, & Sellick, 1984) and other theoretical considerations (B. M. Johnstone, Patuzzi, & Yates, 1986; Nobili & Mammano, 1996). However, this trend is rarely observed in Mossbauer experiments in normal cochlea, and perhaps more importantly, this linearization does not appear to occur in physiologically relevant intensities (up to 110dB), as reported by Ruggero *et al.*, 1997.

The health of the cochlea is a critical factor that affects the function of the active process. As the cochlea becomes more damaged, the nonlinear response tends to become more linear, resulting in a reduction of stimulus responses and ultimately at the death of the cochlea, the response becomes entirely linear (Ruggero *et al.*, 1992; Ruggero *et al.*, 1997).

Potential sources of nonlinearity in the auditory system were investigated by Horst *et al.* (1990). Using Fourier transformations of period histograms from phase-locked discharge patterns in single cat auditory fibre responses, the effect of phase spectrum, number of components and intensity of the centre

component, were investigated. With the exception of phase, strong nonlinearities in response were observed in all of the signals. Importantly, the degree of nonlinearity was observed to increase with increasing intensity and signal complexity. The authors interpreted the nonlinearity of responses as arising from the cochlear mechanics, compression applied to instantaneous discharge rate, and the saturation of the average discharge rate.

Measurements from this study indicate that the number and temporal position of the fine structure peaks observed in the responses are greatly influenced by the harmonic complexity and intensity, previously observed with noise stimuli (Moller, 1977). This observation suggests that, alongside the effect of the tuning shape filtering of components contributing to the fibres response, suppression may also be operating. Furthermore, suppression strength appears to be dependent on the temporal waveform of the stimulus (Horst *et al.*, 1990).

Nonlinearity is important to allow perception of wide dynamic range and frequency range tuning present in the auditory system. However, other properties are also determined by this process. Studies by Young and Sachs (1979) and Delgutte and Kiang (1984) suggest that an increase in the intensity can improve the representation of spectral peaks (or formants) in temporal response spectra. This suggests that amplification of spectral contrast is an important outcome of nonlinear cochlear processing.

1.3.1 Combination Tone Generation

Combination tone generation is one consequence of nonlinear interactions between two tones, also known as a distortion product. This occurs when two tones are presented, resulting in humans often perceiving a third, lower tone that is not present in the original stimulus. The most prominent of these being $2f_1 - f_2$ and $2f_2 - f1$, where f_2 is greater than f_1. Goldstein (1967) proposed that these arise in the cochlea, after ruling out production in the middle ear, with the site of origin being the cochlear region most sensitive to the primary tones, and postulated that these mechanical distortion products propagate along the basilar membrane to a region where the characteristic frequency matches its own. This in turn is detected by the cochlear nerve and transmitted to the brain (J. R. Johnstone, 1980).

While some form of rapid compression within the cochlear is required to account for such phenomena as combination tones (Goldstein, 1967; Arthur, Pfeiffer, & Suga, 1971), simple compressive nonlinearity does not account for others, such as low-frequency suppression (Sachs & Abbas, 1976).

1.3.2 Two Tone Rate Suppression

One of the better studied nonlinear phenomena in cochlear nerve responses is that of two-tone suppression, in which the average firing rate in the region most sensitive to a probe tone is reduced by the addition of a suppressor tone at a different nearby frequency. Whether or not a tone is supressed is influenced by a number of factors, such as the intensity and frequency of the suppressing tone (Wever, Bray, & Lawrence, 1940; Sachs & Kiang, 1968; Javel, 1981; Javel, McGee, Walsh, Farley, & Gorga, 1983; Greenberg *et al.*, 1986). The two-tone suppression phenomena has been observed in nearly every auditory response of cochlear origin, including the cochlear microphonic, single neurons, hair cell responses, acoustic emissions and the vibration patterns of the basilar membrane (Rhode & Robles, 1974; Cheatham & Dallos, 1982; Javel *et al.*, 1983; Cheatham & Dallos, 1989). The overall suppression effect can be quite large, with discharge reductions equivalent to approximately 40-50 dB in the input level being observed (Delgutte, 1990).

One of the most significant properties of two-tone suppression is the dependency on the frequency of the excitatory tone; only tones with frequencies close to the neurones CF can be strongly supressed by tones with frequencies below or above (Schmiedt, 1982). This suggests that the suppression may arise in the cochlear mechanics, as a result of the sharp frequency tuning evident in the vibrations observed on the basilar membrane. This also indicates that the sharp frequency tuning is established early in the transduction chain. This dependency is further evidenced by research that shows the two-tone suppression persists even after sectioning of the auditory nerve central to the site of recording the cochlear afferents (Kiang, 1965).

When using discharge rate of single auditory nerves as an index, measurements suggest that the phenomenon behaves in an orderly but nonlinear manner, with the suppression being limited to the

frequencies and intensities on either side of the tuning curves of the nerve fibres. This indicates that the suppression bandwidth, or range, is greater than that of the excitatory bandwidth of the fibre (Javel *et al.*, 1983).

Suppression tends to be greatest from suppressor tones below the CF and weakest from suppressor tones above the CF. Additionally, it has been shown that suppression by characteristic frequency tones grows faster as a function of intensity in lower tuned fibres than in higher tuned fibres. However, this may be due to interference by phase-locking responses (Javel *et al.*, 1983).

Javel (1981) investigated two-tone suppression in feline auditory nerve fibres using synchronisation of discharges to the tone being suppressed (vector strength) as a measure of suppression strength. This was achieved by measuring the contribution of each component of the complex sound by timing the occurrence of fibre discharges. The current study emulates this measurement through the use of Fast Fourier analysis of peri-stimulus histograms of the fibres response. The limitation in this technique is that it can only be measured for components with frequencies within the range of phase-locking. However, this method overcomes the limitation in recording suppression when only discharge rate is considered. When the overall discharge rate is maximal, it cannot be determined if the response exhibits suppression. Other measures of suppression through the use of amplitudes of response in period histograms had previously been employed by other authors (Arthur, 1976). However, these techniques resulted in unnatural measures of suppression when the overall discharge rate varied with changing stimuli. Differentiating by fibre response index gives rise to the terms two-tone rate suppression (discharge rate) or two-tone suppression (synchronisation), as described in Holton and Weiss (1978).

Using the synchronisation technique, recorded responses showed that even at levels where the overall discharge rate was saturated, suppression was able to continue increasing. Furthermore, it was observed that suppression was greatest at the fibre's characteristic frequency when the suppressor was fixed in intensity. The recorded suppression in this study was in general agreement with previous studies on two-tone suppression (Sachs & Abbas, 1976).

Investigations into the origin of suppression by Javel *et al.* (1983) suggest that the suppression may occur in the inner hair cells themselves. This is indicated through the apparent generation of suppression occurring before the release of neurotransmitter in the auditory neurone synapse. Additionally, the basilar membrane function alone cannot account for all of the properties of suppression. Examples of this are the short latency exhibited in suppression and that the phase of excitation that causes suppression is also the phase that produces synchronisation to the suppressor. This indicates that suppression is dependent on excitation (Sachs & Hubbard, 1981). The authors suggest that suppression may be a property of the half wave rectification characteristic of the inner hair cell, where one half cycle of the stimulus cycle has a 'potential for excitation', that is, the activation of neurotransmitter release, whereas the other half of the cycle has a 'potential for suppression', in which the effect is to diminish the response to other tones (Javel *et al.*, 1983). Further investigation into the transforms occurring within, and the role in suppression of the inner hair cell, is needed.

Two-tone rate suppression may be important for the coding of speech and other complex sound stimuli, with the dominant components reducing the neural response to the less intense components and thereby, increasing the relative neural response to the dominant components (Sachs & Young, 1979).

Investigation into the response of fibres to two harmonically related tones simulating the lowest formants of a set of vowels indicated that when one tone was at the fibres characteristic frequency, that tone controlled the fibres discharge timing. Furthermore, the response to the second tone was suppressed. However, this domination was also intensity dependent; at threshold, the tone near the fibres characteristic frequency was dominant while at higher intensity levels (~60 dB and above) the lower frequency tone was favoured (Reale & Geisler, 1980). This feature may have implications for the encoding of the first and second formants in complex sounds such as speech.

1.4 Strong Synchrony Capture

While two-tone suppression is a nonlinear phenomenon exhibited with two-tone stimuli, strong synchrony capture, sometimes termed synchrony suppression, is also observed in the temporal

representation of low harmonics of complex sounds in which suppressive effects are exhibited when phase-locked response components are involved. This occurs when a component of a complex sound (i.e. harmonic tones and speech) tends to dominate other amplitude components and 'captures' the nerve fibre firing synchrony in a 'winner takes all' scenario (Deng, Geisler, & Greenberg, 1987).

Strong synchrony capture was first reported by Sachs & Young 1979, while investigating the role of two-tone suppression and other nonlinearities in the encoding of feline auditory nerve fibre responses to synthetic steady-state vowels. Observations were made in which the driven discharge rate profiles of the responses exhibited peaks in the regions containing the first, second and third formants, with a reduction in the latter two regions at higher intensities. This reduction in formant peaks was suggested as being a result of a combination of the two-tone suppression phenomenon and rate saturation. As with studies in two-tone suppression (Horst *et al.*, 1990), a difference between high spontaneous rate and low spontaneous rate fibres was noted; with low spontaneous rate fibres retaining the higher formant peaks at higher intensity levels to those of high spontaneous rate fibres.

The authors concluded that the rate suppression seen in the rate functions of auditory fibres with characteristic frequencies above that of the first formant peak shares the same underlying mechanism as that of two-tone suppression.

It was found that this suppression has a significant effect in the shaping of auditory nerve fibre responses to steady-state vowel stimuli, contributing to the loss of a separate peak in the second formant region and did not sharpen the representation of the stimulus rate spectrum, as had been initially hypothesised (Sachs & Young, 1979).

These findings were further discussed in Young and Sachs (1979) and Sachs and Young (1980). The phase locking to the formant frequencies was observed to be stronger than that of the other harmonics in the stimulus. As the stimulus intensity increased, the synchrony to the formant frequency saturated, however, the response to the other harmonics was concurrently suppressed, allowing the phase-locking (or synchronisation) to the formant frequencies to dominate even at higher intensities, when the response activity to non-formant frequencies would otherwise be increasing. From this, synchrony

suppression may have a role in the preservation of information about the stimulus spectrum in the response's temporal pattern. That is, if the harmonics between the formants are not suppressed, as the intensity of the stimulus increased, these harmonics would also increase, leading to saturation of synchronised rate at high intensities. This, in turn, would flatten the spectrum representation in the fibre response, leading to a loss of information important to the perception of spectrally complex stimuli (Young & Sachs, 1979).

Another observation in the fibre responses was that in recordings in which synchrony to the second harmonic was large, response activity was seen in frequency components that were interpreted as rectifier distortion products of the second harmonic. It was suggested that these may arise from second harmonic tone combination tone propagation due to nonlinearities in the cochlea (Sachs & Young, 1980). Alternatively, these products may be a consequence of the method used for analysis and not having a true physiological basis.

The auditory nerve fibre responses findings of Sachs and Young (1979) were generally supported by Delgutte and Kiang (1984). Using a set of steady-state two-formant vowels presented at 60 and 75 dB SPL, it was found that the largest components of the Fourier transforms of the period histograms were nearly always a harmonic of the fundamental frequency situated close to one of the formant frequencies. The position of the formant frequency relative to the fibre's characteristic frequency appeared to determine which component of the fibre response was dominant. Furthermore, the response of fibres of various characteristic frequencies were able to be generally assigned. For fibres with characteristic frequencies in the frequency region below the first stimulus formant, the largest response components were closest harmonics of the fundamental frequency to the characteristic frequency of that fibre. In fibres where the characteristic frequencies were in regions centred on either the first or second stimulus formant, the largest response components were those closest to that formant frequency and its harmonics. For the frequency region between the two formants, large components were seen at both the fibres characteristic frequency and the fundamental frequency, whereas in fibres with frequencies above the second formant, broad multiple peaks were seen at both formant frequencies and the fundamental.

Measurements of fibre responses to broadband stimuli show the largest components near the characteristic frequency, unlike in the responses to vowel stimuli, in which the fibre response is centred on the formant frequencies (Delgutte & Kiang, 1984).

The authors noted that differences in the distortion component amplitudes were likely to be due to the increased relative intensity of the second formant over the first used in their stimuli. The first formant frequency components were found to dominate the response in fibres whose characteristic frequency was close to that of the second formant in Sachs and Young (1979), but not in responses measured by Delgutte and Kiang (1984). It was suggested that this difference in stimulus parameter was also responsible for this result.

Further research by Sinex and Geisler (1983) investigated the auditory nerve fibre responses to consonant-vowel syllables, rather than the steady-state vowel stimuli used by Sachs and Young (1979). The use of slightly more complex stimuli allowed the investigation of discharge patterns in responses to sounds in which the spectra vary in time, a characteristic property in real speech patterns. The results of this study differed to that of Sachs and Young (1979) in that more information about the spectra of formant transitions rather than steady-state vowels appeared to be provided by the discharge rate. The analysis of synchrony suggested that many fibres track a stimulus formant from its onset through to its steady-state frequency. However, in some stimulus situations, fibres were observed to track one formant momentarily before switching to a different one. This is thought to have arisen due to the formant structure of the stimulus being characterised by a number of spectral peaks with different relative amplitudes. As the frequencies of these peaks moved in relation to the fibres characteristic frequency, the most ‘effective’ peak for that fibre could change, such as with a decrease in amplitude of components near the characteristic frequency, allowing components near another formant to become dominant.

Furthermore, it was suggested that more information about the consonant-vowel spectra is provided by the synchronisation of discharges, rather than the average discharge rate. From this, the response from a fibre could be identified by the ‘dominant component’, defined as the largest peak in a Fourier

transform of a period histogram. Changes to the dominant components in a sample of fibres could then be used to infer the trajectories of the first three formants, especially in moderate to high stimulus intensities. This is not as reliable, however, at lower intensities as some fibres have a tendency to synchronise their discharges to frequencies near their characteristic frequencies at onset of the stimulus (Sinex & Geisler, 1983).

Perhaps the most significant research for the present study, is the study by Sinex, Guzik, Li, and Sabes (2003). Investigations were made into responses of auditory nerve fibres to harmonic tones, in which one component harmonic could be mistuned by various amounts to evaluate the neural processing of acoustic cues that contribute towards spectral segregation (Moore *et al.*, 1985; Moore *et al.*, 1986). From this, it was found that most of the neural activity in the response was synchronised to a small number of stimulus components around the fibre's characteristic frequency, which 'dominated' the fibres response in a nonlinear fashion with increasing intensity. This was the case whether those components were harmonically linked to the other components or if they deviated harmonically from the series. Although the mistuning of a component within a harmonic tone produces striking changes to the temporal discharge patterns at the level of the inferior colliculus (Sinex, Sabes, & Li, 2002; Sinex, Li, & Velenovsky, 2005), the response changes in the peripheral neural coding do not provide any explanation for the perceptual changes of mistuning (Sinex *et al.*, 2003). The results of this study were consistent with previous studies in that the responses of the auditory nerve fibres were predominately synchronised to components around their characteristic frequencies. This is particularly so at lower stimulus intensities and with broader stimulus bandwidths.

One difference in this study compared to others is the use of the high fundamental frequency of 400Hz. Due to this, the fibre responses show only two or three stimulus components. In view of this, it was suggested that the widely spaced components may behave in a similar way as two tones, and that a more appropriate comparison of the result would be to studies investigating synchrony capture through the use of two tone stimuli, such as that by Reale and Geisler (1980).

In Deng *et al.* (1987), the responses of auditory nerve fibres to multiple-tone complexes were investigated, in which the amplitude of a single component (probe) was increased. Measurements of the relative synchrony to the probe tone, against that to the characteristic frequency component, were then utilised as a measure of the fibre's frequency selectivity to synchronisation. From this, it was shown that an iso-capture curve could be generated from observation of the dominant component as a function of intensity and the distance of the components frequency from the fibres characteristic frequency. However, this is based on the assumption that synchronisation magnitude can be used as a measure of a fibre's neural response. The advantage of this method is the ability to reliably assess the fibres frequency selectivity at high intensity levels, without interference from properties such as saturation. One limitation to this study was that while the amplitudes of components below the characteristic frequency were investigated to an extent to show an increase of relative intensity being necessary for the dominant component switch, this was not investigated as thoroughly in component frequencies above the characteristic frequency. Due to this, there is a gap in the results of a fibre's ability for strong-component capture above its characteristic frequency.

Sinex and McDonald (1989) demonstrated that the dominant component changes frequency depending on the voice-onset time, further suggesting the potential of synchrony encoding being relevant to human perception of voicing. This was explored in greater detail by Kluender, Lotto, and Jenison (1995)**,** who found a small but consistent effect of presentation level, and thus synchrony capture, on the perception of voicing as a function of frequency separation between the first formant and higher formants.

This finding, however, has since been questioned by its authors in subsequent studies, which examined the role of synchrony capture in the perception of voicing stimuli. The findings showed manipulations to the stimuli that should have impacted synchrony capture ability had no effect on voiceless perception ability, with the effect of amplitude itself being unaltered (Lotto & Kluender, 2002). This suggests further research is needed to investigate the exact role synchrony capture may have in this element of speech perception.

1.4.1 Significance of Synchrony Capture

Synchrony capture has significance in two main functions: i) the neural representations of the periodicity and spectrum of a sound; and ii) fundamental frequency pitch formation and associated sound separation.

The effect of synchrony capture neural representations, as described previously, enhances the temporal representations of individual resolved harmonics, at the expense of unresolved harmonics (Sachs & Young, 1979). This effect is generated through suppression effects enhancing the relative intensity relationships of a particular sound's frequency components, bolstering the 'relevant' stimulus components like the formant frequencies while obstructing the 'irrelevant' components. This ability to encode temporal features in the auditory system is critical for accurate perception of complex sounds.

The second significant aspect of synchrony capture is its role in the fundamental frequency based sound separation. Individuals are most commonly placed in situations where there are multiple competing sound sources that overlap in time and frequency (Sinex *et al.*, 2005). In order to separate multiple sounds occurring simultaneously, listeners rely on differences in the fundamental frequencies of the signals. Other properties of the stimuli, such as onset times, are also utilised in sound separation. Research suggests that the separation of multiple sound sources relies heavily on the presence of perceptually resolved harmonics (Darwin, 1997), and the estimation of the fundamental frequencies of one or more of the sounds being separated (Sinex, 2005). Fundamental frequency has a significant role in the development of pitch perception (Micheyl & Oxenham, 2010). While complex tones contain multiple components, they tend to be perceived as a single sound, linked together by the fundamental frequency. This common fundamental frequency is the origin of the pitch of the sound. When a component does not fall within an integer multiple of the fundamental frequency of other components, it is perceived as a separate sound with its own pitch (Sinex, 2005). This perception of various streams of sound is important for the separation of different sound sources. In this, synchrony capture has the effect of enhancing the representation of individual harmonic components.

Palmer (1990) demonstrated that the distribution of synchronised activity across the auditory nerve fibre array allowed estimation of the fundamental frequencies of synthetic double vowels. From the information provided by the synchronised activity of the fibre population, the vowel spectra were able to be reconstructed. It was also found that the timing of the auditory nerve fibre activity generated important cues for the fundamental frequency identification. However, research by Oxenham, Bernstein, and Penagos (2004) suggests that the tonotopic placement along the cochlea may have a more significant role in the extraction of the fundamental frequency of a sound. In this study, the temporal information of low frequency pure-tone sounds was presented to locations in the cochlea tuned to high frequencies. This had the effect of isolating the temporal information in the stimulus from the cochlea placement. Results showed poor fundamental frequency estimation from all participants based on the temporal information of the stimulus alone. As such, further research is needed in this area to investigate the relative importance of neural representations and tonotopical placement in the role of fundamental frequency estimation.

Speech perception in noise is known to be more difficult for individuals with hearing loss (Carhart & Tillman, 1970). However, this reduction in intelligibility is not accounted by the shift in hearing thresholds alone (Plomp, 1978). This research suggested that the difference between these hearing losses was the introduction of distortion into the auditory signal.

Fundamental frequency coding may have a role in masker release in the presence of fluctuating maskers. These maskers may be sounds such as other speech signals. It has been suggested that listeners may take advantage of momentarily favourable signal-to-noise ratios that appear in the temporal valleys of fluctuating competing sound sources (Festen & Plomp, 1990). This ability is thought to rely on the ability to code for the fundamental frequency of the stimulus. This in turn is dependent on the ability to process the temporal fine structure (Hopkins, Moore, & Stone, 2008).

Further research into the role of synchrony capture in the encoding of fundamental frequency through enhancing the representation of individual harmonics may have implications in improving the benefit provided to users of rehabilitative listening devices. Chatterjee and Peng (2008) suggest that one of the

greatest challenges for cochlear implants is providing pitch information in complex sounds. The increased ability to encode for fundamental frequency, and therefore pitch, that research into synchrony capture may provide, will be a significant step forward in cochlear implant use.

1.5 Aims and Rationale

1.5.1 Rationale for investigating auditory model functionality

Computer modelling is an invaluable instrument in research, with significant interest over the last few decades in the development of signal processing models (Stern & Morgan, 2012).

Computational models of the auditory system have a wide range of potential uses; allowing for hypothesis testing of the mechanisms that underlie response properties without the need for extensive and expensive experimental research conducted in laboratories that can have ethical considerations, as well as implications of other resources, such as time and the ability for consistent testing results (Lopez-Poveda & Meddis, 2001; Zhang, Heinz, Bruce, & Carney, 2001).

Due to the complexity of the auditory system, in both the individual processing stages and their interactions with one another, many auditory models simply simulate an observed input-output function without specifically modelling the internal auditory mechanisms involved. The model described by Seneff (1988) is one of these functional models. The inherent structural limitations of these models, such as oversimplification of the outer and middle ear function, can restrict the scope of their utilisation (Guigere & Woodland, 1994).

While computational models can help reduce a number of these issues, they need to be stringently tested to ensure that they are providing correct and accurate responses in regards to the outputs that they are designed to emulate. Furthermore, the testing of these models expands our understanding of their limitations and allows these shortcomings to be addressed, providing a means for more robust models to be created.

The aim of this study is to test two computational models of the auditory nerve and compare outputs with experimental data previously gathered with the explicit aim of examining their efficacy in demonstrating the phenomenon of synchrony capture.

1.5.2 Models implemented in the current study

The first model being used in the current study is a phenomenological model of the inner hair cell synapse and auditory nerve as presented in Zilany, Bruce, Nelson, and Carney (2009), referred to as the 'Carney' model.

This model includes an initial filter for middle ear simulation, from which the stimulus is split into three parallel filter paths. The control path filter features a broadband filter, simulating outer hair cell function, while the signal path consists of two parallel filters, C1 and C2, which account for level-dependent properties of the cochlea and a two-factor cancellation hypothesis (based on Kiang (1990) respectively. The inner hair cell signals are then combined and passed into an inner hair cell low pass filter, the output of which drives the inner hair cell- synapse model.

For the synapse modelling, a rate-adaption model is used, with an exponential adaptation component flowing into parallel power-law functions, a 'slow' path, in which fractional Gaussian noise is also added at appropriate rates to simulate spontaneous firing of the fibre, and a 'fast' power-law channel. Both paths connect at a 'spike generator' function from which the output of the fibre, as auditory neurone spike times, can be plotted. In this final stage, refractory effects of the fibre are added.

The slow path is used to improve the predicted recovery of the auditory nerve response after a stimulus offset, while the fast path is used to account for 'additivity' of the rate function in response to increasing stimulus intensity (Zilany *et al.*, 2009).

Overall, the Carney model emulates each major functional component of the auditory system from middle ear to auditory nerve fibre response (Figure 1).

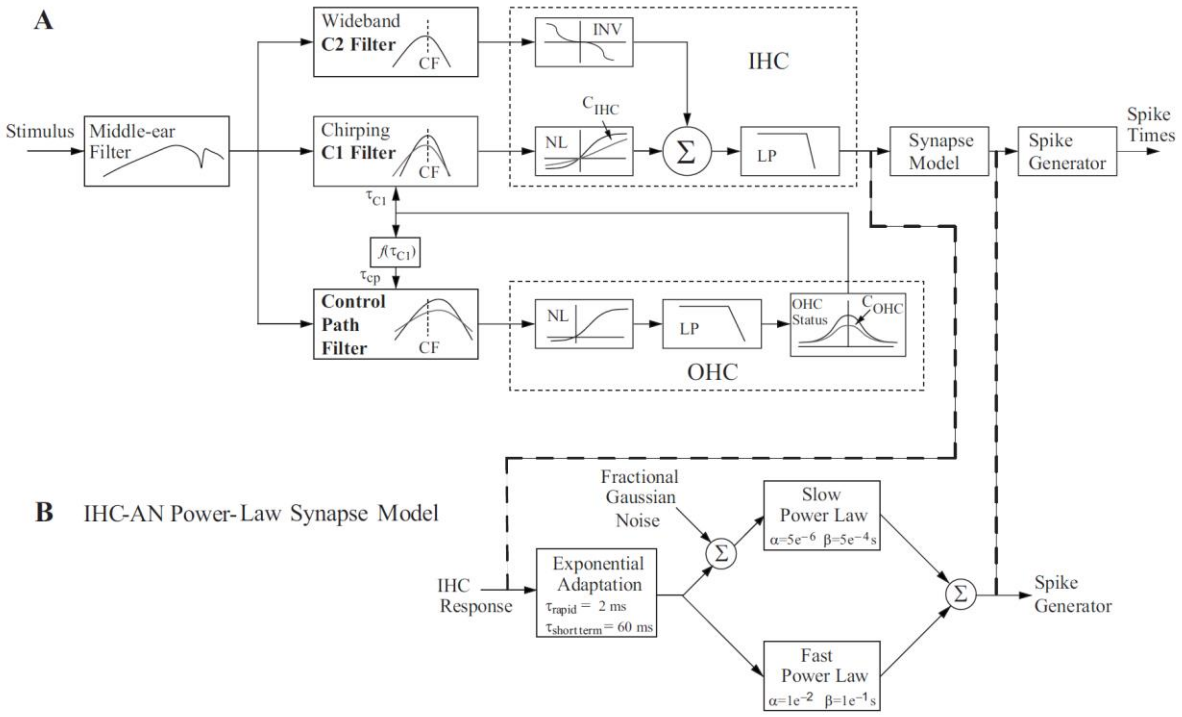

Figure 1: Schematic diagram of the Carney model structure.
Each major element of the peripheral auditory pathway (from the middle ear to the auditory nerve) is simulated in segmented components, as demonstrated above. Reproduced from Zilany *et al.* (2009).

The second model used in this study is a joint synchrony/mean-rate model of auditory speech processing, as described by Seneff (1988). This model is referred to as the 'Seneff' model in the current study. This functional model is based on properties of the auditory system, using parameters adjusted to simulate experimental results of the auditory peripheral physiology.

As seen in figure 2, this model consists of three stages: a critical band filter bank which defines the initial spectral analysis, a second stage modelling the hair cells synapse and a third stage, consisting of parallel detector modules. The first of these is the 'envelope detector', which determines the envelope magnitude as it corresponds to the average discharge rate of the response. The second module is the 'synchrony detector', which determines the synchronous response, through measurement of the extent that information near the centre frequency of the linear filter dominates the output.

The second stage of this model is comprised of four subcomponents, each corresponding to different aspects of the inner hair cell synapse. Hair cell function is modelled through half wave rectification saturating nonlinearity, followed by the synapse, modelled via a short-term adaption circuit. The nerve

fibre response is constructed through the last two subcomponents, a low pass filter to reduce synchrony and a rapid automatic gain control (AGC) to simulate the refractory effect of the fibre (Seneff, 1988).

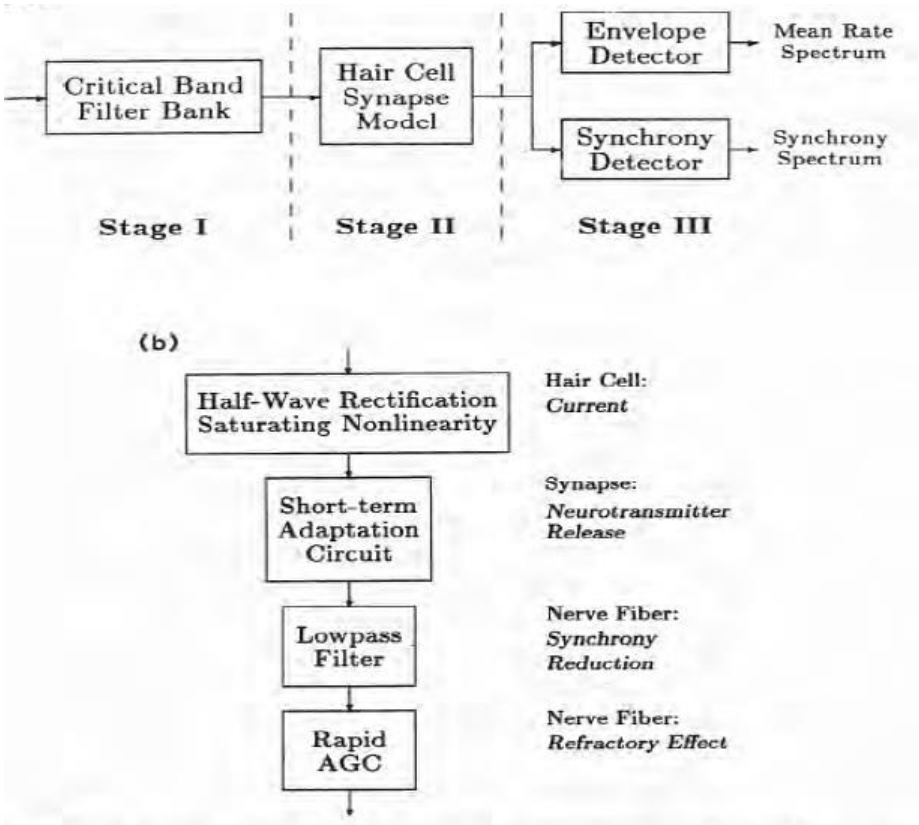

Figure 2: Schematic diagram of the Seneff model structure.
Displayed top is the overall structure of the Seneff model, showing each of the three stages. The subcomponents that comprise stage II are displayed below, with suggested auditory system affiliations indicted to the right. Reproduced from Seneff (1988)

Outputs from these models will be visually compared to previous research papers containing experimental data exhibiting the synchrony capture phenomenon; Sinex *et al.* (2003) and Deng *et al.* (1987).

The first study exhibits synchrony in a harmonic tone against increasing overall intensity, with the relative intensity of the stimulus components being equal and using a comparatively high fundamental frequency of 400Hz. From this, the effect of increasing overall stimulus level on the dominant component of the fibre response can be observed.

The study by Deng *et al.* (1987) explores the relationship between the relative amplitude of the stimulus components and stimulus, and the frequency difference between the stimulus and characteristic frequency of the fibre, on the presentation of synchrony capture. This is demonstrated through increasing the intensity of a single harmonic component in relation to the rest of the stimulus and observing the effect that this has on the dominant component being expressed by the fibre response. This relationship was explored over a number of harmonic components, allowing the effect of component frequency distance from the characteristic frequency of the fibre to also be explored.

Methods

The current study assesses two models of the peripheral auditory system, defined by Zilany *et al.* (2009), referred to here as the Carney model, and Seneff (1988), referred to here as the Seneff model. The modelled outputs were compared to responses of auditory nerve fibres to harmonic complex tones reported in two previous studies by Sinex *et al.* (2003) and (Deng *et al.*, 1987).

2.1 Equipment

MATLAB™ R2014a (Student) was used to operate the models on a PC with Microsoft Windows™ 7 running Microsoft Visual C++ 2010 Compiler.

The model coding was supplied as either C source code with MATLAB wrapper functions (Carney), or already coded as MATLAB function files (Seneff). The source files were originally retrieved from http://www.urmc.rochester.edu/labs/carney-lab/publications/auditory-models.cfm and https://engineering.purdue.edu/~malcolm/interval/1998-010/ respectively.

Additional MATLAB function files were written to call the supplied models with input parameter sets and to manage the resulting output data files.

The resulting output data files were later transferred to an Excel spreadsheet.

2.2 Procedure

A two-step procedural approach was taken. The first step was to verify that the models were functioning as the original authors described. The second step was to compare the model output with auditory nerve fibre responses recorded in previous research, specifically, from Sinex *et al.* (2003) and Deng *et al.* (1987).

2.2.1 Determination of Model Functioning

Confirmation that the supplied models being implemented as described by the original authors was achieved by replicating figures presented in both Seneff (1988) and Zilany *et al.* (2009). These comparisons used single tones and formant stimuli for the Seneff model comparison. A formant is a consolidation or 'peaks' of acoustic energy around a frequency, for example, vowels present in a speech stimuli. Single tone and amplitude modulated stimuli were used for the Carney model comparisons.

The resulting model outputs were visually compared against the original author's results. Minor coding changes were required to account for coding variations between the version of MATLAB originally used and MATLAB R2014. The models themselves were not affected by these changes. However, the rate level properties of both models were adjusted to match each other.

The models were then compared against each other using a basic rate-level curve consisting of a 1 kHz tone in 10 dB SPL increments measuring the model average spike rate output to confirm that the models produced realistic threshold results. Response variation built into the Carney model was minimised through utilising model responses averaged 50 times. This was selected through a balance of computational time and variation in the averaged responses.

A rate-level curve was generated for both of the tested models in order to confirm that the model thresholds were appropriate. In both cases, the rate curves increased between 0 and 10 dB SPL, indicating that the thresholds of the models in question are consistent with expected real world auditory thresholds (Figure 3). The rate levels of the models were adjusted in the initial modelling stage to produce similar rate levels. This was performed in order to generate model outputs that were consistent with each other.

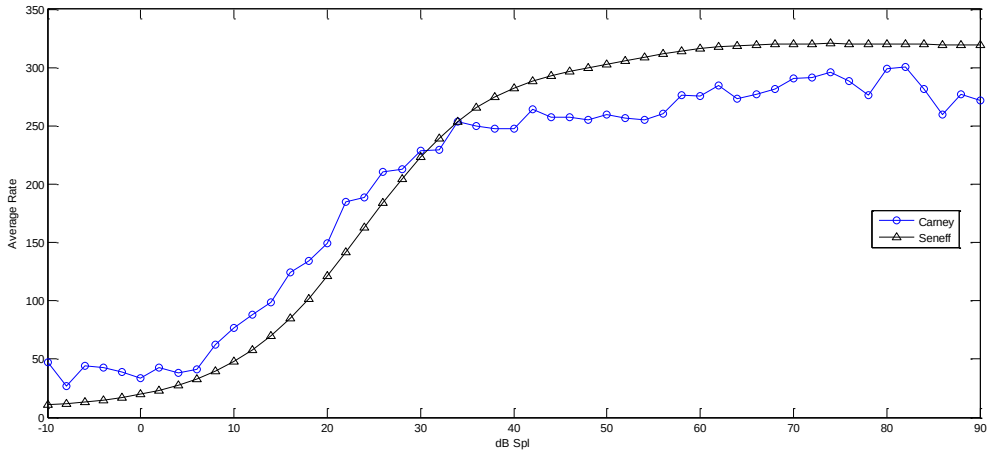

Figure 3: Rate-level comparison of the Carney and Seneff model outputs.
Generated rate-level curve outputs to a 1 kHz pure-tone from the Carney and Seneff models, demonstrating auditory thresholds, as indicated by an increase of firing rate at approximately 5-10 dB SPL

The Seneff model PSTH output was visually compared to the PSTH response to a 2 kHz tone reported in Seneff (1988) (Figure 4). The tone was generated at 70dB SPL with a duration of 80ms. The modelled response generated shows a similar response pattern overall. However, the variation showing in the initial firing rate spike at the stimulus onset is not as pronounced as expected when compared to the reported figure. Additionally, the rate of adaptation to the stimulus is slower in the generated PSTH. Due to changes made to the Seneff model rate level function, this stimulus was run at both higher and lower intensity levels (50 – 100 dB SPL) to eliminate the possibility that this was the case of the differences from the response reported in Seneff 1988. Presented in Seneff 1988 is another PSTH of the model response before the output is processed by an automatic gain control function. This output response has a greater degree of similarity to the output generated by the Seneff model response, which may suggest that this function is not operating optimally in the current model. Comparison of the generated Seneff model output and the reported model before processing of the automatic gain control is shown in figure 5. These responses were generated with the same stimulus parameters as above.

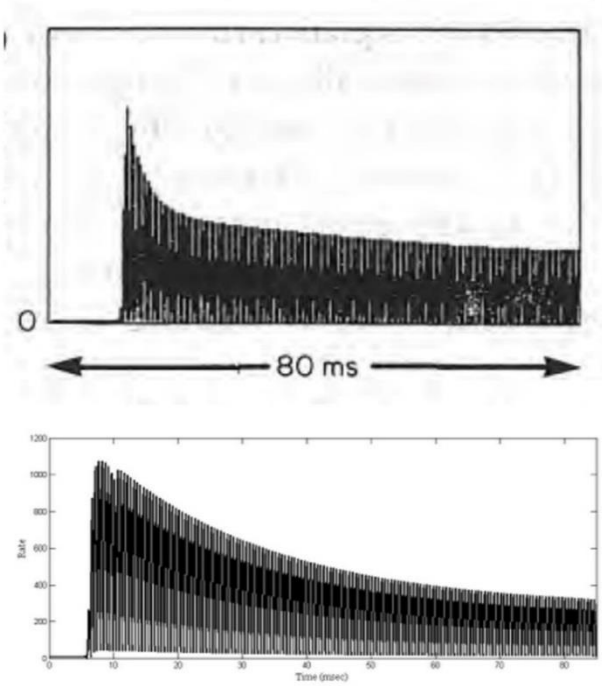

Figure 4: Comparison of Seneff model and Seneff (1988) pure-tone PSTH.
Peri-stimulus time histogram responses to a 2 kHz pure-tone presented at 70 dB SPL of a 80ms period were visually compared for similarity to determine the accuracy of the modelled response. The response presented in figure 3 of Seneff (1988) is above and the generated Seneff model response is below.

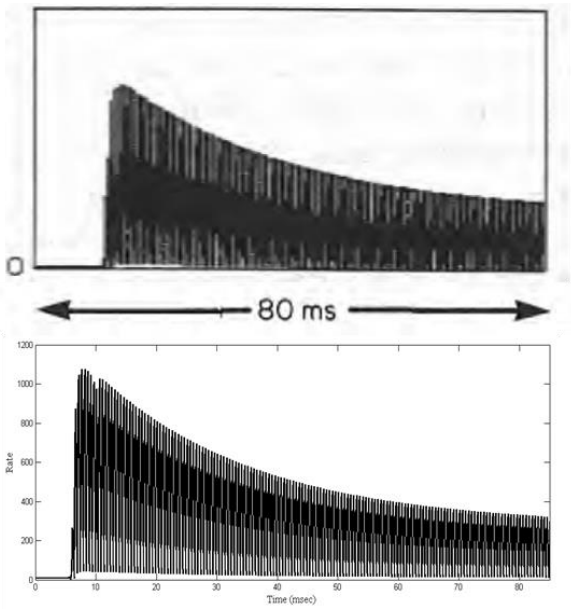

Figure 5: Comparison of pure-tone PSTH between Seneff model and Seneff (1988) without AGC.
Peri-stimulus time histogram responses to a 2 kHz pure-tone presented at 70 dB SPL of a 80ms period were visually compared for similarity to determine the accuracy of the modelled response. The response presented in figure 3 of Seneff (1988) without automatic gain control processing (AGC) is above and the generated Seneff model response is below.

Visual comparisons were made between the responses of the Seneff model and the responses presented in Seneff (1988) to formant stimuli over increasing intensity (Figure 6). The formant stimulus was a synthetic stimulus designed to mimic vowels in a speech stimulus. The formant stimulus was generated with a formant frequency of 0.8 kHz to a fibre with a characteristic frequency of 0.8 kHz. The bandwidth of the formant peak was 0.070 kHz and the fundamental frequency was 0.1 kHz. These stimulus parameters were repeated over a range of intensities.

Observations of the resulting outputs suggest that while the pattern of the generated responses is consistent with those reported in Seneff (1988), the stimulus levels between the responses sets appear mismatched. It would appear the generated histograms are more similar to the original responses generated at a lower nominal level, i.e., 62 dB SPL in the generated response appear closer to the 47 dB SPL response in the reported histogram.

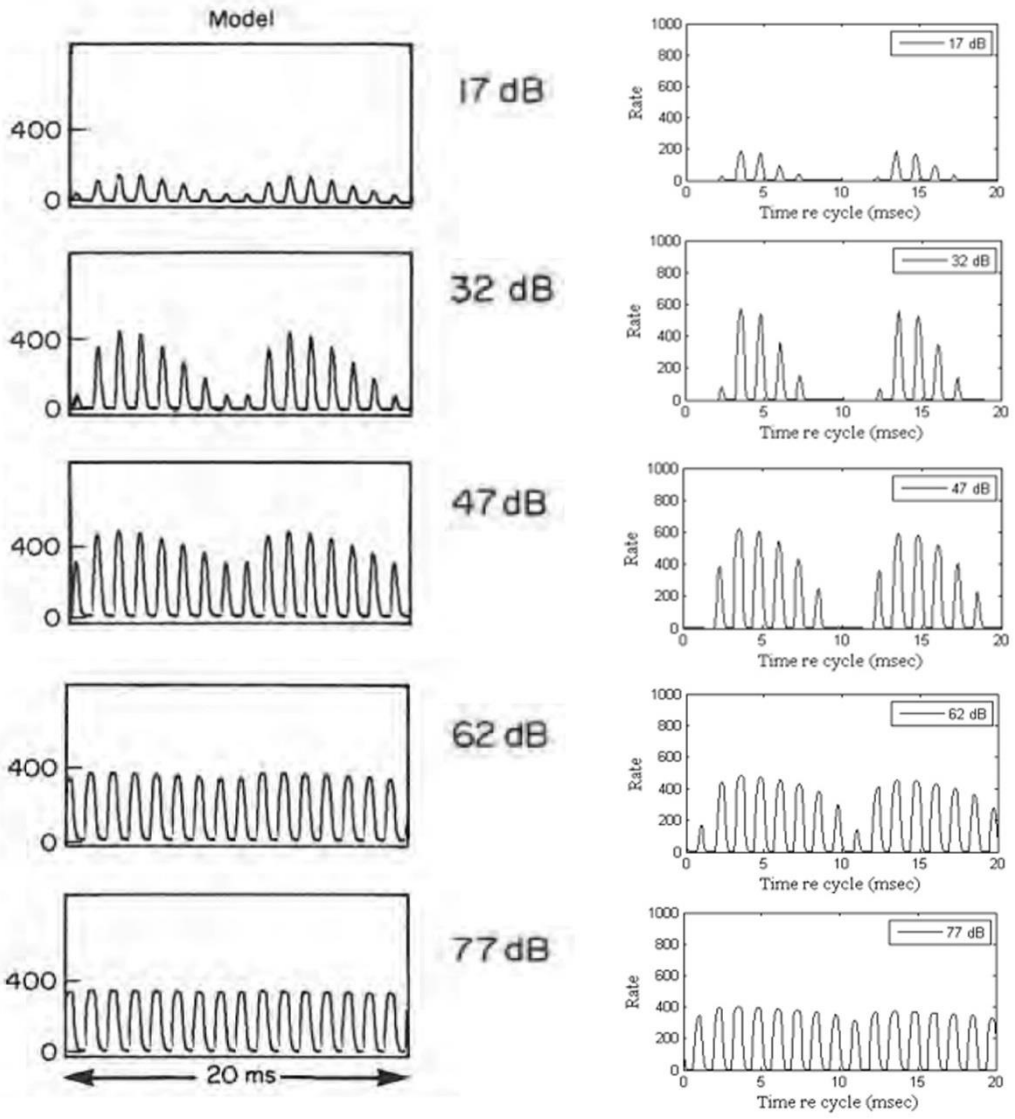

Figure 6: Comparison of Seneff model and Seneff (1988) responses to formant stimuli.
Cyclic histogram outputs of the Seneff model (right) and figure 6 in Seneff (1988) (left) over a 20ms period were visually compared to determine Seneff model output accuracy. A formant frequency of 0.8 kHz with a fundamental frequency of 0.1 kHz to a fibre with a characteristic frequency of 0.8 kHz was used. Intensities of 17, 32, 47, 62 and 77 dB SPL were used.

Response outputs using the Carney model were compared to reported outputs of single tones of 1.82 kHz at 25 dB SPL presented in Zilany *et al.* (2009) **(**Figure 7).

Random variations in the PSTH present in the reported response are not present in the generated response. Possible reasons for this may include differences in sampling rate. While the Carney model has a native sampling rate of 100 kHz, the model used was down sampled to 16 kHz to scale to the sampling rate of the Seneff model. This results in a larger bin-width for the generated PSTH, consequently smoothing out the response in the generated response as the firing is averaged over a longer time period. Rate scaling of the Carney model accounts for the asymmetry between the firing rates of the two responses. However, the overall pattern of the generated response adaptation and spontaneous rate recovery is consistent with the reported response in Zilany *et al.* (2009).

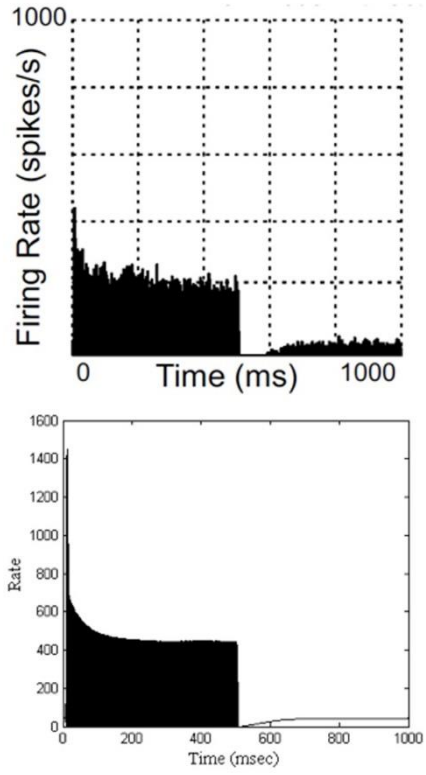

Figure 7: Comparison of PSTH outputs to a pure-tone from the Carney model and Zilany *et al.* (2009).
Peri-stimulus time histograms generated by Zilany *et al.* (2009) (top) and the Carney model (bottom) were visually compared to determine the accuracy of the Carney model outputs. A pure-tone of 1.82 kHz at 25 dB SPL over 500ms was used.

Responses generated by the Carney model were compared to amplitude modulated stimuli reported in figure 12 of (Zilany *et al.*, 2009).

Auditory nerve fibre responses were modelled to stimuli varying from 0 to 0.99 in modulation depth. A characteristic frequency of 20.2 kHz and a stimulus intensity of 32 dB SPL was used with the model and the outputs were represented in a cyclic histogram. A strong similarity between the reported responses and the generated responses can be seen (Figure 8), with the increase in modulation depth eliciting similar response pattern changes in both response sets. Random variation in the reported responses was present. This is likely due to the high sampling rate in the reported responses by Zilany *et al.* (2009) compared to the relatively slow sampling rate and wide bin-width used in the generated model outputs.

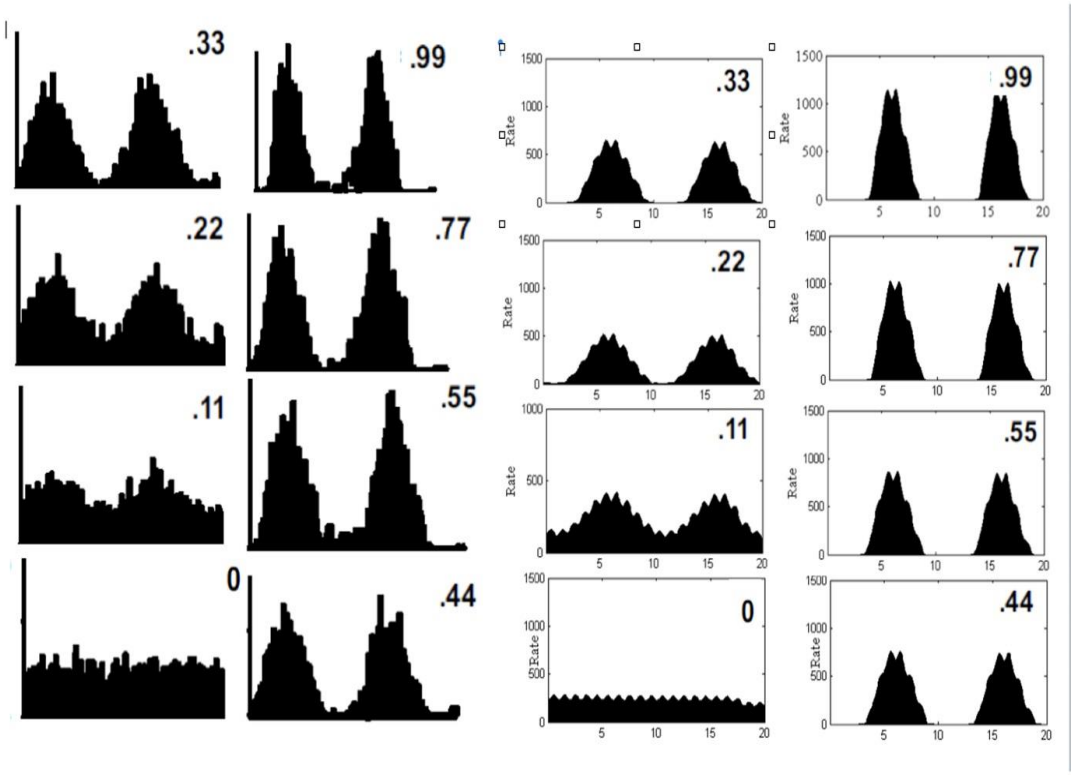

Figure 8: Comparison of Carney model and Zilany *et al.* (2009) outputs to amplitude modulated stimuli.
Visual comparisons between Carney model outputs and figure 12 in Zilany *et al.* (2009) were made to determine the accuracy of the model outputs. Cyclic histograms to a 20.2 kHz tone presented at 32 dB SPL over 20ms (two stimulus cycles) were generated, across amplitude modulation depths 0 to 0.99.

2.2.2. Comparison of Model Outputs to Sinex *et al* 2003

Carney and Seneff model response outputs were compared to auditory nerve responses to harmonic tones over increasing intensities as described in Sinex *et al.*, 2003, with the procedure outlined below.

Responses from four chinchilla auditory fibres were acquired from data produced by Sinex *et al.* (2003), with characteristic frequencies of 1.3, 1.5, 1.7 and 1.7 kHz. One of these data sets was described in Sinex *et al.* (2003) while the other three sets were summarised within a larger data set in the paper. Evidence of synchrony capture was present in each of the four response data sets.

The models were configured to produce responses to the same complex tone stimuli described in Sinex *et al.*, (2003). The stimuli were complex tones consisting of 8 equal-amplitude components added in phase. In the harmonic tone, the components were the first 8 components of 400 Hz. These stimuli were modelled at levels from 10 to 90 dB SPL in 10 dB steps. The tone duration was 300ms with a preceding 5ms silent period and a following silent period of 305ms. An example of the stimulus duration is shown by the black bar above the PSTH of Figure 10, showing the modelled response to a harmonic tone.

The responses were recorded in an analysis window implemented from 55ms to 305ms in order to avoid adaptation artefacts. PSTH of the modelled responses were generated. Bin widths of the modelled responses were 62.5μs (0.625ms) due to a 16 kHz sampling rate implemented in the Seneff model. Modelled responses from the Carney model were down-sampled to 16 kHz from a native 100 kHz for consistency.

Fast Fourier transformations (FFT) of the PSTH were performed to calculate the synchrony index of components in the generated response. Synchrony index was calculated by dividing the amplitude of each frequency in the FFT by the total response. The resulting model response output was displayed as a plot of the PSTH with an accompanying lower plot with the generated FFT showing the response synchrony of the modelled fibre to each frequency component in the response (Figure 10).

The modelled response to a puretone of 2.4 kHz at 60 dB SPL is shown (Figure 9). The top plot is the PSTH of the response output. With this, the average firing rate of the modelled neurone can be seen

over time. As for all of the modelled responses presented, the bin width in which the average firing rate is calculated is 62.5μs. The lower plot shows the FFT of the PSTH response. As the stimulus for this response is a pure-tone (i.e. only one component), a single frequency component can be seen.

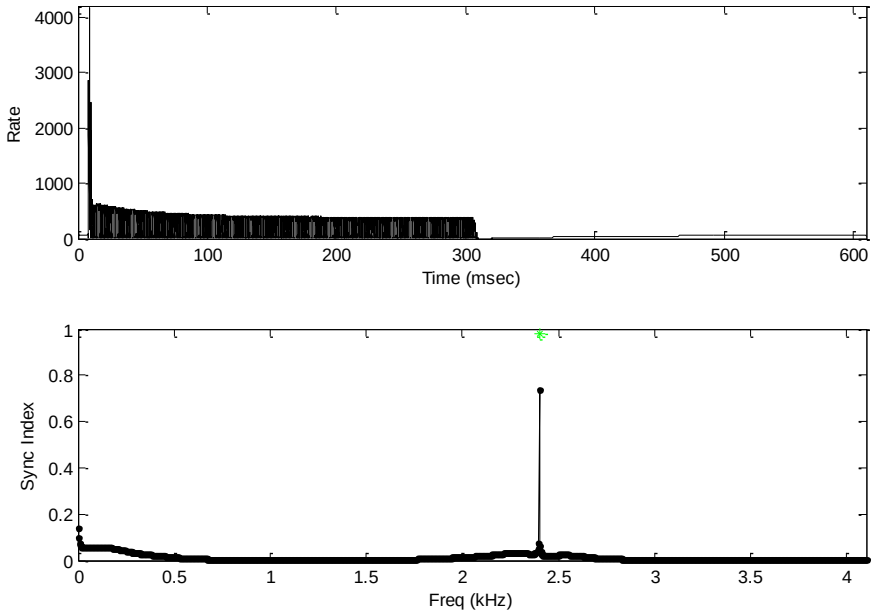

Figure 9: Response PSTH and FFT of a pure-tone generated by the Carney model
Response output to a 2.4 kHz pure-tone presented at 60 dB SPL to a modelled fibre with a characteristic frequency of 2.4 kHz. The modelled peri-stimulus time histogram is displayed above and the Fast Fourier Transformation generated frequency component response synchrony is displayed below.

Demonstration of synchrony index responses to harmonic tones is shown in Figure 10. Responses were modelled to a harmonic tone consisting of 8 components of 400 Hz presented at 60dB SPL. The characteristic frequency of the modelled fibre was 2.4 kHz. As more components are present in the stimulus, the FFT of the PSTH indicates the response activity of the fibre to each frequency component, the 'synchrony' to that response component.

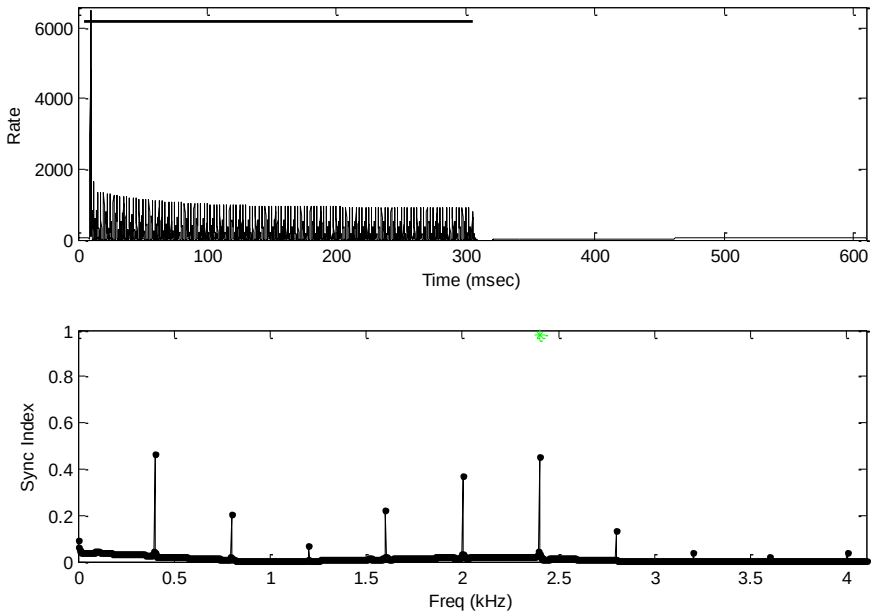

Figure 10: Response PSTH and FFT of a harmonic tone generated by the Carney model
Response output to a 2.4 kHz pure-tone presented at 60 dB SPL to a modelled fibre with a characteristic frequency of 2.4 kHz. The modelled peri-stimulus time histogram is displayed above and the Fast Fourier Transformation generated frequency component response synchrony is displayed below, demonstrating the response sycnhrony to various frequency components in the response output.

The resulting data sets consisted of frequency components calculated from the FFT of the PSTH and their corresponding synchrony indexes. For each input intensity level, a list of frequency components was generated, and sorted in descending order of amplitude. The frequencies that produced the 10 largest response amplitudes were selected and saved in spreadsheets for further analysis.

Characteristic frequencies were chosen based on the characteristic frequencies of fibres used by Sinex *et al.*, 2003. These frequencies were 1.3, 1.5, 1.7 and 1.7 kHz. The characteristic frequencies used by the Seneff model were 1.350 kHz, 1.476 kHz and 1.712 kHz respectively. This variation is present as the Auditory Toolbox version of the Seneff model has a bank of predetermined CFs; this model utilised the nearest frequencies to those used by Sinex *et al.*, 2003.

The modelled response data sets were graphed, with each frequency component that occurred after the first selection stage being plotted as a function of synchrony index over the intensity range, allowing a graphical representation of the relative synchronies of all significant components as a function of

increasing intensity. The resulting plots of synchrony over intensity were referred to as component curves.

A final round of selection was added to eliminate any component curves that did not reach a threshold value of 0.1 Synchrony index over the range of SPL intensities modelled. The minimum threshold level was identified by visual inspection of the plotted figures. Most of the plots had a number of results that never exceeded the 0.1 value and these components were essentially consistently low level and did not contribute to the useful results. Trials of other threshold levels were run to confirm that frequency components present in the experimental data were not excluded erroneously.

This process was repeated for both models over a range of different characteristic frequencies beyond those presented in the experimental recordings. This was performed in order to determine whether the models were consistent in their outputs over a wide frequency range, and to show that the modelling of synchrony capture was not limited to a select few frequencies. Examples of these outputs showing the model responses against increasing intensity are provided (Appendix A).

Visual comparisons of the modelled responses and the recorded responses provided by Sinex *et al.* (2003) were made. The measured data sets are shown below in figures 11- 14 below.

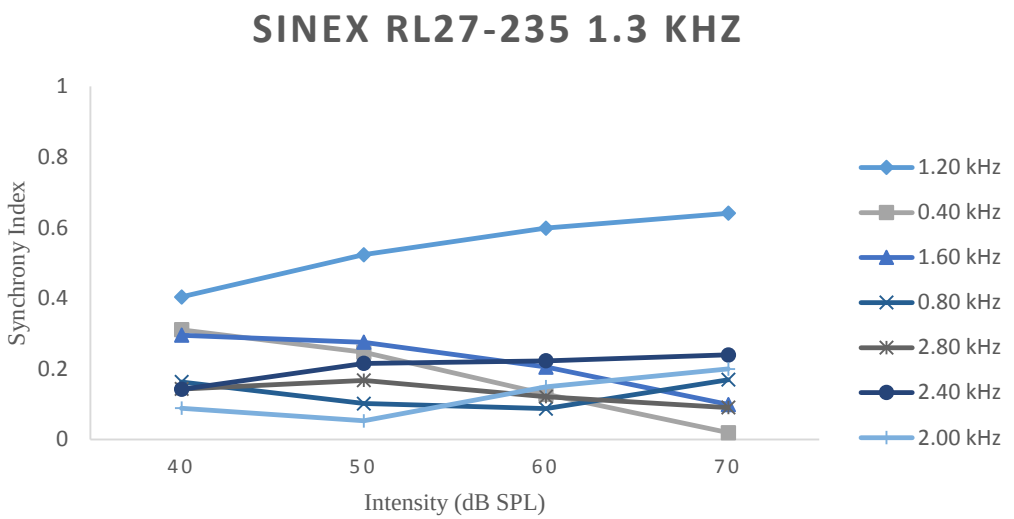

Figure 11: Responses to harmonic tones recorded by Sinex *et al.* (2003) in a 1.3 kHz characteristic frequency nerve fibre. Auditory nerve fibre response synchronies to various frequency components in a fibre with a characteristic frequency of 1.3 kHz at each tested intensity are displayed. The stimulus used was an 8 component harmonic tone with a fundamental frequency of 400Hz.

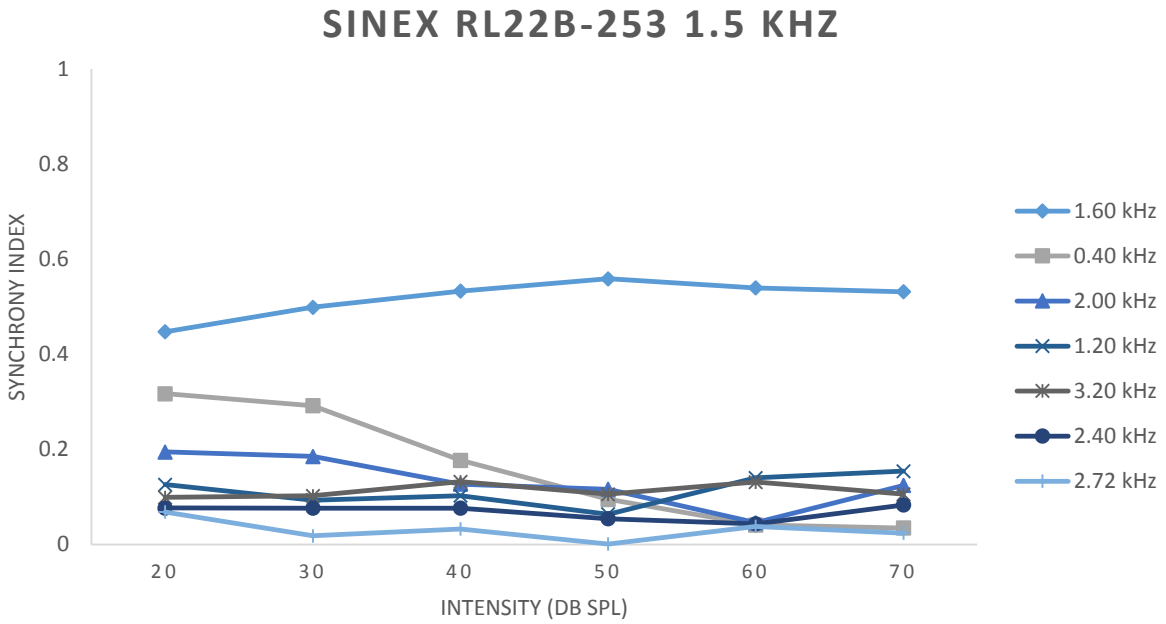

Figure 12: Responses to harmonic tones recorded by Sinex *et al.* (2003) in a 1.5 kHz characteristic frequency nerve fibre. Auditory nerve fibre response synchronies to various frequency components in a fibre with a characteristic frequency of 1.5 kHz at each tested intensity are displayed. The stimulus used was an 8 component harmonic tone with a fundamental frequency of 400Hz.

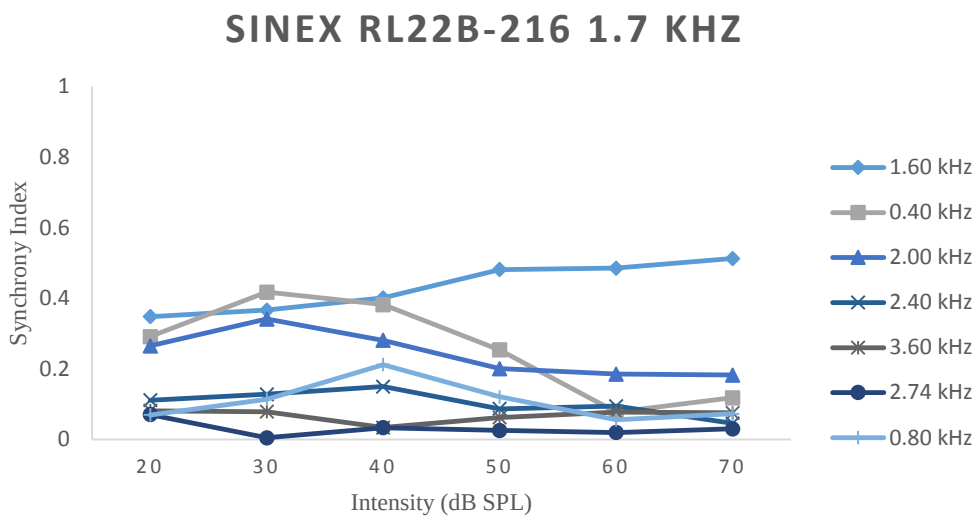

Figure 13: Responses to harmonic tones recorded by Sinex *et al.* (2003) in a 1.7 kHz characteristic frequency nerve fibre.
Auditory nerve fibre response synchronies to various frequency components in a fibre with a characteristic frequency of 1.7 kHz at each tested intensity are displayed. The stimulus used was an 8 component harmonic tone with a fundamental frequency of 400Hz.

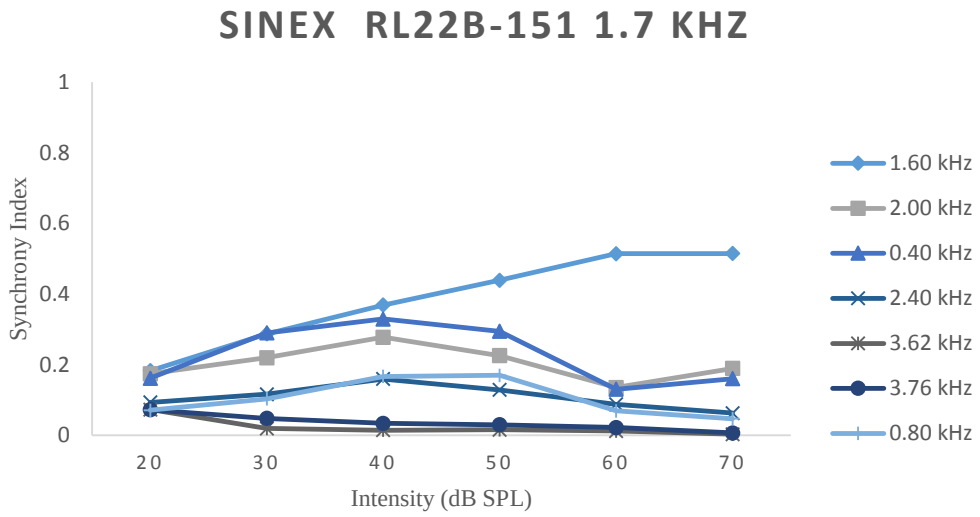

Figure 14: Responses to harmonic tones recorded by Sinex *et al.* (2003) in a second 1.7 kHz characteristic frequency nerve fibre.
Auditory nerve fibre response synchronies to various frequency components in a fibre with a characteristic frequency of 1.7 kHz at each tested intensity are displayed. The stimulus used was an 8 component harmonic tone with a fundamental frequency of 400Hz.

Finally, the plotted curves for each component frequency over increasing intensity were individually compared to the measured component curves over intensity produced by Sinex *et al.* (2003). This was performed to provide a rudimentary comparison of the modelled frequency component patterns over increasing intensity to the measured frequency component patterns over increasing intensity provided by Sinex *et al.*, 2003.

The overall modelling procedure is shown below (Figure 15).

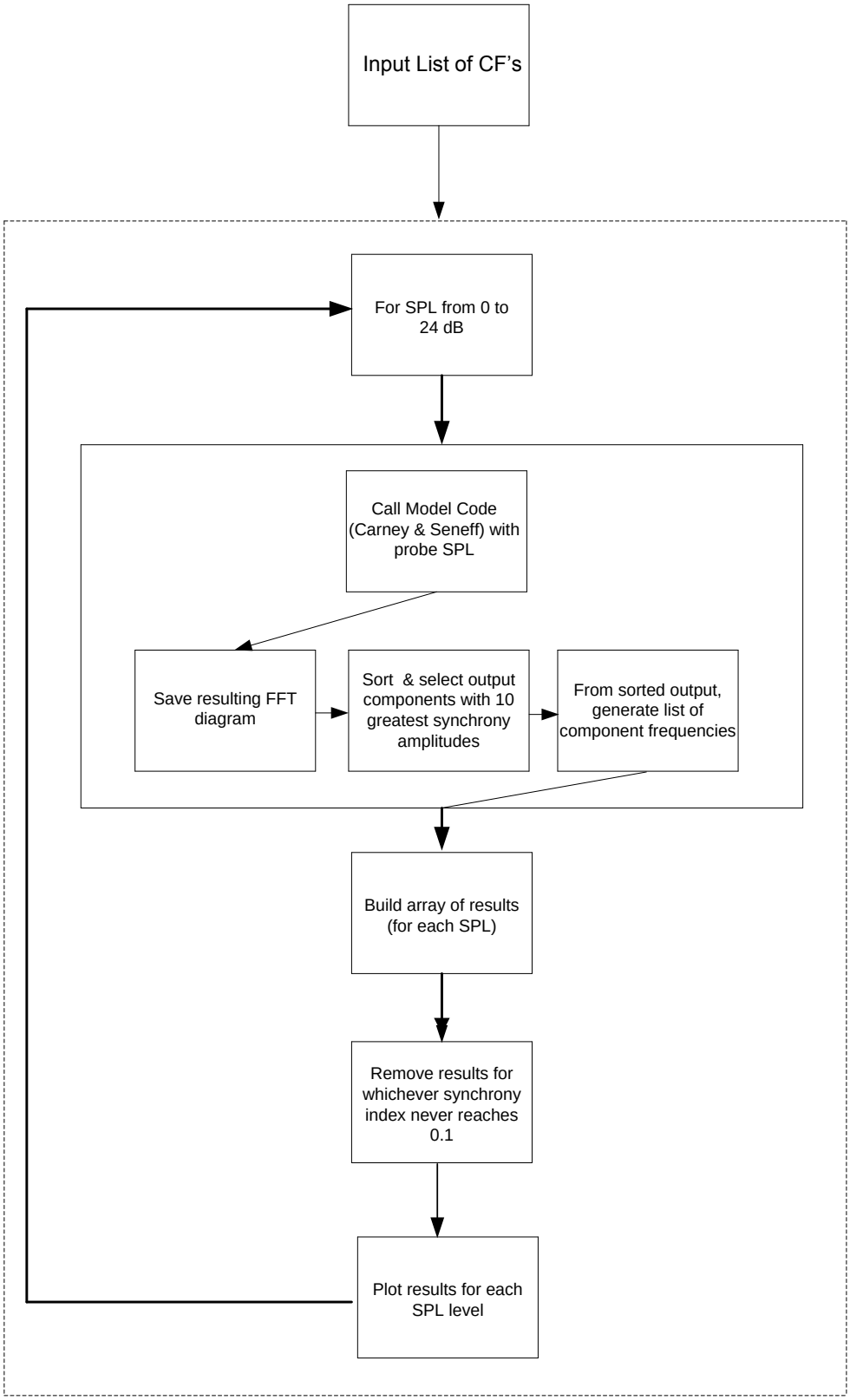

Figure 15: Procedural map of running the Carney and Seneff models to generate outputs for comparison to auditory nerve fibre responses measured by Sinex *et al* (2003).

2.2.3 Comparison of Model Outputs to Deng & Geisler 1987

Responses using stimulus parameters described in Deng *et al.* (1987) were modelled.

Auditory nerve responses of adult cats to harmonic tones exhibiting synchrony capture in which a single harmonic component was manipulated were presented by Deng *et al.* (1987).

The harmonic complex tone stimuli were generated with parameters used in Deng *et al.* (1987), utilising a harmonic tone with f_0 of 125Hz, 60 components a characteristic frequency of 2.625 kHz and a stimulus phase of 0°. The stimulus was presented at 70dB SPL, with selected individual harmonic components being presented in 3dB steps from 0 – 30dB relative to the main stimulus level. The exception to this was the 21st harmonic, which was increased in 2 dB steps, and the 24th harmonic where the relative intensity was from 0 – 24dB SPL, as per Deng & Geisler 1987. The stimulus had a tone duration of 200ms with 10msec and 100msec silence periods before and after the tone presentation respectively. An analysis window from 100ms to 250ms was implemented.

The fundamental frequency used by Deng *et al.* (1987) was 122.07 Hz. For the modelled responses, a fundamental frequency of 125 Hz was utilised. This was necessitated due to the sampling rate employed by the models, in which the use of 122.07 Hz would present an erroneous PSTH as components fell in-between sampling bins. Similarly, a characteristic frequency of 2.625 was used rather than the estimated 2.6 kHz described in Deng *et al.* (1987) due to imprecise recording of responses due to the model sampling rates.

The models were run largely as described previously. The most significant difference was that instead of ordering and selecting out the smaller components that had been produced by the model, this investigation required the plotting of three select components, to allow comparison to responses measured by Deng *et al.* (1987).

To accomplish this, the closest frequency components to the characteristic frequency (CF), the fundamental frequency (f_0) and the probe frequency (nth harmonic of f_0), along with their respective

synchronies were identified and extracted. The models were run for each of the intensities of the manipulated component and the respective synchronies recorded.

The three components were then plotted as a function of synchrony index against change in stimulus level (of the probe harmonic).

This process was repeated for each of the frequency components produced by Deng *et al* (1987); via 0.854 kHz, 1.465 kHz, 2.075 kHz, 2.197 kHz, 2.563 kHz and 2.930 kHz. These frequencies correspond to the harmonic components of a 122.07 Hz fundamental complex tone numbering 7, 12, 17, 18, 21, and 24 respectfully. Due to the changes in fundamental frequency required by the sampling rate of the models, there was slight variation in the frequency components used by the models. However, the same number harmonic component was used in the modelling stimulus.

The compound outputs were then visually assessed in comparison to the exhibited synchrony capture presented by Deng *et al.* (1987). The recorded responses to which the modelled responses were compared to are shown below in figures 16 to 21.

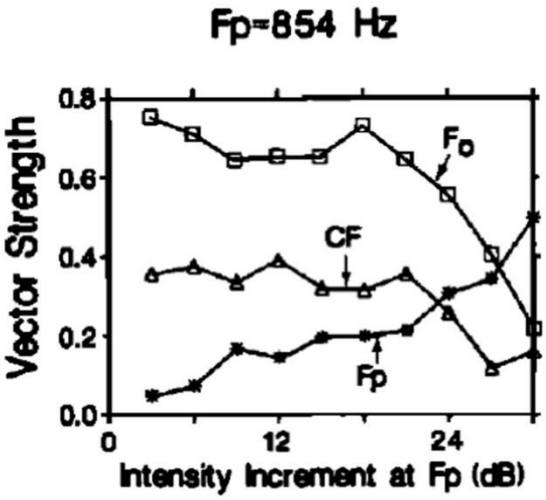

Figure 16: Recorded responses to harmonic tones with an intensity manipulated (7^{th}) harmonic component as presented in figure 3 of Deng *et al.* (1987).
Measured auditory nerve responses to a harmonic tone with a fundamental frequency of 0.12207 kHz presented at 70 dB SPL in a fibre with a characteristic frequency of 2.6 kHz. Response synchronises to the probe component (Fp), the fundamental frequency harmonic component (F_0) and the characteristic frequency component (CF) are displayed over increasing intensities of the manipulated component, where the probe component is the 7^{th} harmonic.

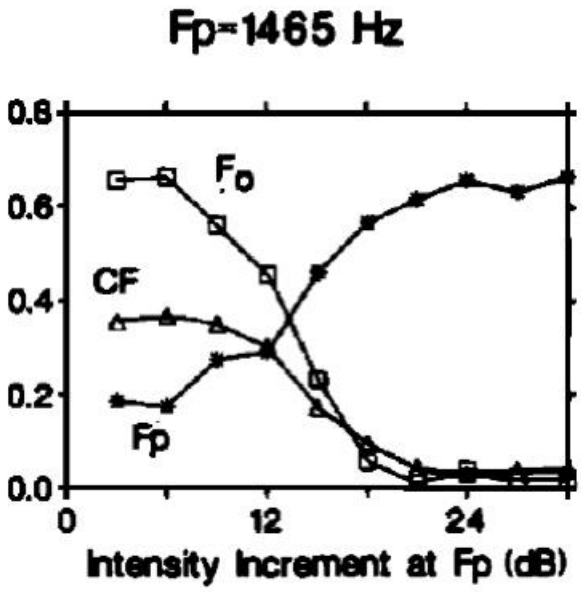

Figure 17: Recorded responses to harmonic tones with an intensity manipulated (12th) harmonic component as presented in figure 3 of Deng *et al.* (1987).
Measured auditory nerve responses to a harmonic tone with a fundamental frequency of 0.12207 kHz presented at 70 dB SPL in a fibre with a characteristic frequency of 2.6 kHz. Response synchronises to the probe component (Fp), the fundamental frequency harmonic component (F_0) and the characteristic frequency component (CF) are displayed over increasing intensities of the manipulated component, where the probe component is the 12th harmonic.

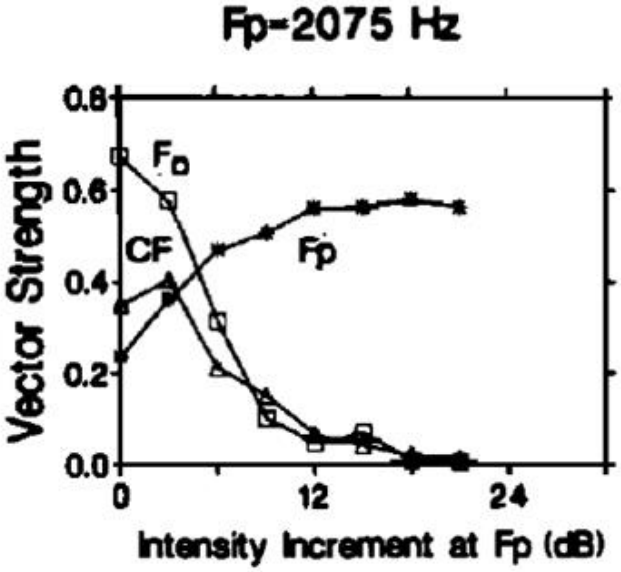

Figure 18: Recorded responses to harmonic tones with an intensity manipulated (17th) harmonic component as presented in figure 3 of Deng *et al.* (1987).
Measured auditory nerve responses to a harmonic tone with a fundamental frequency of 0.12207 kHz presented at 70 dB SPL in a fibre with a characteristic frequency of 2.6 kHz. Response synchronises to the probe component (Fp), the fundamental frequency harmonic component (F_0) and the characteristic frequency component (CF) are displayed over increasing intensities of the manipulated component, where the probe component is the 17th harmonic.

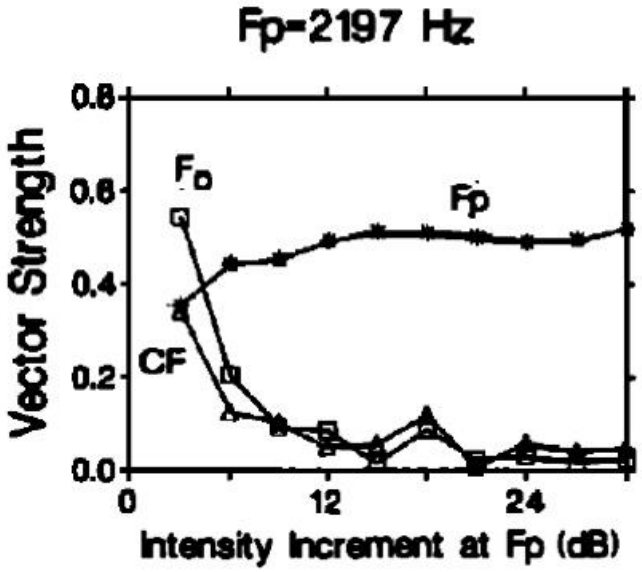

Figure 19: Recorded responses to harmonic tones with an intensity manipulated (18th) harmonic component as presented in figure 3 of Deng *et al.* (1987).
Measured auditory nerve responses to a harmonic tone with a fundamental frequency of 0.12207 kHz presented at 70 dB SPL in a fibre with a characteristic frequency of 2.6 kHz. Response synchronises to the probe component (Fp), the fundamental frequency harmonic component (F_0) and the characteristic frequency component (CF) are displayed over increasing intensities of the manipulated component, where the probe component is the 18th harmonic.

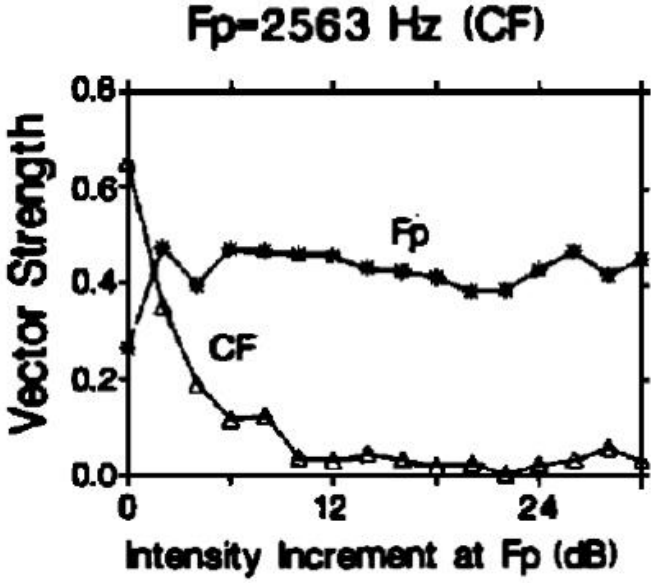

Figure 20: Recorded responses to harmonic tones with an intensity manipulated (21st) harmonic component as presented in figure 3 of Deng *et al.* (1987).
Measured auditory nerve responses to a harmonic tone with a fundamental frequency of 0.12207 kHz presented at 70 dB SPL in a fibre with a characteristic frequency of 2.6 kHz. Response synchronises to the probe component (Fp), the fundamental frequency harmonic component (F_0) and the characteristic frequency component (CF) are displayed over increasing intensities of the manipulated component, where the probe component is the 21st harmonic.

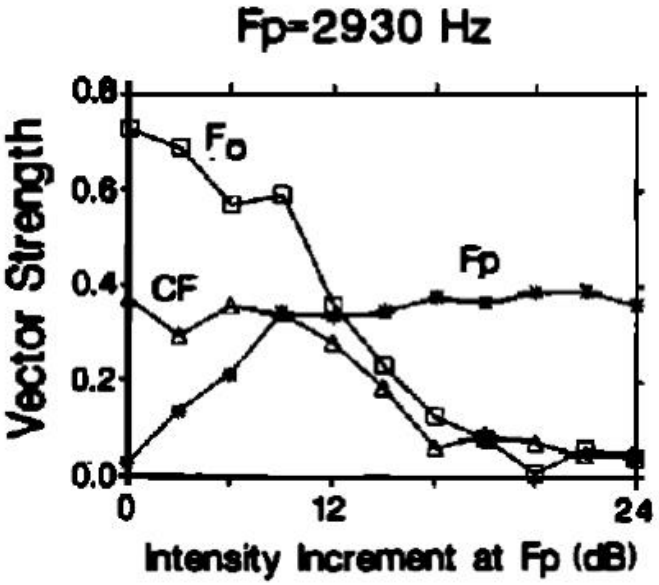

Figure 21: Recorded responses to harmonic tones with an intensity manipulated (24th) harmonic component as presented in figure 3 of Deng *et al.* (1987).
Measured auditory nerve responses to a harmonic tone with a fundamental frequency of 0.12207 kHz presented at 70 dB SPL in a fibre with a characteristic frequency of 2.6 kHz. Response synchronises to the probe component (Fp), the fundamental frequency harmonic component (F_0) and the characteristic frequency component (CF) are displayed over increasing intensities of the manipulated component, where the probe component is the 24th harmonic.

The overall modelling procedure for this is shown below (Figure 22).

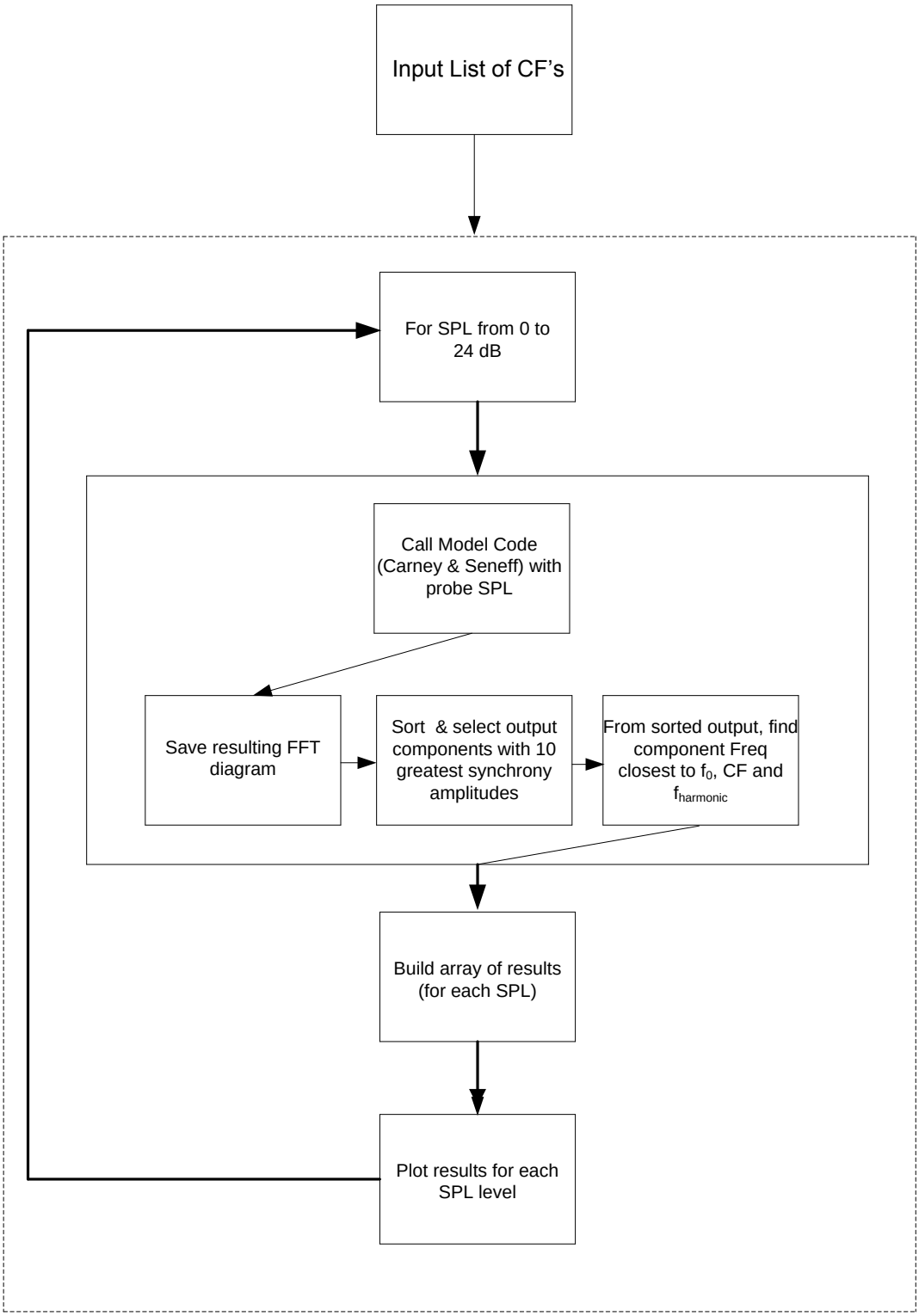

Figure 22: Procedural map of running the Carney and Seneff models to generate outputs for comparison to auditory nerve fibre responses measured by Deng *et al.* (1987).

Results

3.1 Comparison of Sinex *et al* 2003 Dataset

The generated model outputs were plotted against increasing stimulus intensity.

Model outputs were plotted against increasing stimulus intensity to enable identification of synchrony capture (and suppression of non-dominant components). The modelled responses utilised characteristic frequencies of 1.3, 1.5 and 1.7 kHz. A harmonic tone using a fundamental frequency of 400Hz was used. These plots were then visually compared to plots of the same design produced by the experimental results.

Modelled responses from the Carney outputs show the 1.20 kHz frequency component being dominant in the 1.3 kHz characteristic frequency fibre. However, clear synchrony capture is not apparent (Figure 23). A reduction in the synchrony to this component occurred for intensities above 60 dB SPL with a complementary increase in synchrony to lower frequency components (0.40 and 0.80 kHz) occurring. At the highest modelled intensity (90 dB SPL), synchrony to the 1.20 kHz component drops below that of these lower frequency components.

The Seneff model output for a fibre with a characteristic frequency of 1.3 kHz shows a clear synchrony capture effect by the 1.20 kHz component, with increasing synchrony apparent at approximately 40 dB SPL (Figure 24). The second large component that can be seen is the second closest frequency component to the characteristic frequency of the fibre (1.60 kHz). Evidence of suppression of this component can be seen in the reduction of synchrony, concurrently occurring with the increase in fibre synchrony in the 1.20 kHz components. An increase in synchrony can also be observed in the 0.80 kHz component, arising from approximately 30 dB SPL.

Visual comparison to auditory nerve responses in a fibre with an estimated characteristic frequency of 1.3 kHz as produced by Sinex *et al.* (2003) (Figure 11) suggests that the Seneff model demonstrates expected fibre responses, showing a dominant component near the characteristic frequency with limited

response synchrony to the other frequency components present. The Carney model outputs for a characteristic frequency fibre of 1.3 kHz exhibits the dominant component near the characteristic frequency for the low to moderate intensities but, unlike in the measured responses, synchrony to this component steadily declines over the intensity range.

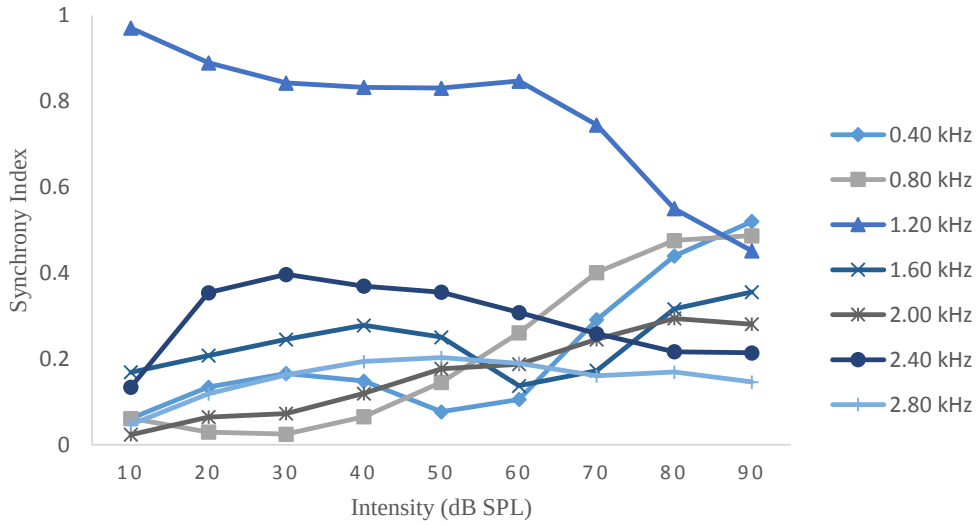

Figure 23: Carney model outputs of the response synchronies produced by a 1.3 kHz characteristic frequency fibre to harmonic tones over increasing intensity
Pattern of modelled response synchrony to individual harmonic components against increasing intensity to a 1.3 kHz auditory fibre to an 8 component harmonic tone with a fundamental frequency of 0.400 kHz.

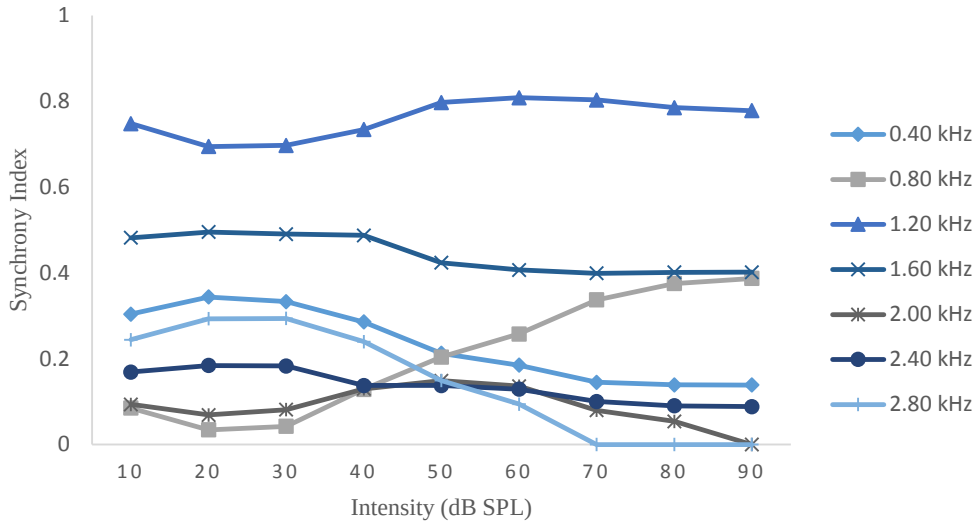

Figure 24: Seneff model outputs of the response synchronies produced by a 1.3 kHz characteristic frequency fibre to harmonic tones over increasing intensity
Pattern of modelled response synchrony to individual harmonic components against increasing intensity to a 1.3 kHz auditory fibre to an 8 component harmonic tone with a fundamental frequency of 0.400 kHz.

Response outputs for the Carney model at a fibre characteristic frequency of 1.5 kHz show a similar pattern to those observed in Carney model responses for the 1.3 kHz fibre (Figure 25). A dominant component with a frequency close to the characteristic frequency of the fibre is seen (1.60 kHz), showing a reduction in response synchrony above 60 dB SPL. Again, response synchrony to lower harmonic components of 0.40 and 0.80 kHz increases simultaneously with the decline in the 1.6004 kHz component, with the 0.80 kHz component becoming dominant at 90 dB SPL.

The Seneff model responses to a 1.5 kHz characteristic frequency fibre shows strong synchrony capture (Figure 26). Response synchrony is greatest to the 1.6004 kHz component, increasing further at 30 dB SPL with a concurrent reduction in all other modelled harmonic components.

Visual comparison to the measured outputs of an auditory nerve fibre with an estimated characteristic frequency of 1.5 kHz (Figure 12) again suggests that the Seneff model gives accurate representations of auditory fibre responses with a strong dominant component close to the characteristic frequency supressing the response synchrony to the other frequency components. Conversely, the Carney model again shows a dominant component close to the characteristic frequency. However, the decline in synchrony is not as pronounced within the measured intensity range as is seen with the 1.3 kHz modelled outputs.

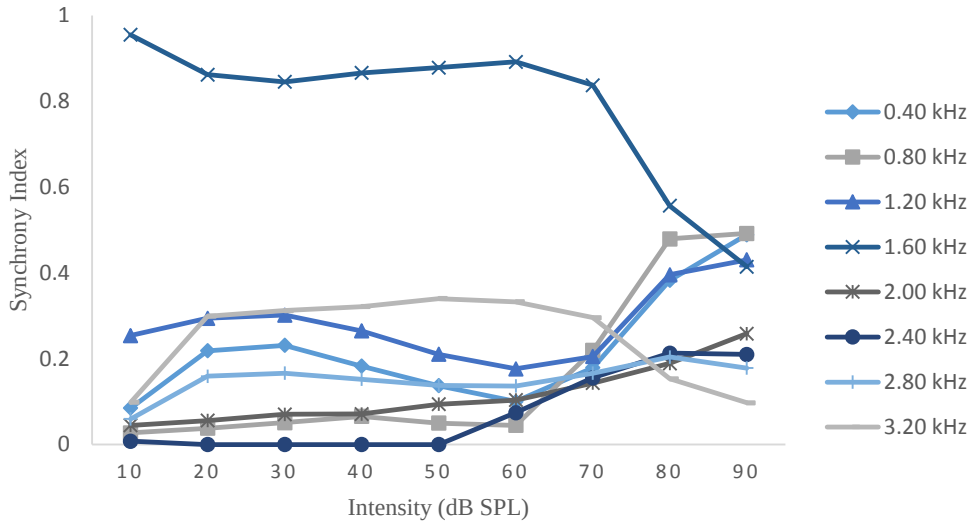

Figure 25: Carney model outputs of the response synchronies produced by a 1.5 kHz characteristic frequency fibre to harmonic tones over increasing intensity
Pattern of modelled response synchrony to individual harmonic components against increasing intensity to a 1.5 kHz auditory fibre to an 8 component harmonic tone with a fundamental frequency of 0.400 kHz.

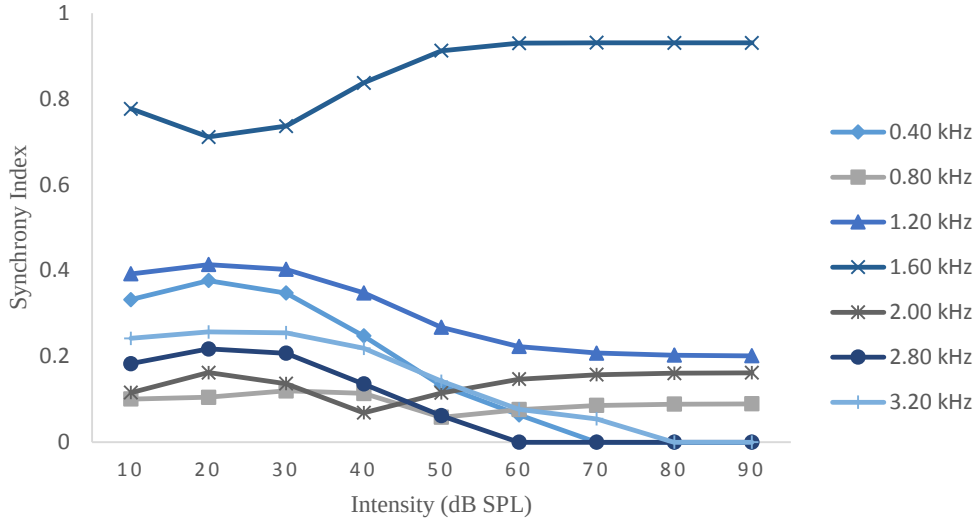

Figure 26: Seneff model outputs of the response synchronies produced by a 1.5 kHz characteristic frequency fibre to harmonic tones over increasing intensity
Pattern of modelled response synchrony to individual harmonic components against increasing intensity to a 1.5 kHz auditory fibre to an 8 component harmonic tone with a fundamental frequency of 0.400 kHz.

Finally, the Carney response outputs for an auditory fibre with a characteristic frequency of 1.7 kHz indicates a dominant component (1.6004 kHz) close to the characteristic frequency of the fibre showing a reduction in response synchrony at intensities above 60 dB SPL (Figure 27). Lower harmonic

components show an increase in response synchrony at moderate intensities, with the fundamental frequency of the stimulus becoming dominant at the highest modelled intensity of 90 dB SPL.

Seneff model responses for a fibre with a characteristic frequency of 1.7 kHz show clear synchrony capture (Figure 28). A dominant component of 1.6004 kHz increases in response synchrony concurrent to reductions in synchrony of the next largest harmonics, 2.00 kHz and the fundamental frequency of 0.40 kHz.

Visual comparisons between the modelled responses and the measured 1.7 kHz auditory nerve responses produced by Sinex *et al.* (2003) follow a similar pattern as in the 1.3 kHz and 1.5 kHz comparisons above. Two measured responses were obtained for comparison, with the second response output showing a high level of synchrony fundamental frequency component at low intensity levels with the component closest to the characteristic frequency becoming dominant at higher intensities (Figure 13). The first response output follows a similar component pattern to those seen in the 1.3 and 1.5 kHz response outputs (Figure 14).

The Carney output does not appear to show much similarity to the measured responses, with the synchrony to the closest component to the characteristic frequency dominating the response with a slow decline at the higher intensities with no significant synchrony to any other modelled components.

The Seneff model output shows a similar response pattern to the measured responses, with the fundamental and two closest components to the characteristic frequency of the fibre showing the highest levels of response synchrony in the lower intensities. As the intensity increases further, the closest component to the characteristic frequency of these two increases in fibre synchrony to the detriment of synchrony to the other frequency components.

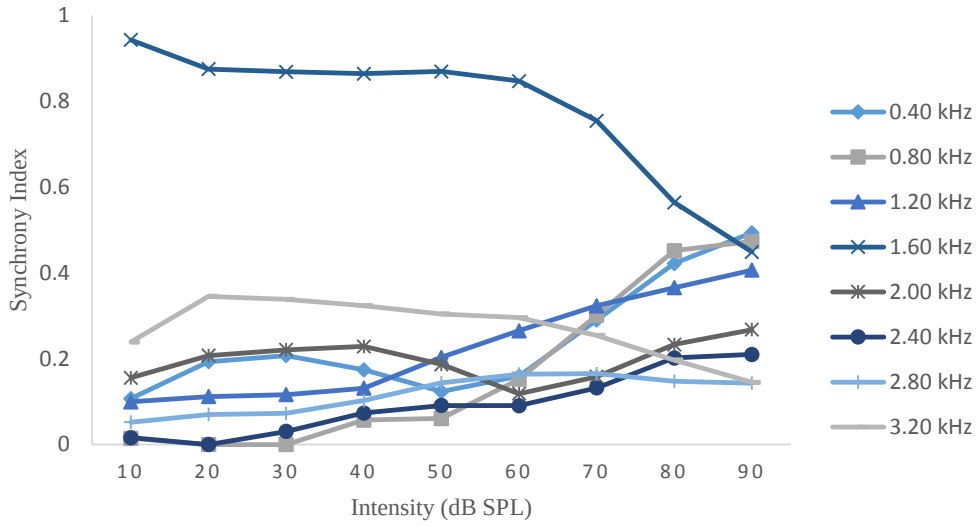

Figure 27: Carney model outputs of the response synchronies produced by a 1.7 kHz characteristic frequency fibre to harmonic tones over increasing intensity
Pattern of modelled response synchrony to individual harmonic components against increasing intensity to a 1.7 kHz auditory fibre to an 8 component harmonic tone with a fundamental frequency of 0.400 kHz.

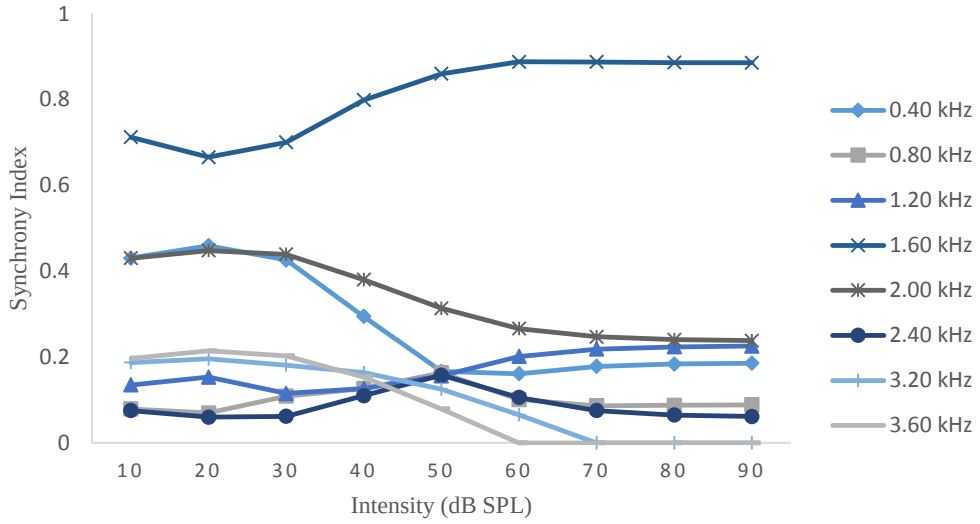

Figure 28: Carney model outputs of the response synchronies produced by a 1.7 kHz characteristic frequency fibre to harmonic tones over increasing intensity
Pattern of modelled response synchrony to individual harmonic components against increasing intensity to a 1.7 kHz auditory fibre to an 8 component harmonic tone with a fundamental frequency of 0.400 kHz.

Overall, the pattern and relationships between the frequency components modelled in the Seneff model show strong agreement with the experimental data. This is exemplified in the dominant frequency component being closest in frequency to the characteristic frequency of the fibre and suppressing the remaining frequencies, even at higher intensities.

Consistently, the next largest components in the Seneff outputs are the second closest harmonic to the characteristic frequency and the component with the same periodicity as the fundamental frequency of the stimulus. This fundamental frequency component is possibly a rectifier distortion product. This trend is not observed in the Carney model outputs, with no significant response synchrony to the other modelled components being prevalent in the outputs.

Correlations between the modelled component curves and the measured response components curves produced by Sinex *et al.* (2003) were measured (*tables 1-4*). Correlations were only calculated within intensity levels measured by Sinex *et al.* (2003) for a more accurate representation between the component curves. However, it should be recognised that adjustments made to the rate level functions of both models limit the overall accuracy of the labelled intensities generated by the models.

The use of individual correlations of the curves is not a particularly robust analysis of the overall phenomena of synchrony capture, only allowing comparison of the behaviour of individual components to similar frequency components in other measurements. The relationships between the harmonic synchronicity is unable to be quantified in this measure.

Table 1: Correlations of harmonic component response synchrony patterns to Sinex *et al.* (2003) in a fibre with a CF of 1.7 kHz.
Correlation (r) of measured frequency components and closest modelled frequency components of auditory nerve responses in a fibre with a characteristic frequency of 1.7 kHz. Measured frequency component curves were provided by Sinex *et al.* (2003). NA has been used where the modelled output did not generate a near match for the measured frequency component.

Component freq. (kHz)	**1.60**	**2.00**	**0.40**	**2.40**	**0.80**	**3.62**
Carney (r)	-0.67	0.82	-0.30	-0.29	-0.50	NA
Seneff (r)	0.98	0.34	0.16	0.47	0.87	0.67

Table 2: Correlations of harmonic component response synchrony patterns to Sinex *et al.* (2003) in a fibre with a CF of 1.7 kHz.
Correlation (r) of measured frequency components and closest modelled frequency components of auditory nerve responses in a second fibre with a characteristic frequency of 1.7 kHz. Measured frequency component curves were provided by Sinex *et al.* (2003). NA has been used where the modelled output did not generate a near match for the measured frequency component.

Component freq. (kHz)	**1.60**	**0.40**	**2.00**	**2.40**	**0.80**	**3.62**
Carney (r)	-0.71	-0.17	0.84	-0.69	-0.35	-0.65
Seneff (r)	0.97	0.73	0.89	-0.06	0.56	-0.09

Table 3: Correlations of harmonic component response synchrony patterns to Sinex *et al.* (2003) in a fibre with a CF of 1.5 kHz.
Correlation (r) of measured frequency components and closest modelled frequency components of auditory nerve responses in a fibre with a characteristic frequency of 1.5 kHz. Measured frequency component curves were provided by Sinex *et al.* (2003). NA has been used where the modelled output did not generate a near match for the measured frequency component.

Component freq. (kHz)	**1.60**	**0.40**	**2.00**	**1.20**	**3.20**	**2.40**	**2.72**
Carney (r)	0.78	0.87	-0.34	-0.32	0.56	0.084	0.051
Seneff (r)	0.87	0.99	0.13	-0.36	-0.27	NA	0.38

Table 4: Correlations of harmonic component response synchrony patterns to Sinex *et al.* (2003) in a fibre with a CF of 1.3 kHz.
Correlation (r) of measured frequency components and closest modelled frequency components of auditory nerve responses in a fibre with a characteristic frequency of 1.3 kHz. Measured frequency component curves were provided by Sinex *et al.* (2003). NA has been used where the modelled output did not generate a near match for the measured frequency component.

Component freq. (kHz)	**1.20**	**0.40**	**1.60**	**0.80**	**2.80**	**2.40**	**2.00**
Carney (r)	-0.53	-0.69	0.71	0.12	0.95	-0.81	0.75
Seneff (r)	0.92	0.95	0.76	0.04	0.77	-0.63	-0.85

3.2 Comparison of Deng & Geisler 1987 Dataset

The model outputs emulating the synchrony capture exhibited in Deng *et al.* (1987) were plotted and visually inspected.

Manipulation of the 7th harmonic component (0.87 kHz) produced similar response patterns in both the Carney and Seneff models (Figures 29 and 30**)**. The component closest to the fundamental frequency of the stimulus dominates the response synchrony over the intensity range modelled. In the higher probe component intensities, there is a switch between the characteristic frequency and probe components exhibited in the Carney model, with the probe component seeing a decrease in synchrony index; this being the opposite to the pattern shown in Deng & Geisler (1987). The Seneff model amplitudes stay relatively constant over increasing intensity. However, as with the Carney model, there is no increase in the probe synchrony index coupled with the decrease in fundamental component synchrony index.

Both of the models generated responses that were dissimilar to the measured responses produced by Deng *et al.* (1987) in which the synchrony to the fundamental frequency was eclipsed by synchrony to the probe component at high relative intensity levels (Figure 16).

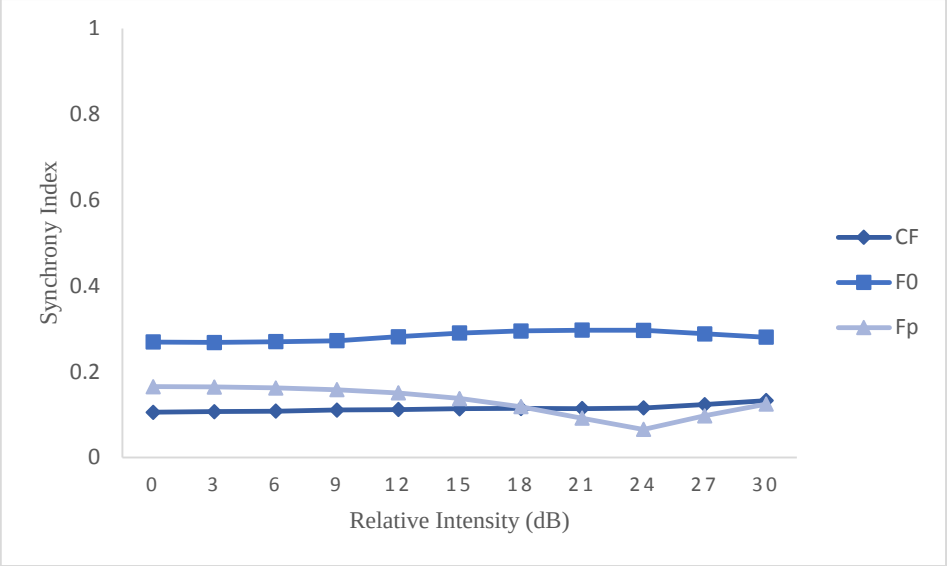

Figure 29: Carney model output showing response synchrony to components against increasing 7th harmonic intensity. Auditory nerve fibre synchrony to harmonic components generated in the Carney model of a 2.625 kHz characteristic frequency (CF) fibre to a 70 dB SPL harmonic one with a fundamental frequency (F_0) of 0.125 kHz with manipulation of the 7th stimulus harmonic, termed the probe component (Fp). Relative intensity of the Fp was increased to determine change in synchrony response with regards to the CF and F_0 components.

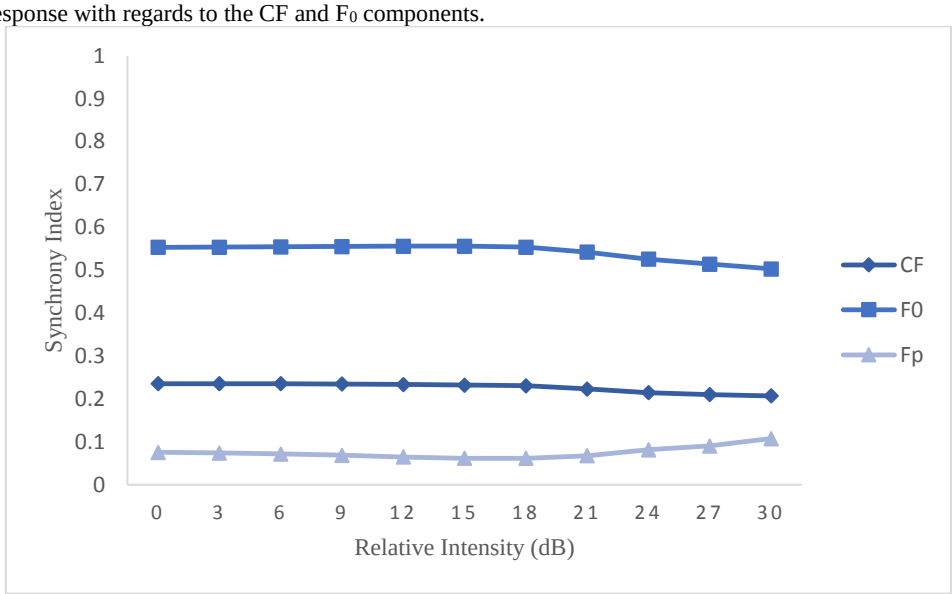

Figure 30: Seneff model output showing response synchrony to components against increasing 7th harmonic intensity. Auditory nerve fibre synchrony to harmonic components generated in the Carney model of a 2.625 kHz characteristic frequency (CF) fibre to a 70 dB SPL harmonic one with a fundamental frequency (F_0) of 0.125 kHz with manipulation of the 7th stimulus harmonic, termed the probe component (Fp). Relative intensity of the Fp was increased to determine change in synchrony response with regards to the CF and F_0 components.

The model outputs for a probe frequency of 1.5 kHz, or the 12th harmonic component both show a greater similarity to the expected pattern. The Carney model (Figure 31) has a strong agreement with the figure presented in Deng *et al.* (1987) (Figure 17), showing an increase in the probe component coupled with the simultaneous decrease in synchrony index for the fundamental, and to a lesser extent, the characteristic component.

The Seneff model also shows agreement. However, the increase of the probe component does not eclipse the fundamental component until higher intensities are reached, although the initial increase starts at a similar intensity (Figure 32). Furthermore, the Seneff model generates the characteristic component with a larger initial synchrony index than the probe component, which parallels the relationship of the components in the measured auditory fibre responses.

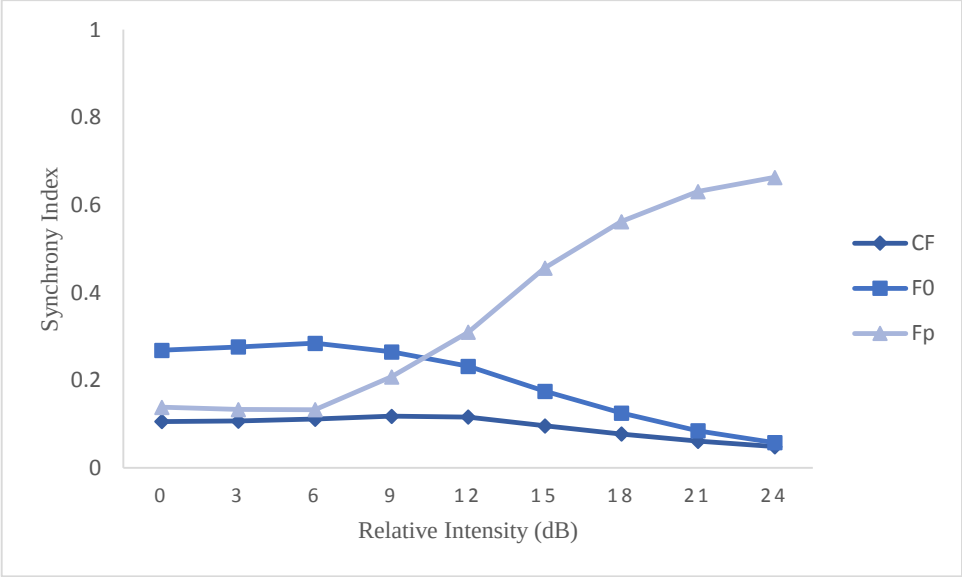

Figure 31: Carney model output showing response synchrony to components against increasing 12th harmonic intensity. Auditory nerve fibre synchrony to harmonic components generated in the Carney model of a 2.625 kHz characteristic frequency (CF) fibre to a 70 dB SPL harmonic one with a fundamental frequency (F_0) of 0.125 kHz with manipulation of the 12th stimulus harmonic, termed the probe component (Fp). Relative intensity of the Fp was increased to determine change in synchrony response with regards to the CF and F_0 components.

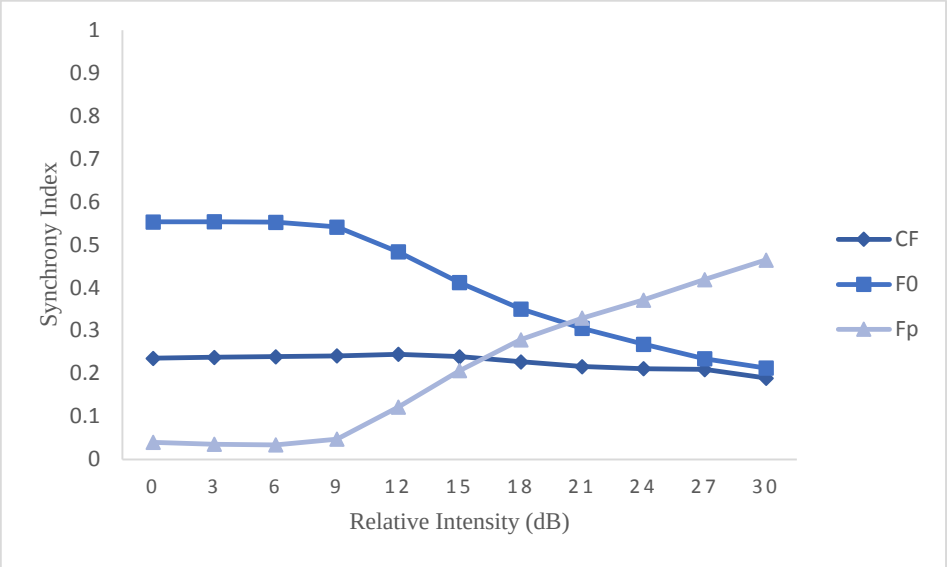

Figure 32: Seneff model output showing response synchrony to components against increasing 12th harmonic intensity. Auditory nerve fibre synchrony to harmonic components generated in the Carney model of a 2.625 kHz characteristic frequency (CF) fibre to a 70 dB SPL harmonic one with a fundamental frequency (F_0) of 0.125 kHz with manipulation of the 12th stimulus harmonic, termed the probe component (Fp). Relative intensity of the Fp was increased to determine change in synchrony response with regards to the CF and F_0 components.

For the 17th harmonic component of the stimulus (2.075 kHz), a similar pattern was observed to that seen in the 12th harmonic manipulation. An increase in the probe component was recognised in both models, along with the simultaneous decrease of both of the other components. Again, the Carney model generated the probe frequency at a higher initial synchrony index than the characteristic component, with the cross-over point between the fundamental frequency and the probe frequency dominance occurring at a lower intensity (Figure 33). The Seneff model generated the probe component with the lowest initial synchrony index, although at this probe frequency, the increase and crossover materialised at approximately the same point as in the presented figure, indicating a strong agreement with the experimental data (Figure 34).

Visual comparison of the measured responses to the modelled outputs (Figure 18) suggest strong agreement of synchrony capture in both the Carney and Seneff models, with the probe harmonic component becoming dominant at similar relative intensity levels.

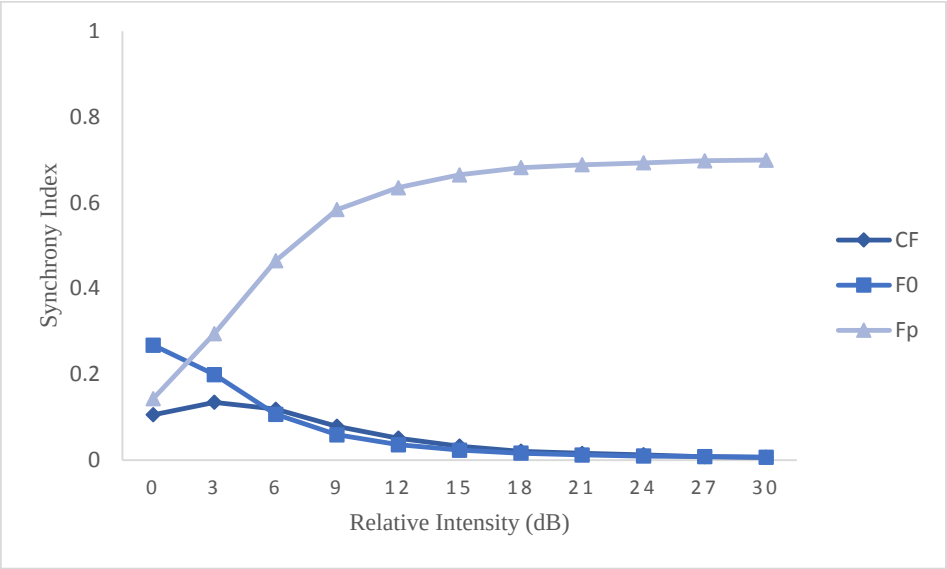

Figure 33: Carney model output showing response synchrony to components against increasing 17th harmonic intensity. Auditory nerve fibre synchrony to harmonic components generated in the Carney model of a 2.625 kHz characteristic frequency (CF) fibre to a 70 dB SPL harmonic one with a fundamental frequency (F_0) of 0.125 kHz with manipulation of the 17th stimulus harmonic, termed the probe component (Fp). Relative intensity of the Fp was increased to determine change in synchrony response with regards to the CF and F_0 components.

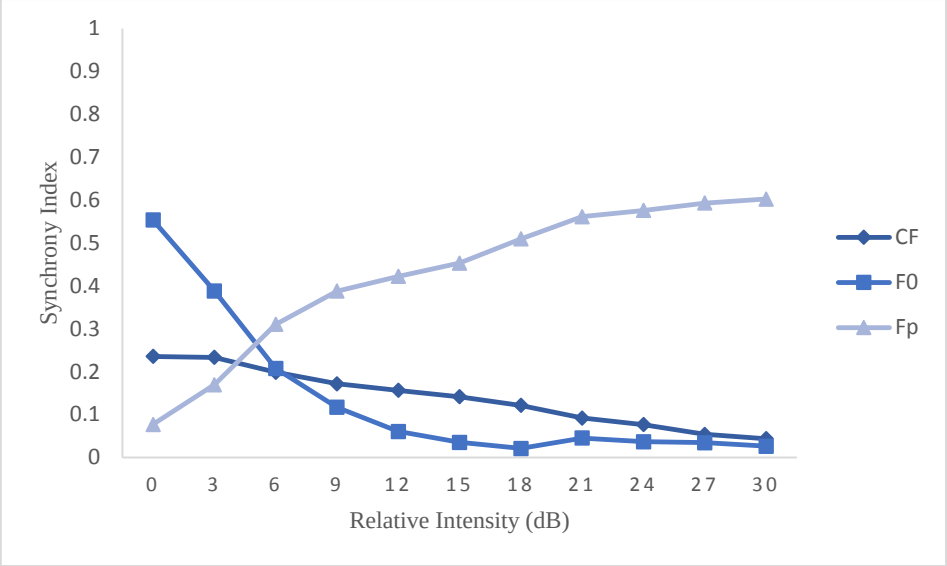

Figure 34: Seneff model output showing response synchrony to components against increasing 17th harmonic intensity. Auditory nerve fibre synchrony to harmonic components generated in the Carney model of a 2.625 kHz characteristic frequency (CF) fibre to a 70 dB SPL harmonic one with a fundamental frequency (F_0) of 0.125 kHz with manipulation of the 17th stimulus harmonic, termed the probe component (Fp). Relative intensity of the Fp was increased to determine change in synchrony response with regards to the CF and F_0 components.

The 18th harmonic component (2.197 kHz) again showed a similar trend between the Carney and Seneff model outputs (Figure 35 and 36 respectively) and the measured responses in Deng *et al.* (1987) (Figure 19). Observation shows the characteristic frequency and fundamental frequency components being suppressed in response synchrony, whilst the probe frequency dominates the response synchrony where the relative intensity is above 0 dB SPL in the Carney model, and above 3 dB SPL in the Seneff model.

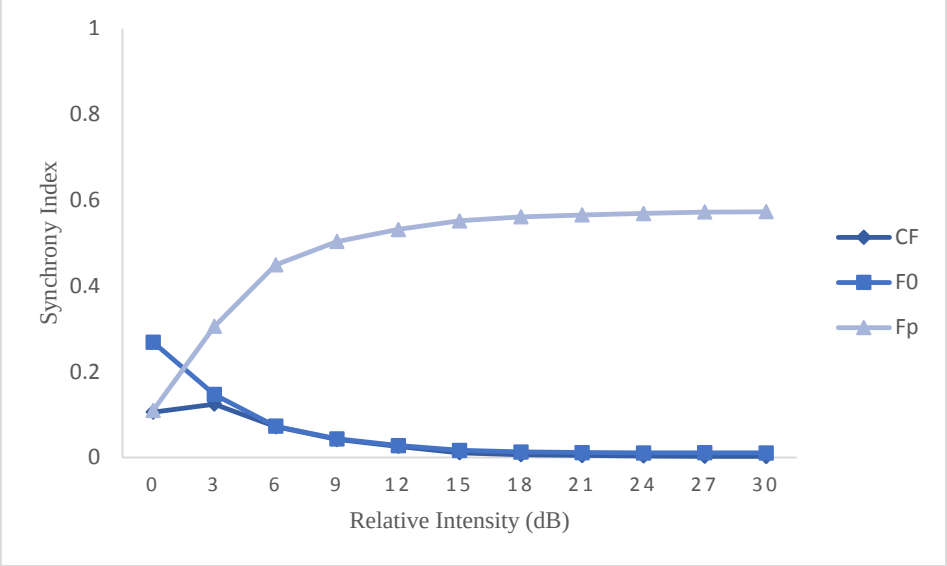

Figure 35: Carney model output showing response synchrony to components against increasing 18th harmonic intensity. Auditory nerve fibre synchrony to harmonic components generated in the Carney model of a 2.625 kHz characteristic frequency (CF) fibre to a 70 dB SPL harmonic one with a fundamental frequency (F_0) of 0.125 kHz with manipulation of the 18th stimulus harmonic, termed the probe component (Fp). Relative intensity of the Fp was increased to determine change in synchrony response with regards to the CF and F_0 components.

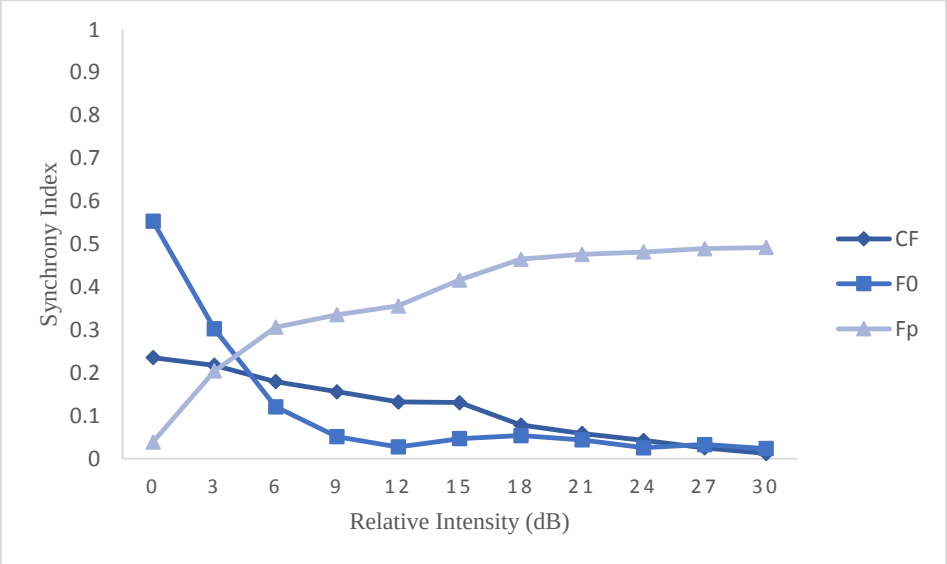

Figure 36: Seneff model output showing response synchrony to components against increasing 18th harmonic intensity. Auditory nerve fibre synchrony to harmonic components generated in the Carney model of a 2.625 kHz characteristic frequency (CF) fibre to a 70 dB SPL harmonic one with a fundamental frequency (F_0) of 0.125 kHz with manipulation of the 18th stimulus harmonic, termed the probe component (Fp). Relative intensity of the Fp was increased to determine change in synchrony response with regards to the CF and F_0 components.

The intensity interval for the 21st component (2.563 kHz) was changed to a 2 dB step as per Deng *et al.* (1987), which was replicated with the Carney and Seneff model outputs (Figure 37 and 38 respectively). At this probe frequency, the characteristic and probe components share the same frequencies, giving rise to identical component outputs. Both models show strong correlation with the measured fibre responses in this condition (Figure 20), showing strong synchrony capture to the manipulated harmonic component at low relative intensity levels.

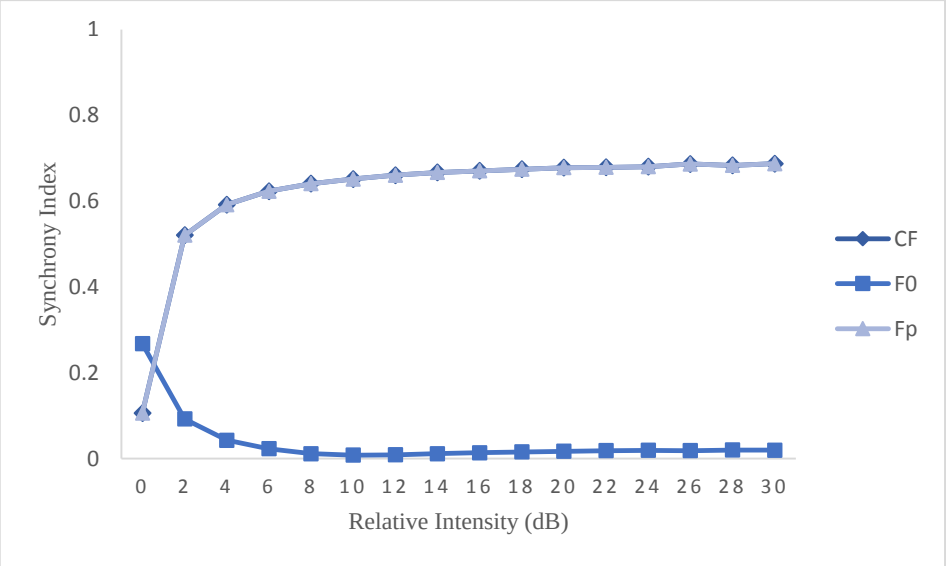

Figure 37: Carney model output showing response synchrony to components against increasing 21st harmonic intensity. Auditory nerve fibre synchrony to harmonic components generated in the Carney model of a 2.625 kHz characteristic frequency (CF) fibre to a 70 dB SPL harmonic one with a fundamental frequency (F_0) of 0.125 kHz with manipulation of the 21st stimulus harmonic, termed the probe component (Fp). Relative intensity of the Fp was increased to determine change in synchrony response with regards to the CF and F_0 components.

.

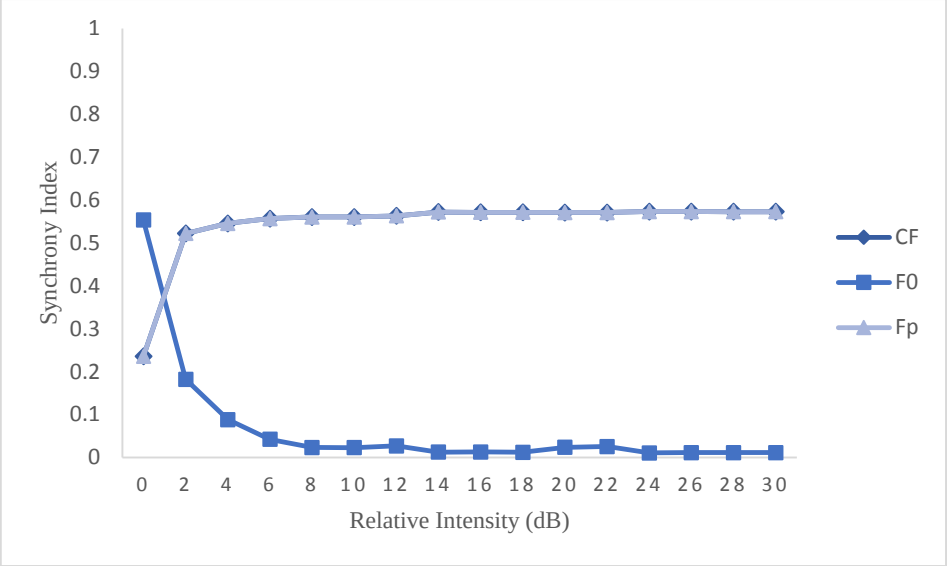

Figure 38: Seneff model output showing response synchrony to components against increasing 21st harmonic intensity. Auditory nerve fibre synchrony to harmonic components generated in the Carney model of a 2.625 kHz characteristic frequency (CF) fibre to a 70 dB SPL harmonic one with a fundamental frequency (F_0) of 0.125 kHz with manipulation of the 21st stimulus harmonic, termed the probe component (Fp). Relative intensity of the Fp was increased to determine change in synchrony response with regards to the CF and F_0 components.

The last probe frequency modelled was the 24th harmonic component (2.930 kHz). Both the Carney and Seneff model responses exhibit strong synchrony capture to the probe harmonic at low intensity levels (Figures 39 and 40), consistent with the previous modelled responses. Visual comparison to Deng *et al.* (1987) (Figure 21) show the modelled capture occurs at a relative intensity lower than exhibited in measured auditory fibre responses, suggesting the agreement between the model outputs and the measured responses may be weaker in cases where the probe harmonic frequency is higher than the characteristic frequency of the auditory fibre.

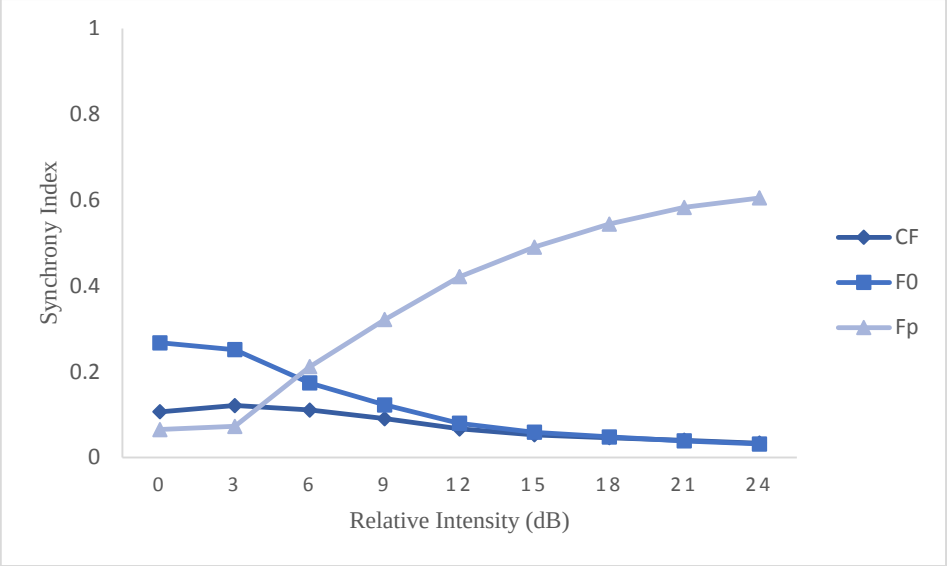

Figure 39: Carney model output showing response synchrony to components against increasing 24th harmonic intensity. Auditory nerve fibre synchrony to harmonic components generated in the Carney model of a 2.625 kHz characteristic frequency (CF) fibre to a 70 dB SPL harmonic one with a fundamental frequency (F_0) of 0.125 kHz with manipulation of the 24th stimulus harmonic, termed the probe component (Fp). Relative intensity of the Fp was increased to determine change in synchrony response with regards to the CF and F_0 components.

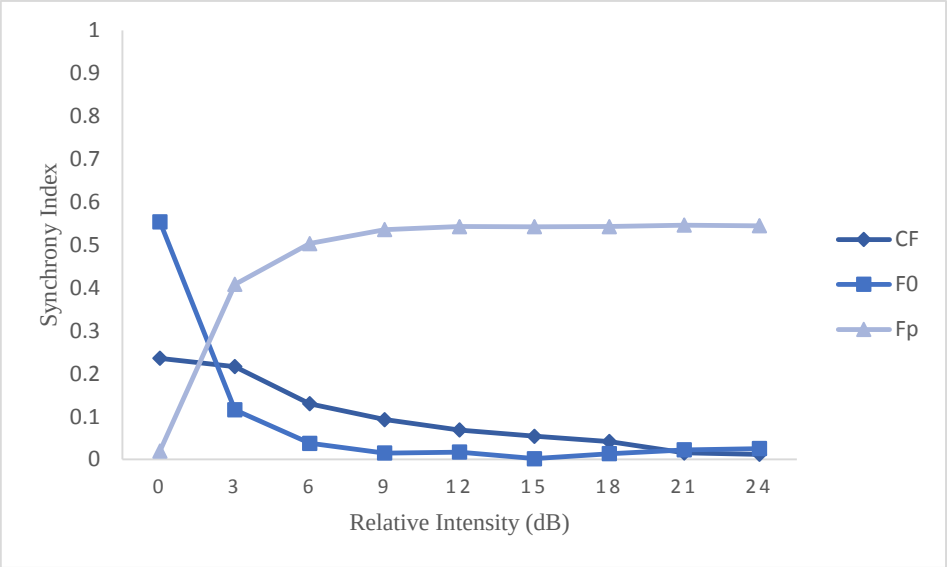

Figure 40: Seneff model output showing response synchrony to components against increasing 24th harmonic intensity. Auditory nerve fibre synchrony to harmonic components generated in the Carney model of a 2.625 kHz characteristic frequency (CF) fibre to a 70 dB SPL harmonic one with a fundamental frequency (F_0) of 0.125 kHz with manipulation of the 24th stimulus harmonic, termed the probe component (Fp). Relative intensity of the Fp was increased to determine change in synchrony response with regards to the CF and F_0 components.

.

3.3 Summary of Main Findings

Visual comparisons of the model output with the model response presented in their parent papers (Seneff (1988) and Zilany *et al.* (2009)) indicated minor variations in response rate. However, overall response patterns were similar to the presented model responses.

Visual comparisons of the model outputs to the measured responses produced by Sinex *et al.* (2003) suggest that the Seneff model response outputs produce an accurate representation of synchrony capture in the frequency components, with the modelled responses demonstrating a similar pattern in the frequency components against intensity. The Carney model did not produce especially similar frequency component patterns to the measured responses within the given parameters.

Visual comparisons of the model outputs to the measured responses produced by Deng *et al.* (1987) suggest that within this set of stimulus and modelling parameters, both models demonstrate synchrony capture in their responses. Deviations from the component patterns shown in the measured responses did occur, however, with neither model demonstrating synchrony capture in the 7^{th} harmonic component, whereas this was observed in the measured responses at higher relative intensities, and in the 24^{th} harmonic component, where both models exhibited synchrony capture but at lower relative intensity levels of the harmonic component than was presented in the measured responses.

Discussion

The purpose of this study was to examine the efficacy of two models in the simulation of synchrony capture. Both models were executed with parameters from experimental auditory nerve responses that exhibited synchrony capture, and the outputs were visually compared to determine if either model was able to reproduce the expected response patterns in a consistent manner.

Two different stimulus frameworks were employed to assess the models, the first being a steady increase in a complex harmonic tone intensity at a specific characteristic frequency, and observing the relationships in synchrony index between the various components.

The second was through increasing the relative intensity of individual components in the complex harmonic tone at a specific characteristic frequency, and observing the interactions of different component's synchrony index over increasing component level.

In both of these scenarios, the expected outcome was that one component would become dominant over the others, with a concurrent decrease in synchrony index observed in the 'lesser' components.

4.1 Discussion of model outputs in relation to Sinex *et al* 2003

In the present study, there is an appreciable difference in how the auditory nerve responses have been represented by the two tested models. The output from the Seneff model showed strong agreement with the experimental data presented in Sinex *et al.* (2003). While the absolute rates of the fibres are dissimilar, the behaviour of the response components exhibits the expected synchrony capture of the dominant component, coupled with the suppression of the 'minor' components.

One difference of note between the experimental data and the model output is that the smaller components that appear in the outputs are not well matched. While the dominant components are analogous, there is some separation in terms of which of the smaller frequency components have been

plotted as significant components. This is most obvious in the correlation tables presented above, in which each of the four fibre comparison plots are missing two of the components present in the experimental response data. While this should be noted, this outcome may be due to the filtering process used in the model plotting function, where component curves below a threshold were eliminated from the resulting graph in order to allow for more coherent interpretation.

In contrast to the strong agreement shown by the Seneff model, the response outputs from the Carney model do not show the same overall pattern in the component relationships shown in the experimental data. Whereas the data produced by Sinex *et al.* (2003) showed the harmonic component closest to the characteristic frequency of the fibre dominating the neurone activity with reduced activity from the other components, the modelled responses in the Carney outputs showed a reduction in 'dominance' appearing in the higher intensities. While this largest component was in agreement with the recorded responses in its frequency, the fibre synchronisation to this component dramatically drops in higher intensities, with lower frequency components 'capturing' the fibres synchronisation.

Overall statistical comparisons between synchrony capture exhibited in the model outputs and the recorded responses presented in Sinex *et al.* (2003) were not possible. However, correlations were calculated between the individual component curves of the responses (*tables 1-4*). These correlations corroborate with the visual comparisons, revealing that, in general, the Seneff model outputs have a strong agreement with the responses presented in Sinex *et al.* (2003), while there is less agreement to the responses generated by the Carney model.

Although the recorded measurements by Sinex *et al.* (2003) did not reach the highest intensities modelled where the loss of synchronisation was most obvious, this decline in fibre synchrony seen in this component was evident at even moderate intensities. That the reduction in dominance of the component closest to the characteristic frequency coincides with the increase of synchrony to lower frequency components may be partly explained by the asymmetry in auditory fibre tuning curves. The significant low frequency tails, as shown in auditory nerve fibres by Kiang and Moxon (1974), may have some erroneous influence being exhibited through the Carney model responses at higher

intensities. This is noted by Kumaresan, Peddinti, and Cariani (2013), where the captured, or suppressed, fibres often have characteristic frequencies higher than the dominant component due to the asymmetrical nature of the cochlear. Exceptions to this have been noted, however, such as fibre locking to the harmonic and intermodulation components of two formant frequencies of a stimulus, which increase in amplitude at higher sound levels (Sachs & Young, 1980).

Based on the results of the current study, it is appropriate to conclude that the Seneff model resulted in responses in strong agreement with the synchrony capture presented responses by Sinex *et al.* (2003), while no strong agreement was found in the Carney model responses to these stimuli.

4.2 Discussion of model outputs in relation to Deng & Geisler 1987

Unlike the modelled results based on parameters described in Sinex *et al.* (2003), both model responses to a stimulus where a single harmonic component intensity was manipulated showed strong agreement with the responses measured in Deng *et al.* (1987) over the majority of manipulated harmonics.

Two conditions did not show the same pattern of synchrony capture as presented in Deng *et al.* (1987); manipulation of the 7^{th} and the 24^{th} harmonic components. The 7^{th} harmonic was the lowest manipulated harmonic below the characteristic frequency of the modelled fibre and the 24^{th} harmonic was the only manipulated harmonic component above the characteristic frequency. The deviation from the expected responses was present in a similar fashion in both the Carney and Seneff models.

These differences may indicate inherent differences in the tuning curves utilised by both models to that measured by Deng *et al.* (1987). The lack of synchrony capture exhibited in the models by this low harmonic component even at high relative intensities could suggest that the low frequency tail of the fibre tuning is not representative of expected fibre tuning. Additionally, the reverse is true in harmonic components higher in frequency than the fibres characteristic frequency. Both models responses exhibited synchrony capture at lower than expected levels of relative intensity of the manipulated harmonic. The level of synchrony capture by the higher frequency manipulated harmonic component

may suggest that the high frequency tail of the tuning curves used in the models may be broader than the higher frequency tail measured by Deng *et al.* (1987). This would indicate that both model's tuning curves do not accurately match the expected tuning response. It should be noted, however, that this higher frequency condition was only able to be compared to one measured response set, limiting the strength of any conclusions.

From comparisons between the modelled responses and the responses presented in Deng *et al.* (1987), it can be concluded that both models show relatively accurate representations of synchrony capture to complex stimuli where a single harmonic component is being manipulated.

4.3 Differences between parameter comparisons

The observed differences in model efficacy in simulating synchrony capture between the different stimuli parameters may have a number of origins. One of the more significant of these is the adjusted rate-levels in the models creating disruptions to the Carney model response outputs, especially at higher intensity levels. This is most apparent in the comparison to the synchrony capture presented in Sinex *et al.* (2003), where the effect of increasing overall stimulus intensity was investigated. However, it should also be noted that the overall downwards trend in response synchrony for the 'dominant' component in the Carney model outputs was observed at relatively low levels. This would suggest that even taking possible changes in model output from the adjusted rate-level into account, the overall ability of this version of the Carney model to emulate the measured synchrony capture in auditory nerve fibre responses is not as accurate as that of the Seneff model, when the pattern of synchrony capture over increasing intensity is being investigated.

Other explanations for the modelling differences are likely to be due to the differing model structures and mathematical applications; investigations that are beyond the scope of the current study.

4.3.1 Model Functionality

Notwithstanding the modelling outcomes described above, it should be noted that both of the tested models in the current study approach the scenario of auditory nerve responses outputs in two different ways. The overall aim of both models is to generate representations of the auditory nerve response to various stimuli.

The Seneff model operates as a functional model where a statistical algorithm provides the same answer for a set of input parameters, providing an average auditory nerve fibre response. The average in this context means that the output values describe the mean of 'normal auditory performance'. This has the benefit of generating the exact same output response to a given input stimulus. The functioning of the Seneff model was previously alluded to in figure 2.

The Carney model, on the other hand, is built using representations of the individual elements of the auditory pathway, as previously described in figure 1. The model includes components to simulate expected random firing of neurons. This has the effect of guaranteeing that two runs of the same parameters will not have the exact same outputs, but will provide responses within a given range derived from measured data.

These differences mean that both models have distinct advantages depending on the application that needs to be modelled.

The strong agreement of the Seneff model to the examples of synchrony capture presented in Deng *et al.*, (1987); Sinex *et al.* (2003) and Deng *et al.* (1987) suggests that this model may have applications in the investigation of the effects of synchrony capture on neural representations in regards to normal hearing individuals. Furthermore, the apparent consistency in synchrony capture exhibited by the Seneff model may lend itself as a benchmark for synchrony capture representation, both for confirming experimental investigation and for further development of other models.

The Carney model has other potential applications, due to the individual elements of the auditory pathway being accounted for in the model structure. This model naturally lends itself to investigation

into the effect of disruptions to various structures in the auditory pathway. This could be achieved through adapting the structures of individual elements of the auditory pathway (within the model) to simulate various complications that arise within different auditory structures in individuals. The effect of damage, such as reduction of outer hair cells, to the representation of synchrony capture may open up avenues of research into improving technologies such as rehabilitative devices. As overall agreement was weak between the Carney model outputs and the Sinex *et al.* (2003) examples, further research and adjustments to the model may be needed to make this a viable option. The agreement between the Carney model outputs and the Deng *et al.* (1987) examples indicates the potential of this model.

4.4 Future Directions / Clinical Implications

Significant research has been carried out to better understand the effect of synchrony capture in the representation of sounds in the peripheral auditory system. However, the use of auditory fibre models will allow for further research into the role of synchrony capture in the perception of speech, allowing a greater understanding of any associated benefits. One significant area that would benefit a greater understanding of how complex sounds are encoded is that of cochlear prostheses (Sinex & Geisler, 1983).

It has been suggested that the lack of masking release in individuals with hearing loss and cochlear implants partially stems from the reduced ability to encode fundamental frequency (Nelson & Jin, 2004; Stickney, Zeng, Litovsky, & Assmann, 2004). As previously stated, research suggests that this encoding decline arises through a reduced access to temporal fine structure (Miller *et al.*, 2001; Hopkins & Moore, 2007; Hopkins *et al.*, 2008). The enhancement of temporal representation of individual harmonics in complex sounds generated by synchrony capture may help facilitate fundamental frequency pitch formation, and therefore, separation of sound sources.

This may be of particular interest in the processing of cochlear implants, which are known to discard nearly all of the temporal fine structure information (Brown & Bacon, 2010). Hearing in noise is typically where most hearing impaired individuals and cochlear implant users have the most difficulty

(Nelson & Jin, 2004). From this, further research into synchrony capture may give hints into providing access to fundamental frequency coding, as well as other benefits related to enhanced temporal representation of harmonics in complex sound (Kumaresan *et al.*, 2013).

This study is designed to give some insight into the accuracy of synchrony capture representation in two models. From this, it is hoped that further understanding of synchrony capture and its role in the representation of neural encoding of the peripheral auditory system can be achieved.

4.5 Limitations

The present study was designed to investigate the efficacy of two auditory models to simulate synchrony capture. While steps were taken to allow a reasonable comparative examination of both the models to the previous research and between the models, some aspects could have been improved or were unavoidable. These limitations are outlined below.

One of the major elements that must be taken into consideration in the comparison between the modelled responses and the recorded measurements is the difference in mammalian species from which the responses were recorded. The functioning of both the Carney and Seneff models are predominately based on research performed on feline auditory nerve fibres. While the examples of synchrony capture presented in Deng *et al.* (1987) are responses also recorded from feline fibres, responses presented in Sinex *et al.* (2003) were recorded from chinchilla auditory nerve fibres. Over different mammalian species there is a remarkable similarity in the auditory nerve responses (Sumner & Palmer, 2012). However, there can be considerable quantitative variation; differences in tuning broadness, frequency ranges, and spontaneous activity rates have all been reported between various species. While generalisations may be inferred through the comparison of the data sets, variation in responses should be expected.

The adjustment of the rate-level function of the models in order to generate comparable outputs meant that the intensity values in the generated model responses may not be directly comparable to the

stimulus intensities described in Sinex *et al.* (2003) and Deng *et al.* (1987). This adjustment was necessary for consistent model output generation. As the rate function within the models was an arbitrary value, this should not have had any effect on the mode outputs themselves. The thresholds observed in the generated rate-level curve would suggest that this can be assumed to be true. However, the possibility that this adjustment may have had an effect on the model outputs cannot be entirely discounted.

An updated version of the Carney model was released in 2013 with revised parameters for the inner hair cell to auditory nerve fibre synapse. This update was produced to allow the Carney model to better simulate discharge rates at saturation at higher frequencies as reported in recorded responses (Zilany, Bruce, & Carney, 2014). This updated version of the Carney model was not known to the authors at the beginning of this study and was not included in the current study. Therefore, it should be noted that the Carney model used in this study has acknowledged issues that may have since been rectified, and this may have improved the ability for the Carney model to more accurately simulate synchrony capture.

The analysis of the model outputs was executed through visual inspection and through a basic correlation. The response data required for the correlation of synchrony capture component curves was only available for the measured responses described in Sinex *et al.* (2003). Unavailability of the raw response data sets measured by Deng *et al.* (1987) meant that model output comparisons to these responses was only possible through visual inspections of the presented responses. While other studies have used mathematical approaches to analyse auditory nerve fibre model functioning (Zhang & Carney, 2005), the use of the synchrony capture phenomenon did not lend itself to this type of approach.

Visual comparisons of presented figures is not a particularly robust measure of scrutiny, limiting the strength of this study's results. While it allows for a basic interpretation of how similar the models are to experimental data, it lacks any quantitative investigation. The correlations of the component curves are similarly limited in that the correlations only determine the similarity of a single component frequency over intensity to the same component in the recorded responses. While this is useful, it cannot compare the overall relationships between the various components over intensity. From this, the

simulation of synchrony capture, and the suppression of components, cannot be investigated through this measure.

Finally, the comparisons of the model's ability to simulate synchrony capture is limited to the scope of the recorded auditory nerve fibre responses presented in Sinex *et al.* (2003) and Deng *et al.* (1987). The examples of synchrony capture given in these studies are within auditory fibres with a narrow set of characteristic frequencies and overall intensities ranging from 20 to 70 dB SPL. The current study could be strengthened with investigations into how well the models can simulate synchrony capture in a greater dynamic range, as well as over a greater range of characteristic frequency fibres, with comparisons to appropriate examples of synchrony capture in recorded responses. Due to this limitation, any conclusions drawn from the current study may be limited in overall application.

4.6 Summary

The purpose of this study was to examine and compare the ability of two models of auditory nerve fibres, Carney and Seneff, exhibiting the phenomenon of synchrony capture in response to complex sounds. Two studies of auditory fibres demonstrating synchrony capture were selected for comparison. This allowed the production of synchrony capture in the modelled responses to be investigated with multiple stimulus parameters. These included multiple characteristic frequency fibres against increasing stimulus intensity and synchrony to components within harmonic tones with intensity manipulated components.

The results indicated that the Seneff model exhibited synchrony capture in a similar manner to both studies with experimentally recorded auditory nerve fibres. The Carney model exhibited similar responses to one of the compared studies, but displayed dissimilar responses to the recorded responses against increasing intensity.

These outcomes indicate that the Seneff model tends towards an accurate portrayal of the synchrony capture phenomenon, while the Carney model accessed in this study tended towards an accurate

portrayal of synchrony capture with some stimulus parameters only. This outcome may have been affected by adjustments to the model's rate levels prior to comparison to the selected studies.

References

Adrian, E. D., & Zotterman, Y. (1926). The impulses produced by sensory nerve-endings. Part 2. The response of a single end-organ. *The Journal of Physiology, 61*, 151 - 171.

Arthur, R. M. (1976). Harmonic analysis of two-tone discharge patterns in cochlear nerve fibers. *Biol. Cybernetics, 22*, 21 - 31.

Arthur, R. M., Pfeiffer, R. R., & Suga, N. (1971). Properties of 'two-tone inhibition' in primary auditory neurones. *J. Physiol., 212*, 593 - 609.

Ashmore, J., Avan, P., Brownell, W. E., Dallos, P., Dierkes, K., Fettiplace, R., . . . Canlon, B. (2010). The remarkable cochlear amplifier. *Hearing Research, 266*(1-2), 1-17. doi: 10.1016/j.heares.2010.05.001

Ashmore, J. F. (1987). A fast motile response in guniea-pig outer hair cells: The cellular basis of the cochlear amplifier. *J. Physiol., 388*, 323 - 347.

Brown, C. A., & Bacon, S. P. (2010). Fundamental frequency and speech intelligibility in background noise. *Hearing Research, 266*(1-2), 52-59. doi: 10.1016/j.heares.2009.08.011

Butts, D. A., Weng, C., Jin, J., Yeh, C. I., Lesica, N. A., Alonso, J. M., & Stanley, G. B. (2007). Temporal precision in the neural code and the timescales of natural vision. *Nature, 449*(7158), 92-95. doi: 10.1038/nature06105

Carhart, R., & Tillman, T. W. (1970). Interaction of Competing Speech Signals With Hearing Losses. *Archives of Otolaryngology - Head and Neck Surgery, 91*(3), 273-279. doi: 10.1001/archotol.1970.00770040379010

Ceriani, F., & Mammano, F. (2012). Calcium signaling in the cochlea - Molecular mechanisms and physiopathological implications. *Cell Commun Signal, 10*(1), 20. doi: 10.1186/1478-811X-10-20

Chatterjee, M., & Peng, S. C. (2008). Processing F0 with cochlear implants: Modulation frequency discrimination and speech intonation recognition. *Hearing Research, 235*(1-2), 143-156. doi: 10.1016/j.heares.2007.11.004

Chatterjee, M., & Zwislocki, J. J. (1998). Cochlear mechanisms of frequency and intensity coding II. Dynaic range and the code for loudness. *Hearing Research, 124*, 170 - 181.

Cheatham, M. A., & Dallos, P. (1982). Two-tone interactions in the cochlear microphonic. *Hearing Research, 8*, 29 - 48.

Cheatham, M. A., & Dallos, P. (1989). Two-tone suppression in inner hair cell responses. *Hearing Research, 40*, 187 - 196.

Darwin, C. J. (1997). Auditory grouping. *Trends in Cognitive Sciences, 1*(9), 327 - 333.

Dean, I., Harper, N. S., & McAlpine, D. (2005). Neural population coding of sound level adapts to stimulus statistics. *Nat Neurosci, 8*(12), 1684-1689. doi: 10.1038/nn1541

Delgutte, B. (1990). Two-tone rate suppression in auditory-nerve fibers: dependence on suppressor frequency and level. *Hearing Research, 49*, 225 - 246.

Delgutte, B., & Kiang, N. Y. S. (1984). Speech coding in the auditory nerve I: Vowel-like sounds. *J Acoust Soc Am, 75*(3), 866 - 878.

Deng, L., Geisler, C. D., & Greenberg, S. (1987). Responses of auditory-nerve fibers to multiple-tone complexes. *J Acoust Soc Am, 82*(6), 1989 - 2000.

Evans, E. F. (1972). The frequency response and other properties of single fibres in the guinea-pig cochlear nerve. *J. Physiol., 226*, 263 - 287.

Evans, E. F. (1981). The dynamic range problem: Place and time coding at the level of cochlear nerve and nucleus. In J. Syka (Ed.), *Neuronal Mechanisms of Hearing* (pp. 69-85). New York: Plenum Press.

Evans, E. F., & Palmer, A. R. (1980). Relationship between the dynamic range of cochlear nerve fibres and their sponatneous activity. *Exp Brain Res, 40*, 115 - 118.

Festen, J. M., & Plomp, R. (1990). Effects of fluctuating noise and interferign speech on the speech-reception threshold for impaired and normal hearing. *J Acoust Soc Am, 88*(4), 1725 - 1736.

Galambos, R., & Davis, H. (1943). The response of single auditory-nerve fibers to acoustic stimulation. *J Neurophysiol, 6*, 39 - 57.

Goldstein, J. L. (1967). Auditory nonlinearity. *J Acoust Soc Am, 41*, 676 - 699.

Gray, P. R. (1967). Conditional probability analyses of the spike activity of single neurons. *Biophysical Journal, 7*, 759 - 777.

Greenberg, S., Geisler, C. D., & Deng, L. (1986). Frequency selectivity of single cochlear-nerve fibers based on the temporal response pattern to two-tone signals. *J Acoust Soc Am, 79*(4), 1010 - 1019.

Guigere, C., & Woodland, P. C. (1994). A computational model of the auditory periphery for speech and hearing research. I. Ascending path. *Journal of the Acoustic Society of America, 95*(1), 331 - 342.

Harris, D. M., & Dallos, P. (1979). Forward masking of auditory nerve fiber responses. *J Neurophysiol, 42*(4), 1083 - 1107.

Holton, T., & Weiss, T. F. (1978). Two-tone rate suppression in lizard cochlear nerve fibers, relation to receptor organ morphology. *Brain Research, 159*, 219 - 222.

Hopkins, K., & Moore, B. C. (2007). Moderate cochlear hearing loss leads to a reduced ability to use temporal fine structure information. *J Acoust Soc Am, 122*(2), 1055-1068. doi: 10.1121/1.2749457

Hopkins, K., Moore, B. C., & Stone, M. A. (2008). Effects of moderate cochlear hearing loss on the ability to benefit from temporal fine structure information in speech. *J Acoust Soc Am, 123*(2), 1140-1153. doi: 10.1121/1.2824018

Horst, J. W., Javel, E., & Farley, G. R. (1990). Coding of spectral fine structure in the auditory nerve. II. Level-dependent nonlinear responses. *J Acoust Soc Am, 88*(6), 2656 - 2681.

Howard, J., Roberts, W. M., & Hudspeth, A. J. (1988). Mechanoelectrical transduction by hair cells. *Ann. Rev. Biophys. Biophys. Chem., 17*, 99 - 124.

Javel, E. (1981). Suppression of auditory nerve responses I: Temporal analysis, intensity effects and suppression contours. *J Acoust Soc Am, 69*(6), 1735 - 1745.

Javel, E., McGee, J., Walsh, E. J., Farley, G. R., & Gorga, M. P. (1983). Suppression of auditory nerve responses. II. Suppression threshold and growth, iso-suppression contours. *J Acoust Soc Am, 74*(3), 801 - 813.

Johnstone, B. M., Patuzzi, R., & Yates, G. K. (1986). Basilar membrane measurements and the travelling wave. *Hearing Research, 22*, 147 -153.

Johnstone, J. R. (1980). The generation of combination tones. *Hearing Research, 3*, 253 - 256.

Kiang, N. Y. S. (1965). Discharge patterns of single fibers in the cat's auditory nerve. Cambridge: Massachusetts Inst of Tech

Kiang, N. Y. S. (1990). Curious oddments of auditory-nerve studies. *Hearing Research, 49*, 1 - 16.

Kiang, N. Y. S., & Moxon, E. C. (1974). Tails of tuning curves of auditory-nerve fibers. *J Acoust Soc Am, 55*(3), 620 - 630.

Kluender, K. R., Lotto, A. J., & Jenison, R. L. (1995). Perception of voicing for syllable-inital stops at different intensities: Does synchrony capture signal voiceles stop consonants? *J Acoust Soc Am, 97*(4), 2552 - 2567.

Kumaresan, R., Peddinti, V. K., & Cariani, P. (2013). Synchrony capture filterbank: auditory-inspired signal processing for tracking individual frequency components in speech. *J Acoust Soc Am, 133*(6), 4290-4310. doi: 10.1121/1.4802653

Liberman, M. C. (1978). Auditory-nerve response from cats raised in a low-noise chamber. *J Acoust Soc Am, 63*(2), 442 - 455.

Liberman, M. C., & Dodds, L. W. (1984). Single-neuron labeling and chronic cochlear pathology. III. Stereocilia damage and alterations of threshold tuning curves. *Hearing Research, 16*, 55 - 74.

Lim, D. J. (1986). Functional structure of the organ of Corti: a review. *Hearing Research, 22*, 117 - 146.

Lopez-Poveda, E. A., & Meddis, R. (2001). A human nonlinear cochlear filterbank. *J Acoust Soc Am, 110*(6), 3107. doi: 10.1121/1.1416197

Lotto, A. J., & Kluender, K. R. (2002). Synchrony capture hypothesis fails to account for effects of amplitude on voicing perception. *J Acoust Soc Am, 111*(2), 1056 - 1062. doi: 10.1121/1.1433809

Marsalek, P., & Kofranek, J. (2005). Spike encoding mechanisms in the sound localization pathway. *Biosystems, 79*(1-3), 191- 198. doi: 10.1016/j.biosystems.2004.09.022

Micheyl, C., & Oxenham, A. J. (2010). Pitch, harmonicity and concurrent sound segregation: psychoacoustical and neurophysiological findings. *Hearing Research, 266*(1-2), 36-51. doi: 10.1016/j.heares.2009.09.012

Miller, C. A., Abbas, P. J., & Robinson, B. K. (2001). Response properties of the refractory auditory nerve fiber. *Journal of the Association for Research in Otolaryngology, 2*(3), 216-232. doi: 10.1007/s101620010083

Moller, A. R. (1977). Frequency selectivity of single auditory-nerve fibers in response to broadband noise stimuli. *J Acoust Soc Am, 62*(1), 135 - 142.

Moore, B. C. J. (2003). Coding of sounds in the auditory system and its relevance to signal processing and coding in cochlear implants. *Otology and Neurotology, 24*, 243 - 254.

Moore, B. C. J., Glasberg, B. R., & Peters, R. W. (1986). Thresolds for hearing mistuned partials as separate tones in harmonic complexes. *J Acoust Soc Am, 80*(2), 479 - 483.

Moore, B. C. J., Peters, R. W., & Glasberg, B. R. (1985). Thresholds for the detectio of inharmonicity in complex tones. *J Acoust Soc Am, 77*(5), 1861 - 1867.

Müller, U. (2008). Cadherins and mechanotransduction by hair cells. *Curr Opin Cell Biol, 20*(5), 557-566. doi: 10.1016/j.ceb.2008.06.004

Nelson, P. B., & Jin, S. (2004). Factors affecting speech understanding in gated interference: Cochlear implant users and normal-hearing listeners. *J Acoust Soc Am, 115*(5), 2286. doi: 10.1121/1.1703538

Nobili, R., & Mammano, F. (1996). Biophysics of the cochlea II: Stationary nonlinear phenomenology. *J Acoust Soc Am, 99*(4), 2244 - 2255.

Nuttal, A. L., & Dolan, D. F. (1993). Two-tone suppression of inner hair cell and basilar membrane responses in the guinea pig. *J Acoust Soc Am, 93*(1), 390 - 400.

Oxenham, A. J., Bernstein, J. G., & Penagos, H. (2004). Correct tonotopic representation is necessary for complex pitch perception. *Proc Natl Acad Sci U S A, 101*(5), 1421-1425. doi: 10.1073/pnas.0306958101

Palm, G., Aertsen, A. M. H., & Gerstein, G. L. (1988). On the significance of correlations among neuronal spike trains. *Biol. Cybernetics, 59*, 1 - 11.

Palmer, A. R. (1990). The representation of the spectra and fundamental frequencies of steady-state single-and-double-vowel sounds in the temporal discharge patterns of guinea pig cochlear-nerve fibers. *J Acoust Soc Am, 88*(3), 1412 - 1426.

Palmer, A. R., & Russel, I. J. (1986). Phase-locking in the cochlear nerve of the guinea-pig and its relation to the receptor potential of inner hair-cells. *Hearing Research, 24*, 1 - 15.

Patuzzi, R., Johnstone, B. M., & Sellick, P. M. (1984). The alteration of the vibration of the basilar membrane produced by loud sound. *Hearing Research, 13*, 99-100.

Pick, G. F. (1980). Level dependence of pyschophysical frequency resolution and auditory filter shape. *J Acoust Soc Am, 68*(4), 1085 - 1095.

Plomp, R. (1978). Auditory handicap of hearing impairment and the limited benefit of hearing aids. *J Acoust Soc Am, 63*(2), 533 - 549.

Reale, R. A., & Geisler, C. D. (1980). Auditory-nerve fiber encoding of two-tone approximations to steady-state vowels. *J Acoust Soc Am, 67*(3), 891 - 902.

Rhode, W. S. (1971). Observations of the vibration of the basilar membrane in squirrel monkeys using the Mössbauer technique. *J Acoust Soc Am, 49*(4), 1218 - 1231.

Rhode, W. S., & Robles, L. (1974). Evidence from Mössbauer experiments for nonlinear vibration in the cochlea. *J Acoust Soc Am, 55*(3), 588 - 596.

Robles, L., Ruggero, M. A., & Rich, N. C. (1986). Basilar membrane mechanics at the base of the chinchilla cochlea. I. Input-output functions, tuning curves, and response phases. *J Acoust Soc Am, 80*(5), 1364 - 1374.

Rose, J. E., Brugge, J. F., Anderson, D. J., & Hind, J. E. (1967). Phase-locked response to low-frequency tones in single auditory nerve fibers of the squirrel monkey. *J Neurophysiol, 30*(4), 769 - 793.

Ruggero, M. A., Rich, N. C., Recio, A., Narayan, S. S., & Robles, L. (1997). Basilar-membrane responses to tones at the base of the chinchilla cochlea. *J Acoust Soc Am, 101*(4), 2151 - 2163.

Ruggero, M. A., Robles, L., Rich, N. C., Recio, A., Brown, A. M., & Evans, E. F. (1992). Basilar membrane responses to two-tone and broadband stimuli (and discussion). *Philosophical Transactions of the Royal Society B: Biological Sciences, 336*, 307 - 315.

Ruggero, M. A., & Temchin, A. N. (2005). Unexceptional sharpness of frequency tuning in the human cochlea. *Proc Natl Acad Sci U S A, 102*(51), 18614-18619. doi: 10.1073/pnas.0509323102

Sachs, M. B., & Abbas, P. J. (1974). Rate versus level functions for auditory-nerve fibers in cats: tone burst stimuli. *J Acoust Soc Am, 56*(6), 1835 - 1847.

Sachs, M. B., & Abbas, P. J. (1976). Phenomenological model for two-tone suppression. *J Acoust Soc Am, 60*(5), 1157 - 1163.

Sachs, M. B., & Hubbard, A. E. (1981). Responses of auditory-nerve fibers to characteristic frequency tones and low-frequency suppressors. *Hearing Research, 4*, 309 - 324.

Sachs, M. B., & Kiang, N. Y. S. (1968). Two-tone inhibition in auditory fibers. *J. Acoust. Soc. Am., 43*, 1120

Sachs, M. B., & Young, E. D. (1979). Encoding of steady-state vowels in the auditory nerve: Representation in terms of discharge rate. *J Acoust Soc Am, 66*(2), 470 - 479.

Sachs, M. B., & Young, E. D. (1980). Effects of nonlinearities on speech encoding in the auditory nerve. *J Acoust Soc Am, 68*(3), 858 - 875.

Sachs, M. B., Young, E. D., & Lewis, R. H. (1974). Discharge patterns of single fibers in the pidgeon auditory nerve. *Brain Research, 70*, 431 - 447.

Samson, A. H., & Pollack, G. S. (2002). Encoding of sound localization cues by an identified auditory interneuron: effects of stimulus temporal pattern. *J Neurophysiol, 88*(5), 2322 - 2328. doi: 10.1152/jn.00119.2002

Schalk, T. B., & Sachs, M. B. (1980). Nonlinearities in auditory-nerve fiber responses to bandlimited noise. *J Acoust Soc Am, 67*(3), 903 - 913.

Schmiedt, R. A. (1982). Boundaries of two-tone rate suppression of cochlear-nerve activity. *Hearing Research, 7*, 335 - 351.

Sellick, P. M., Patuzzi, R., & Johnstone, B. M. (1982). Measurement of basilar membrane motion in the guinea pig using the Mössbauer technique. *J Acoust Soc Am, 71*(1), 131 - 141.

Seneff, S. (1988). A joint synchrony/mean-rate model of auditory speech processing. *Journal of Phonetics, 16*, 55 - 76.

Shera, C. A., Guinan, J. J., Jr., & Oxenham, A. J. (2002). Revised estimates of human cochlear tuning from otoacoustic and behavioral measurements. *Proc Natl Acad Sci U S A, 99*(5), 3318-3323. doi: 10.1073/pnas.032675099

Sinex, D. G. (2005). Spectral Processing and Sound Source Determination. *Int Rev Neurobiol., 70*, 371-398. doi: 10.1016/s0074-7742(05)70011-8

Sinex, D. G., & Geisler, C. D. (1983). Responses of auditory-nerve fibers to consonant-vowel syllables. *J Acoust Soc Am, 73*(2), 602 - 615.

Sinex, D. G., Guzik, H., Li, H., & Sabes, J. H. (2003). Responses of auditory nerve fibers to harmonic and mistuned complex tones. *Hearing Research, 182*(1-2), 130-139. doi: 10.1016/s0378-5955(03)00189-8

Sinex, D. G., Li, H., & Velenovsky, D. S. (2005). Prevalence of stereotypical responses to mistuned complex tones in the inferior colliculus. *J Neurophysiol, 94*(5), 3523-3537. doi: 10.1152/jn.01194.2004

Sinex, D. G., & McDonald, L. P. (1989). Synchronized discharge rate representation of voice-onset time in the chinchilla auditory nerve. *J Acoust Soc Am, 85*(5), 1995 - 2004.

Sinex, D. G., Sabes, J. H., & Li, H. (2002). Responses of inferior colliculus neurons to harmonic and mistuned complex tones. *Hearing Research, 168*, 150 - 162.

Smith, R. L. (1977). Short-term adaptation in single auditory nerve fibers: Some poststimulatory effects. *J Neurophysiol, 40*(5), 1098 - 1112.

Stein, R. B., Gossen, E. R., & Jones, K. E. (2005). Neuronal variability: noise or part of the signal? *Nat Rev Neurosci, 6*(5), 389-397. doi: 10.1038/nrn1668

Stern, R. M., & Morgan, N. (2012). Hearing is believing. *IEEE Signal Processing Magazine, 34*.

Stickney, G. S., Zeng, F.-G., Litovsky, R., & Assmann, P. (2004). Cochlear implant speech recognition with speech maskers. *J Acoust Soc Am, 116*(2), 1081. doi: 10.1121/1.1772399

Sumner, C. J., & Palmer, A. R. (2012). Auditory nerve fibre responses in the ferret. *Eur J Neurosci, 36*(4), 2428-2439. doi: 10.1111/j.1460-9568.2012.08151.x

Taberner, A. M., & Liberman, M. C. (2005). Response properties of single auditory nerve fibers in the mouse. *J Neurophysiol, 93*(1), 557-569. doi: 10.1152/jn.00574.2004

Theunissen, F., & Miller, J. P. (1995). Temporal encoding in nervous systems: A rigorous definition. *Journal of Computational Neuroscience, 2*, 149 - 162.

Viemeister, N., F. (1988). Intensity coding and the dynamic range problem. *Hearing Research, 34*, 267 - 274.

Wen, B., Wang, G. I., Dean, I., & Delgutte, B. (2009). Dynamic range adaptation to sound level statistics in the auditory nerve. *J Neurosci, 29*(44), 13797-13808. doi: 10.1523/JNEUROSCI.5610-08.2009

Wen, B., Wang, G. I., Dean, I., & Delgutte, B. (2012). Time course of dynamic range adaptation in the auditory nerve. *J Neurophysiol, 108*(1), 69-82. doi: 10.1152/jn.00055.2012

Wever, E. G., Bray, C. W., & Lawrence, M. (1940). The interference of tones in the cochlea. *J Acoust Soc Am, 12*, 268 - 280.

Winter, I. M., Robertson, D., & Yates, G. K. (1990). Diversity of characteristic frequency rate-intensity functions in guinea pig auditory nerve fibres. *Hearing Research, 45*, 191 - 202.

Young, E. D., & Sachs, M. B. (1979). Representation of steady-state vowels in the temporal aspects of the discharge patterns of populations of auditory nerve fibers. *J Acoust Soc Am, 66*(5), 1381 - 1403.

Zhang, X., & Carney, L. H. (2005). Analysis of models for the synapse between the inner hair cell and the auditory nerve. *J Acoust Soc Am, 118*(3), 1540 - 1553. doi: 10.1121/1.1993148

Zhang, X., Heinz, M. G., Bruce, I. C., & Carney, L. H. (2001). A phenomenological model for the responses of auditory-nerve fibers: I. Nonlinear tuning with compression and suppression. *J Acoust Soc Am, 109*(2), 648-670. doi: 10.1121/1.1336503

Zilany, M. S., Bruce, I. C., & Carney, L. H. (2014). Updated parameters and expanded simulation options for a model of the auditory periphery. *J Acoust Soc Am, 135*(1), 283-286. doi: 10.1121/1.4837815

Zilany, M. S., Bruce, I. C., Nelson, P. C., & Carney, L. H. (2009). A phenomenological model of the synapse between the inner hair cell and auditory nerve: long-term adaptation with power-law dynamics. *J Acoust Soc Am, 126*(5), 2390-2412. doi: 10.1121/1.3238250

Appendix A – Supplementary Model Outputs

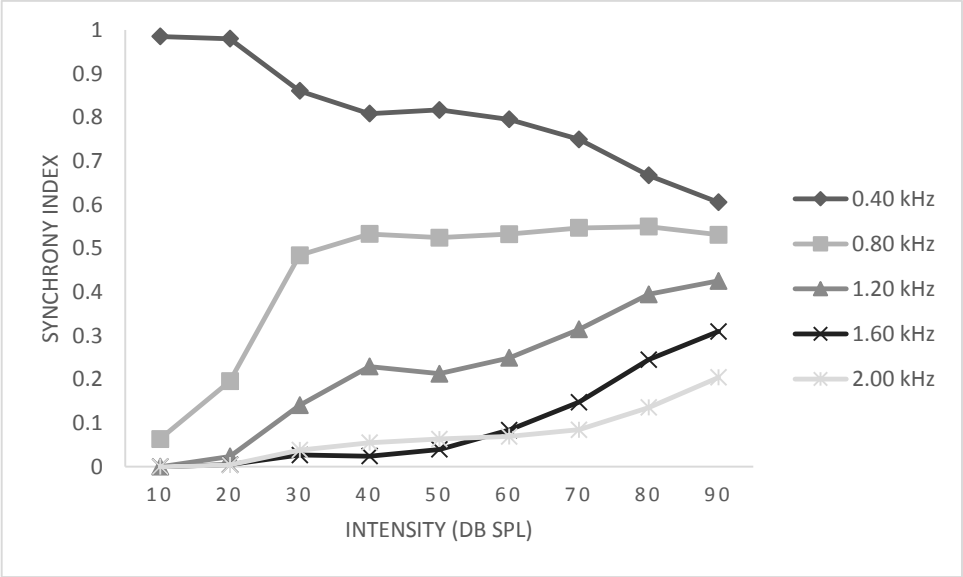

Figure 41: Carney model outputs of the response synchronies produced by a 0.4 kHz characteristic frequency fibre to harmonic tones over increasing intensity
Pattern of modelled response synchrony to individual harmonic components against increasing intensity to a 0.4 kHz auditory fibre to an 8 component harmonic tone with a fundamental frequency of 0.400 kHz.

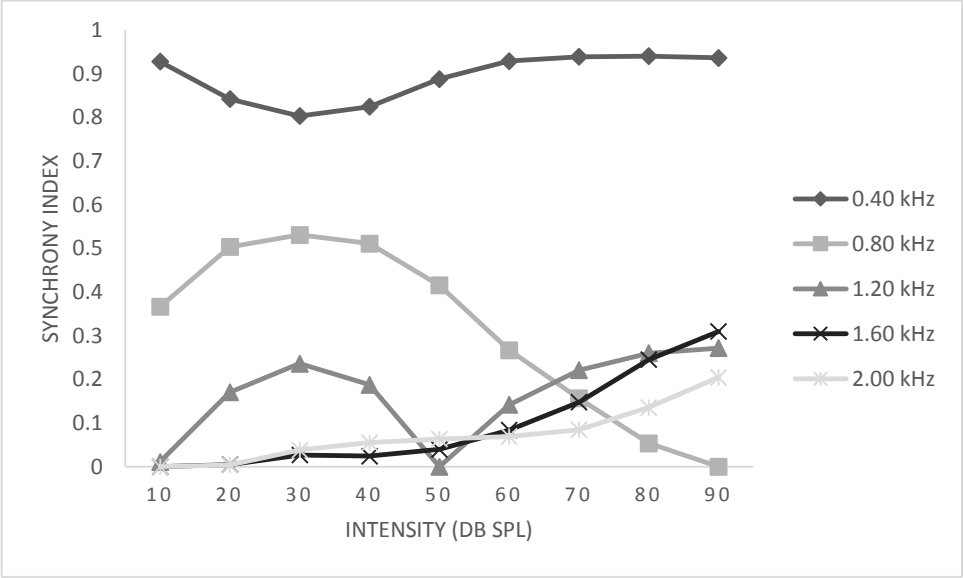

Figure 42: Seneff model outputs of the response synchronies produced by a 0.4 kHz characteristic frequency fibre to harmonic tones over increasing intensity
Pattern of modelled response synchrony to individual harmonic components against increasing intensity to a 0.4 kHz auditory fibre to an 8 component harmonic tone with a fundamental frequency of 0.400 kHz.

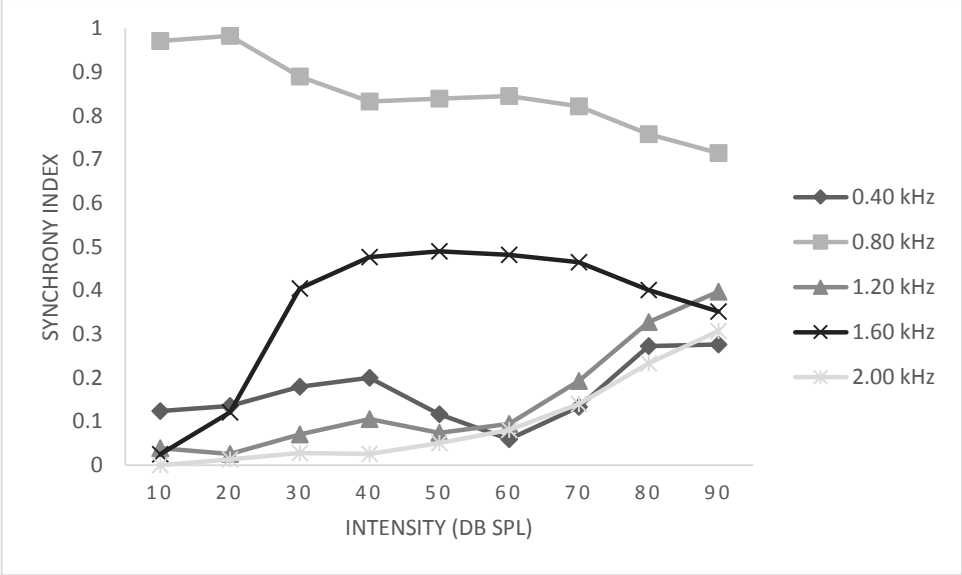

Figure 43: Carney model outputs of the response synchronies produced by a 0.67 kHz characteristic frequency fibre to harmonic tones over increasing intensity
Pattern of modelled response synchrony to individual harmonic components against increasing intensity to a 0.67 kHz auditory fibre to an 8 component harmonic tone with a fundamental frequency of 0.400 kHz.

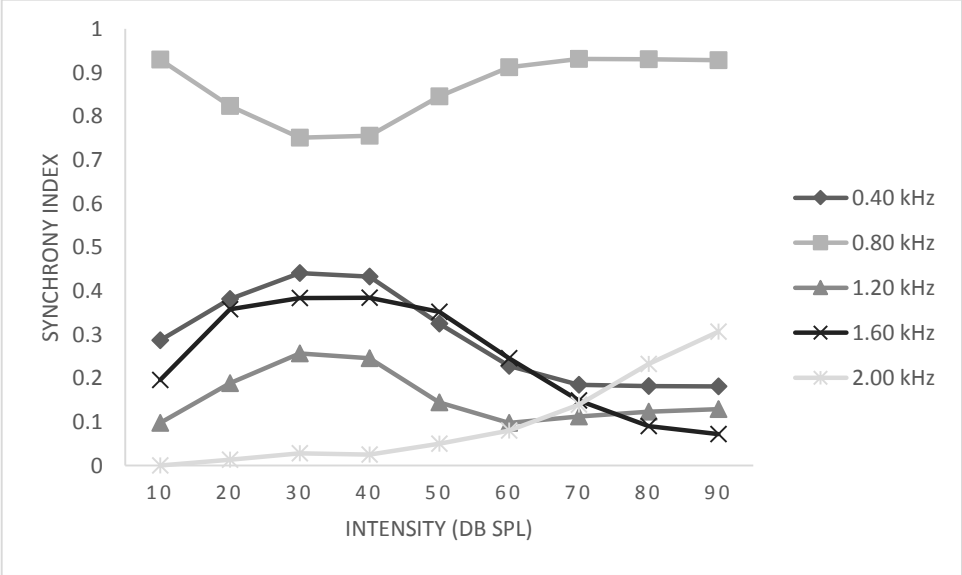

Figure 44: Seneff model outputs of the response synchronies produced by a 0.67 kHz characteristic frequency fibre to harmonic tones over increasing intensity
Pattern of modelled response synchrony to individual harmonic components against increasing intensity to a 0.67 kHz auditory fibre to an 8 component harmonic tone with a fundamental frequency of 0.400 kHz.

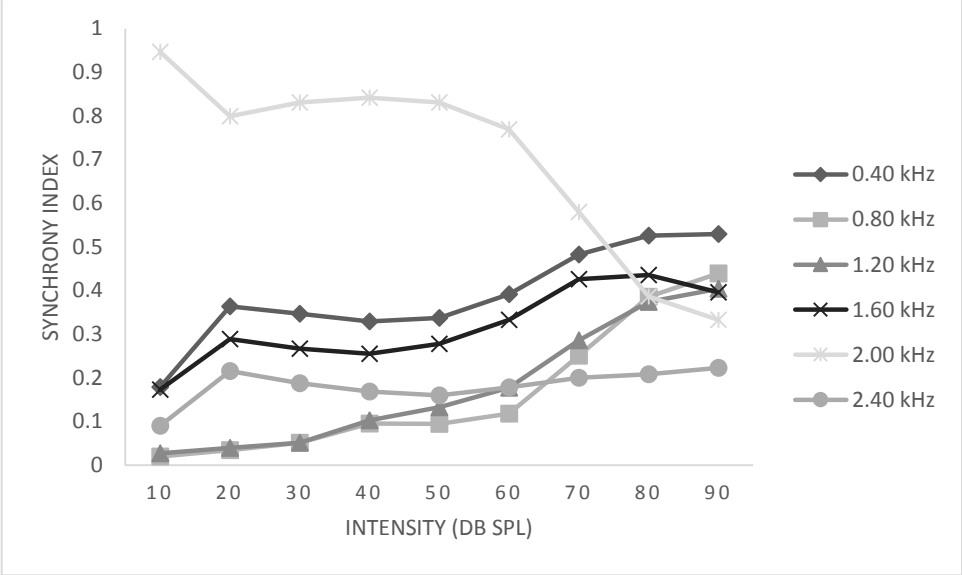

Figure 45: Carney model outputs of the response synchronies produced by a 2.05 kHz characteristic frequency fibre to harmonic tones over increasing intensity
Pattern of modelled response synchrony to individual harmonic components against increasing intensity to a 2.05 kHz auditory fibre to an 8 component harmonic tone with a fundamental frequency of 0.400 kHz.

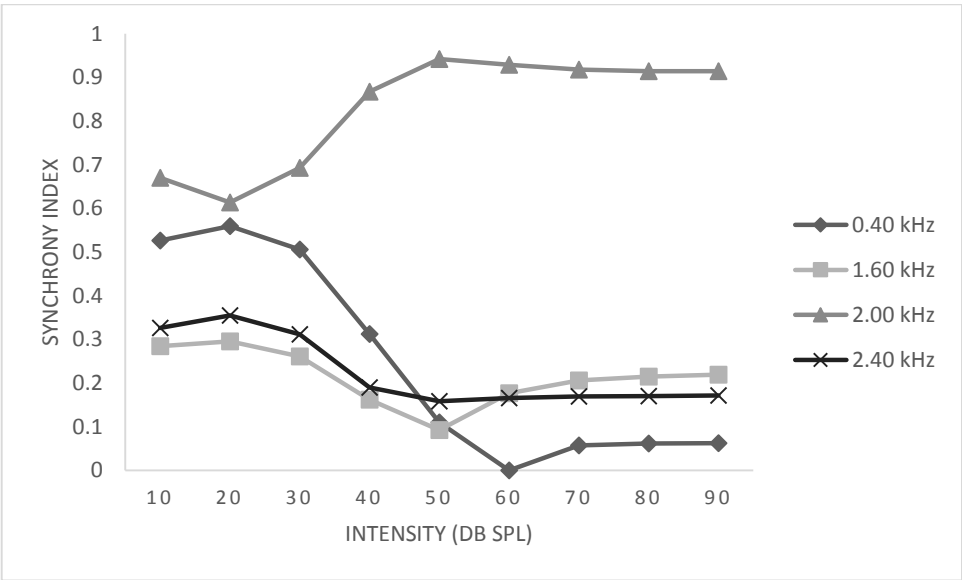

Figure 46: Seneff model outputs of the response synchronies produced by a 2.05 kHz characteristic frequency fibre to harmonic tones over increasing intensity
Pattern of modelled response synchrony to individual harmonic components against increasing intensity to a 2.05 kHz auditory fibre to an 8 component harmonic tone with a fundamental frequency of 0.400 kHz.

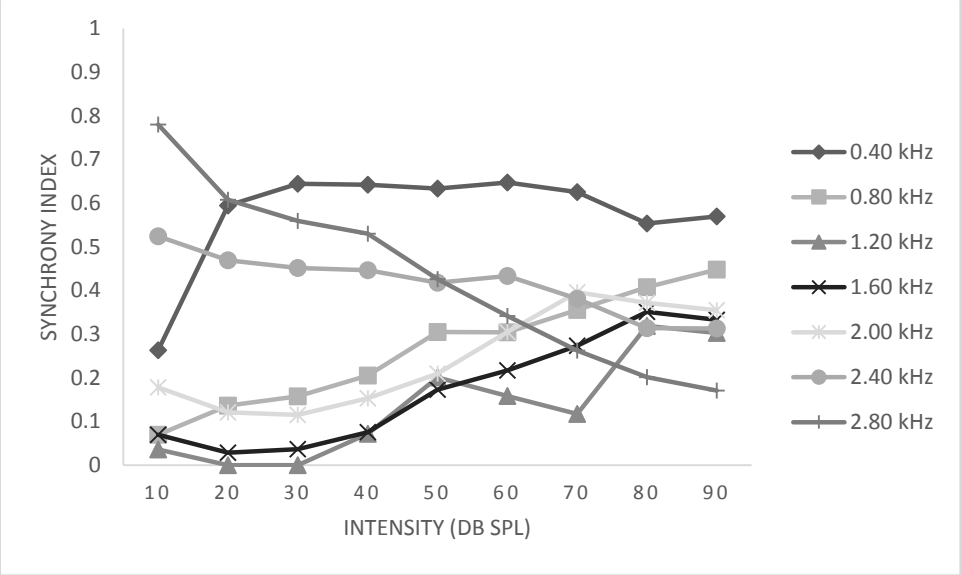

Figure 47: Carney model outputs of the response synchronies produced by a 2.71 kHz characteristic frequency fibre to harmonic tones over increasing intensity
Pattern of modelled response synchrony to individual harmonic components against increasing intensity to a 2.71 kHz auditory fibre to an 8 component harmonic tone with a fundamental frequency of 0.400 kHz.

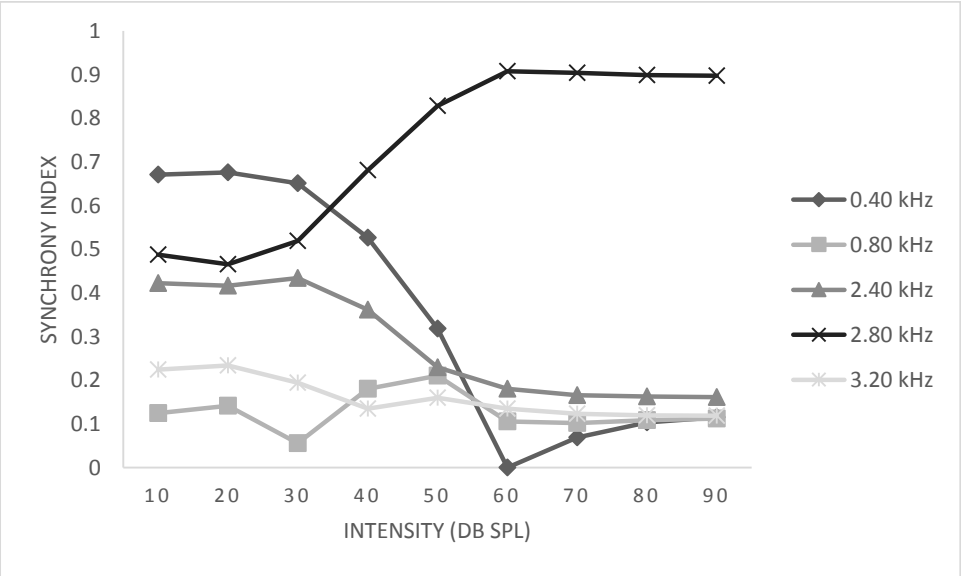

Figure 48: Seneff model outputs of the response synchronies produced by a 2.71 kHz characteristic frequency fibre to harmonic tones over increasing intensity
Pattern of modelled response synchrony to individual harmonic components against increasing intensity to a 2.71 kHz auditory fibre to an 8 component harmonic tone with a fundamental frequency of 0.400 kHz.

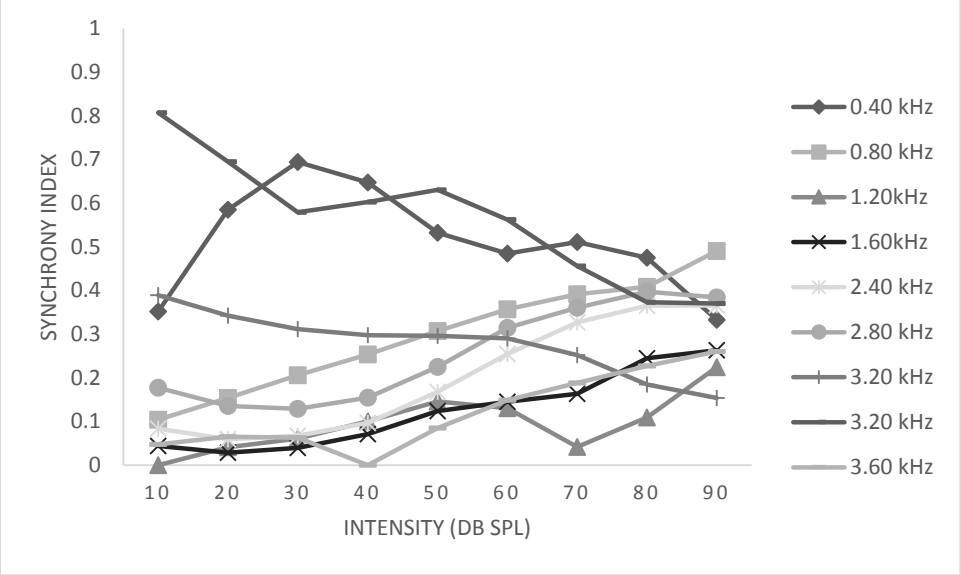

Figure 49: Carney model outputs of the response synchronies produced by a 3.24 kHz characteristic frequency fibre to harmonic tones over increasing intensity
Pattern of modelled response synchrony to individual harmonic components against increasing intensity to a 3.24 kHz auditory fibre to an 8 component harmonic tone with a fundamental frequency of 0.400 kHz.

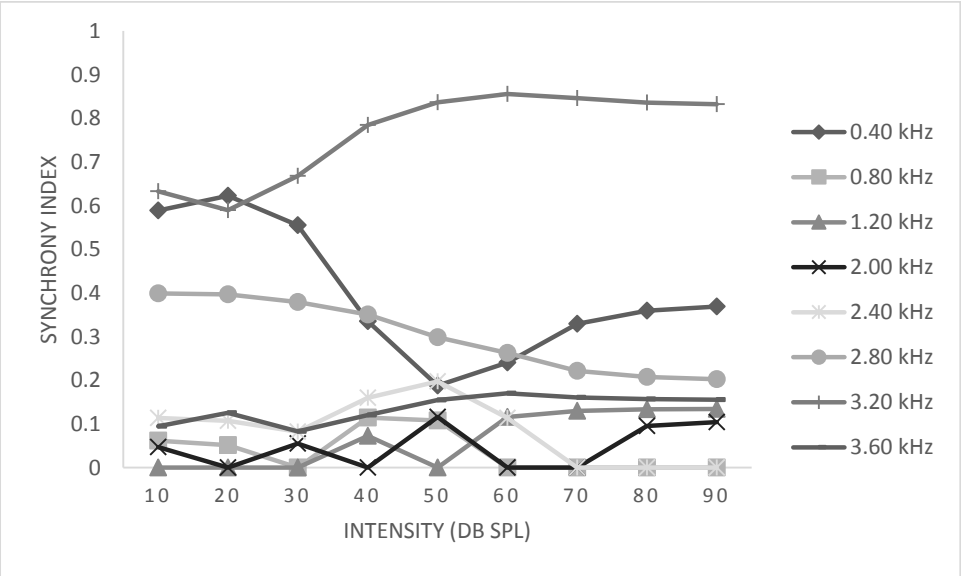

Figure 50: Seneff model outputs of the response synchronies produced by a 3.24 kHz characteristic frequency fibre to harmonic tones over increasing intensity
Pattern of modelled response synchrony to individual harmonic components against increasing intensity to a 3.24 kHz auditory fibre to an 8 component harmonic tone with a fundamental frequency of 0.400 kHz.